

**TOMAS BATA UNIVERSITY IN ZLÍN**  
**FACULTY OF TECHNOLOGY**

Ing. Karin Novotná

**PLANAR ARTICLES FOR TECHNICAL, BIOMEDICAL  
AND THERAPEUTICAL APPLICATIONS**

**PLANÁRNÍ STRUKTURY PRO TECHNICKÉ, BIOMEDICÍNSKÉ A  
THERAPEUTICKÉ APLIKACE**

Doctoral Thesis

<b>Study programme</b>	<b>P 2808 Chemistry and Materials Technology</b>
<b>Supervisor</b>	<b>prof. Ing. Lubomír Lapčík, Ph. D</b>
<b>Year of elaboration</b>	<b>March 2011, Zlín</b>



# ABSTRACT

This work brings results from evaluation of chosen natural polymers and investigation of different factors influences on their physico-chemical properties.

Study also brings review about two different ways of polymerization of natural polymers and afterwards investigation of their disintegration; which is a key factor for pulsed delivery mechanism.

Other critical studied factor is protection of used fibres. It is presented by construction of nanocomposites, which can even improve basic properties of raw material and brings potential of building up other useful compounds.

*Keywords:* pulsed drug delivery, nanocomposites, wound healing dressing, natural polymers

# ABSTRAKT

Tato práce přináší výsledky zkoumání vybraných zástupců z řad přírodních polymerů, stejně jako výsledky zkoumání jejich fyziko-chemických vlastností a vlivů okolních faktorů na průběh těchto charakteristik.

Tato práce se také zabývá popisem dvou polymeračních postupů pro vytvoření gelu z přírodních polymerů, kdy tyto jsou následně rozkládány vlivem okolních podmínek. Studovaný rozklad je nezbytnou podmínkou pro kontrolovaný rozptyl.

Dalším kritickým faktorem, který je v této práci studován, je ochrana použitých vláken. Tento problém je v předložené práci řešen konstrukcí nanokompozitů, které

mohou jednak chránit vlákna, jednak vylepšit základní vlastnosti těchto vláken, nebo mohou sloužit jako podklad pro stavbu dalších jednotek, které obohatí základní vlastnosti nanokompozitů.

Toto vše může přinést další budoucnost pro aplikace přírodních vláken v medicínských aplikacích.

***Klíčová slova:*** kontrolovaný rozptyl léčiva, nanokompozity, povrchová léčba ran, přírodní polymery

Acknowledgement:

I would like to thank to my university colleagues and teachers, to my husband, to my employment colleagues and to my family and friends for their great support during my work. Thank you to all!

This Doctoral Thesis titled Planar articles for technical, biomedical and therapeutical application was disposed at Department of Physics and Materials Engineering, Faculty of Technology, Tomas Bata University in Zlín. Mentioned institution secured financially presented project. That is why this work is its assets. Any data, included in the Doctoral Thesis, might be used technically, technologically and literally only when the head of mentioned department or the Doctoral Thesis supervisor yield consent. In the event of any results publication in any technical papers, I will be betrayed as a corporate author.

I declare, that I disposed respectively whole Doctoral Thesis and all discussed literature was quoted.

Zlin, 11. 03. 2011

.....

Author's signature



# TABLE OF CONTENTS

ABSTRACT	3
ABSTRAKT	3
TABLE OF CONTENTS	5
LIST OF FIGURES	8
INTRODUCTION	13
History of technical textiles	14
Market of technical textiles	15
Medical textiles overview	19
List of references	22
<b>1 EVALUATION OF DEX-HEMA FOR CONTROLLED DRUG DELIVERY</b>	<b>23</b>
1.1 Aim of project	27
1.2 Materials and methods	28
<i>1.2.1 Synthesis of dextran derivatized with hydroxyethyl methacrylate (Dex-HEMA)</i>	28
<i>1.2.2 Preparation of buffer</i>	35
<i>1.2.3 Preparation of PEG-solution</i>	35
<i>1.2.4 Preparation of gel</i>	35
<i>1.2.5 Pressure device</i>	37

1.2.6 <i>Rheological Characterisation of Hydrogels</i>	40
1.3 Results and discussion	47
1.4 Conclusions	65
1.5 List of abbreviations	67
1.6 List of references	70
<b>2 PREPARATION OF INORGANIC/ ORGANIC NANOCOMPOSITES</b>	<b>73</b>
2.1 Aim of project	73
2.2 Materials and methods	73
2.2.1 <i>Chemicals</i>	73
2.2.2 <i>Synthesis</i>	76
2.3 Result and discussion	79
2.3.1 <i>List of prepared substances</i>	79
2.4 Conclusion	85
2.5 List of abbreviations	85
2.6 List of references	86
<b>3 EVALUATION OF CELLULOSE DERIVATES FOR WOUND HEALING DRESSING</b>	<b>88</b>
3.1 Aim of this project	88
3.2 Materials and methods	88
3.2.1 <i>Materials</i>	88



3.3 Results and discussion	95
3.3.1 <i>Density measurement</i>	95
3.3.2 <i>Surface tension measurement</i>	97
3.3.3 <i>Contact angle measurement</i>	102
3.3.4 <i>UV-VIS spectroscopy</i>	104
3.3.5 <i>Measurement of the particle diameter</i>	114
3.3.6 <i>Measurement of zeta potential</i>	119
3.4 Conclusion	123
3.5 List of abbreviations	124
3.6 List of References	127
MAIN CONCLUSION	144
CONFERENCE CONTRIBUTION	146
CURRICULUM VITAE	148

## LIST OF FIGURES

Figure 1: World consumption of technical textiles by geographical region [1].	17
Figure 2: World end-use consumption of technical textiles by application area [1].	18
Figure 3: Volume of world consumption of medical textiles in last 20 years [1].	19
Figure 1.1: Schematic picture of a gel particle surrounded by a semi permeable membrane, during degradation of polymer chains. Chains are connected into a three-dimensional network by chemical cross-links → at the end of degradation process polymer solution is inside the semi permeable membrane → after swelling pressure exceeds the tensile strength of the membrane, it ruptures and drug molecules are released [1.8].	24
Figure 1.2: Chemical structure dex-HEMA, that is glucose substituted with HEMA. Degradation of dex-HEMA is caused by hydrolysis of HEMA cross-links and free dextran and HEMA chains are produced.	25
Figure 1.3: Sudden increase of swelling pressure per time. The two curves represent hydrogels with different DS.	26
Figure 1.4: Chemical structure of PEG-HEMA, what is poly (ethylene glycol) substituted with HEMA. Degradation PEG-HEMA is caused by hydrolysis of HEMA cross-links and free PEG chains are produced.	27
Figure 1.5: Reaction schema of dex-HEMA synthesis.	29
Figure 1.6: Pressure and temperature relationship necessary for different water phases	32
Figure 1.7: Small magnetic bar in external magnetic field	33
Figure 1.8: Picture shows orientation of protons without and with external magnetic field.	34
Figure 1.9: Schema of the home made pressure device	38
Figure 1.10: Viscous, elastic and viscoelastic behaviour.	42
Figure 1.11: Diagram of stress and strain as a function of the time	44

Figure 1.12: Schematic picture of oscillation rheological measurement. _____	45
Figure 1.13: Molecule of HEMA-CI with identified protons. _____	47
Figure 1.14: Molecule dex-HEMA with identified protons. _____	50
Figure 1.15: $G'$ during degradation time. Two curves represent different way of polymerisation _____	51
Figure 1.16: Concentration of free dextran molecules in surrounded PB as a function of degradation time. Two curves represent different way of polymerisation and its influent on degradation process. _____	53
Figure 1.17: Variation of $G'$ is presented as a function of degradation time. Two curves represent dex-HEMA gels with different molecular weight: dex-HEMA 5 000 $\text{g}\cdot\text{mol}^{-1}$ and dex- HEMA 19 000 $\text{g}\cdot\text{mol}^{-1}$ . _____	54
Figure 1.18: Concentration of free dextran chains in surrounded PB as a function of degradation time. Two curves represent gels with different molecular weight. _____	59
Figure 1.19: $G'$ as a function of degradation time. Three curves represent different initial dex-HEMA concentration and its influence on $G'$ . _____	59
Figure 1.20: Concentration of free dextran molecules in surrounded buffer as a function of degradation time. Curves represent different initial concentration of dex-HEMA. _____	60
Figure 1.21: Pressure as a function of time. Two curves represent pressure device measurement with two membranes: membrane with molecular weight cut off 2000 and 500 $\text{g}\cdot\text{mol}^{-1}$ . _____	62
Figure 1.22: Pressure of degrading PEG-HEMA gel as a function of time, measured by pressure device. _____	63
Figure 1.23: Swelling pressure as a function of polymer fraction. Graf shows influence of buffer pH (7 and 8.5) as a function of degradation time. _____	63
Figure 1.24: Swelling pressure as a function of polymer fraction. Graf shows influence of buffer pH (7 and 8.5) as a function of degradation time. _____	64

Figure 1.25: Reaction mechanism for alkaline hydrolysis of dex-HEMA. _____	65
Figure 2.1: The curves represent content of SiO <sub>2</sub> or TiO <sub>2</sub> on cellulose fibres by the function of time. _____	83
Figure 2.2: TiO <sub>2</sub> /SiO <sub>2</sub> /cellulose nanocomposite tested by SEM. _____	83
Figure 2.3: Increasing time and NaBH <sub>4</sub> concentration influence colour of samples. _____	84
Figure 3.1: Temperature dependence of OK CEL solution density. _____	96
Figure 3.2: Temperature dependence of HEC solution density. _____	96
Figure 3.3: Temperature dependence of CMC solution density. _____	97
Figure 3.4: Temperature dependence of OK CEL solution surface tension. _____	98
Figure 3.5: Temperature dependence of HEC solution surface tension. _____	99
Figure 3.6: Temperature dependence of CMC solution surface tension. _____	99
Figure 3.7: The diagram presents the OK CEL temperature relation of the surface tension. These linearity and their equations were used to calculate the surface free energy. _____	100
Figure 3.8: The diagram presents the HEC temperature relation of the surface tension. _____	101
Figure 3.9: The diagram presents the CMC temperature relation of the surface tension. _____	101
Figure 3.10: These charts show temperature dependence of advancing and receding contact angle. They also show differences cause by different weight concentration of cellulose solution. _____	102
Figure 3.11: These charts show temperature dependence of advancing and receding contact angle. They also show differences cause by different weight concentration of cellulose solution. _____	103
Figure 3.12: These charts show temperature dependence of advancing and receding contact angle. They also show differences cause by different weight concentration of cellulose solution. _____	104

- Figure 3.13: These graphs are obtained from absorbance measurement. They show absorbance dependence on cellulose solution concentration. \_\_\_\_\_ 105
- Figure 3.14: These graphs are obtained from absorbance measurement. They show absorbance dependence on cellulose solution concentration. \_\_\_\_\_ 106
- Figure 3.15: These charts show the relation between cellulose solution concentration and absorbance. The equations of linear regression were used to calculate extinction coefficient. \_\_\_\_\_ 107
- Figure 3.16: This chart shows the values of pH dependence of 2 w% OK CEL solution absorbance. \_\_\_\_\_ 108
- Figure 3.17: These diagrams present pH dependence of absorbance. These values belong to the wavelength 400 nm. \_\_\_\_\_ 109
- Figure 3.18: These diagrams present pH dependence of UV-VIS (700nm) absorbance. Data are presented for two solution concentrations. \_\_\_\_\_ 109
- Figure 3.19: Diagram presents solution pH influence on absorbance for CMC solution for 400 nm wavelength. \_\_\_\_\_ 110
- Figure 3.20: These curves represent relation between absorbance and increasing ionic concentration in cellulose solution. These values belong to 2w% OK CEL solution. \_\_\_\_\_ 111
- Figure 3.21: These charts present ionic concentration influence on solution UV-VIS light absorbance (400nm). \_\_\_\_\_ 112
- Figure 3.22: These charts present ionic concentration influence on UV-VIS light absorbance (400 nm). \_\_\_\_\_ 112
- Figure 3.23: These curves present dependence of OK CEL solution UV-VIS light absorbance (700nm) on ionic concentration. \_\_\_\_\_ 113
- Figure 3.24: These curves present dependence of CMC solution UV-VIS light absorbance (700 nm) on ionic concentration. \_\_\_\_\_ 113
- Figure 3.25: The changing OK CEL particle size in variable polymer solution pH. 114
- Figure 3.26: The changing HEC particle size with variable polymer solution pH. 115

Figure 3.27: The changing CMC particles size with varying polymer solution pH.	116
Figure 3.28: These curves represent data of particle diameter and their dependence on ionic concentration in OK CEL solution.	117
Figure 3.29: These curves represent data of particle diameter and their dependence on ionic concentration in HEC solution.	117
Figure 3.30: These curves represent data of particle diameter and their dependence on ionic concentration in CMC solution.	118
Figure 3.31: This graph shows the functionality of zeta potential and pH of OK CEL cellulose solution.	119
Figure 3.32: This graph shows the functionality of zeta potential and pH of HEC solution.	120
Figure 3.33: These three graphs show the functionality of zeta potential and pH of cellulose solution.	120
Figure 3.34: These three graphs show the functionality of zeta potential and ionic concentration in cellulose solution.	121
Figure 3.35: These three graphs show the functionality of zeta potential and ionic concentration in cellulose solution.	122
Figure 3.36: These three graphs show the functionality of zeta potential and ionic concentration in cellulose solution.	122

# INTRODUCTION

Until recently textiles were understood as materials for clothing or households, in very narrow view, because they were used as so for ages in whole human civilization. But in the broader one, textiles are materials which can be found in all aspects of our lives and during time there was also modified third field of applications, generally called technical textiles.

The definition of technical textiles says that they are textile materials and products manufactured primarily for their technical and performance properties rather than their aesthetic or decorative characteristics. Nowadays increasing number of technical textiles where combination of functionality with decorative aspects is equal [1].

This very general title covers many different applications from defence, transport and geotextile industry to medical applications and it covers sometimes very diverse products: industrial filters, implants and artificial organs for medicine, motor nozzles, and high performance sport clothing etc. [1].

Manufacturing of technical textiles is great opportunity for evaluations and investigations and it covers up usual technologies as knitting and weaving or technologies more typical for paper industry – nonwovens. Textile industry and paper industry are very close in technical textile view.

Yarns and fabrics are used for various applications other than clothing and furnishing for many years. Technical textiles are not only a result of an application of high-tech materials, but also common raw materials polyethylene, polypropylene, polyamide, viscose, cotton, flex, jute or sisal which are used for centuries. This area of industry is so dynamic that it completely breaks borders between technical textiles and other engineering materials like: paper, films, membranes, filters etc.

In last decades there was enormous growth of research and production in this industry field. Branch of technical textiles is most definitely one of the most potential and developing field of industry. Economic factors, modernization, fashion, development has very great impact on this flexibly developing industry field.

## **History of technical textiles**

History of technical textiles and their manufacturing goes hand by hand with human history; even they were not called technical textiles. Development of technical textiles is very close to developments in other technical fields, especially fibre industry, and reacts on trade needs for industry and human daily life.

Before beginning of 20<sup>th</sup> century the fibres for technical use were various vegetable and animal fibres. The products from them were rather heavy with highly limited water, fungal and flame resistance, what influenced the quantity of applications. The line of investigations in textile manufacturing extends the field of applications, for example whale oil used as lubricant open the way of jute structures to furnishing and household usage. At 1910 the development of technical textiles were influenced by first synthetic fibre viscose rayon, which was highly used as reinforcing material and much later its properties predict it as a first component for non-woven structures. This was followed by other developments of synthetic fibres and manufacturing processes: 1939 polyamide, well known as nylon, 1950' polyester and polyolefin (mostly polypropylene and polyethylene), 1960' tape and film yarns. In 1980' were firstly introduced high performance fibres (aramides), which are usual above mentioned fibres with modification of their properties, they are answer for needs of specific fields of applications.

Carbon fibres are chapter itself with reinforcing applications in military, construction and aerospace markets. New fibres are still developed as well as new way



of fibre and structure manufacturing (polytetrafluoroethylene (PTFE), polyethyletherketone (PEEK). Glass fibres once used as cheap insulation form nowadays 20% of total fibre consumption. They are widely used as reinforcing material in variety of composites for their excellent properties. On the other hand ceramic fibres are predetermined for specialized application due to their high costs and poor mechanical properties.

This industry area is very dynamic with many new developments still coming alive and seems to be very dynamic in the future too.

## **Market of technical textiles**

The production of technical textiles is mostly concentrated in highly developed countries in North America and Western Europe what is caused by the historical development of this industry area in the past.

Before economical crises the technical textile industry employed in sum about 2.3 million workers [1], as was mentioned higher it was the area with the great investment potential, but it was also one of the areas with the highest deficit. Its deficit was second highest after automotive industry one. The example of United States of America is typical and great investments in technical textile manufacturing to stay competitive contrary the smaller customer duties can be one of the factors which influence economic development of countries and bring them to the threshold of the economic crisis.

So what made and still makes this production area so attractive? Many producers do not see themselves as textile producers, but they would rather count their productions as part of car manufacturing, medical or filter products producers. Broad range of applications and end users with their special needs, high norms and specific criteria make products of technical textile manufactures something more than just common

goods. Another factor should be lower dependence of this industry area on economical situation, at least seems to be lower than dependence of common textile industry areas. Other factor of attractiveness should be connection with the fibre industry, where the consumption of fibres for technical textiles reaches almost 50% of all produced fibres [1].

Nowadays developed countries take majority of technical textile production, but there are strong indicators that East European and Far East markets will be significant for this industry and the countries of Asia will be major producers of technical textiles in the future. World consumption of technical textiles by region is presented in Figure 1.

The interest of investors starts increasing with direction to Western Europe, Asia or other world place's markets, where the production is running in almost all technical textile branches and where are strong indicators of growing interest of market about the production in these countries is being driven by many different factors. Some of them are mentioned below:

population growth, changing of demographics, ageing of the population

changes in living standards, attitude to health risks

defence, military, aerospace, automobile industry developments

construction, environmental, safety aspects

increasing demand for standard products with clear market and application

the growing dominance of purchasing which demands increasing value for money

economical stability

changes in industry, a major consumer of technical textiles

	10 <sup>3</sup> tons			\$ million		
	2000	2005	Growth (% pa)	2000	2005	Growth (% pa)
Western Europe	2 690	3 110	2,9	13 770	15 730	2,7
Eastern Europe	420	560	5,9	2 500	3 260	5,5
North America	3 450	3 890	2,4	16 980	18 920	2,2
South America	350	430	4,2	1 870	2 270	3,9
Asia	3 560	4 510	4,8	20 560	25 870	4,7
Rest of the world	870	1 190	6,5	4 590	6 280	6,5
<b>Total</b>	<b>11 340</b>	<b>13 690</b>	<b>3,9</b>	<b>60 270</b>	<b>72 330</b>	<b>3,7</b>

Figure 1: World consumption of technical textiles by geographical region [1].

The production of technical textiles exceeds third of whole textile production on detriment of common textile products, means households, carpets, upholstery. Technical textiles are further divided to other twelve main fields according to the applications. This distribution was decided on the leading international trade exhibition for technical textiles, Techtexil, which is regularly being hold in Frankfurt in Germany and Osaka in Japan [1].

*Agrotech* (agriculture, gardening and forestry)

*Buildtech* (construction)

*Clothtech* (technical components for clothing and shoes)

*Geotech* (geotextile and road construction)

*Homotech* (furniture components, upholstery and floor-coverings)

*Indutech* (filtration, cleaning and other industrial applications)

*Meditech* (medical and hygienic textile)

*Mobiltech* (automotive industry, marine construction, railroad and aviation)

*Oekotech* (products for environment protection)

*Packtech* (packing)

*Protech* (protection of people and property)

*Sporttech* (sport and leisure)

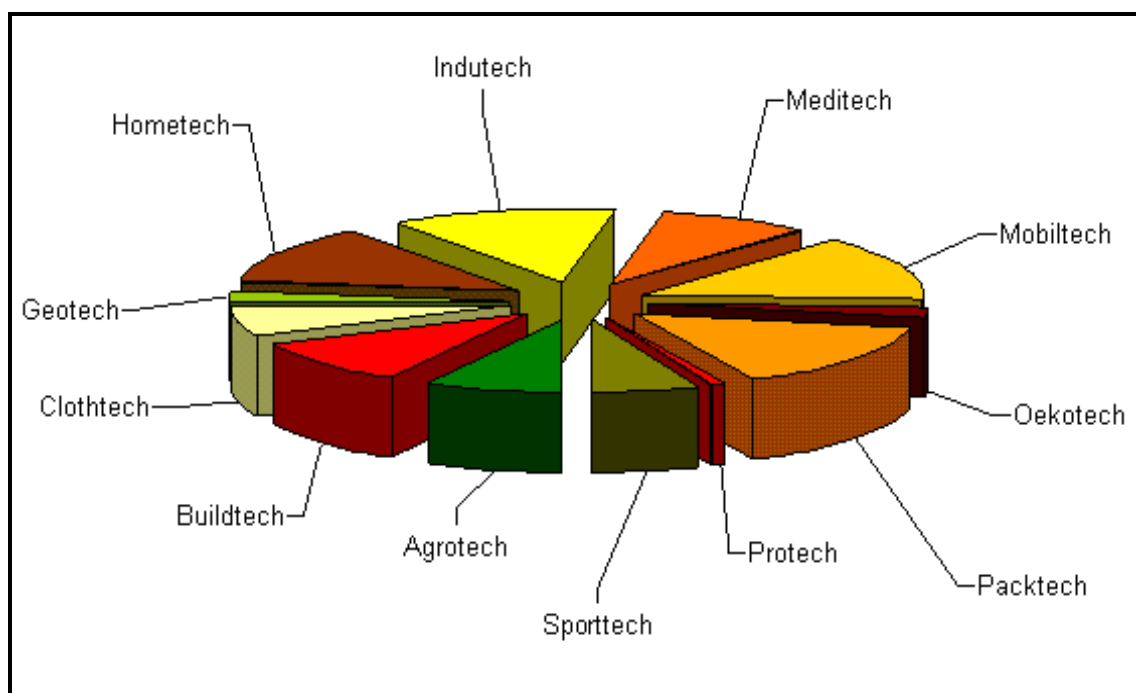


*Figure 2: World end-use consumption of technical textiles by application area [1].*

Each segment of textile application field covers a broad range of applications with many end uses, which are produced from whole scale of fibre materials and production methods.

## Medical textiles overview

The field of medical textiles covers also a very broad range of uses, based materials and applications from plasters to sensoric applicators. This fast and regularly growing area covers materials used in health but also in hygienic applications. World consumption of medical textiles in volume 1 000 tones is presented in Figure 3.

Medical textiles are big opportunities for nonwovens as well as for composite materials, which combine positive characteristics of each from used substances.

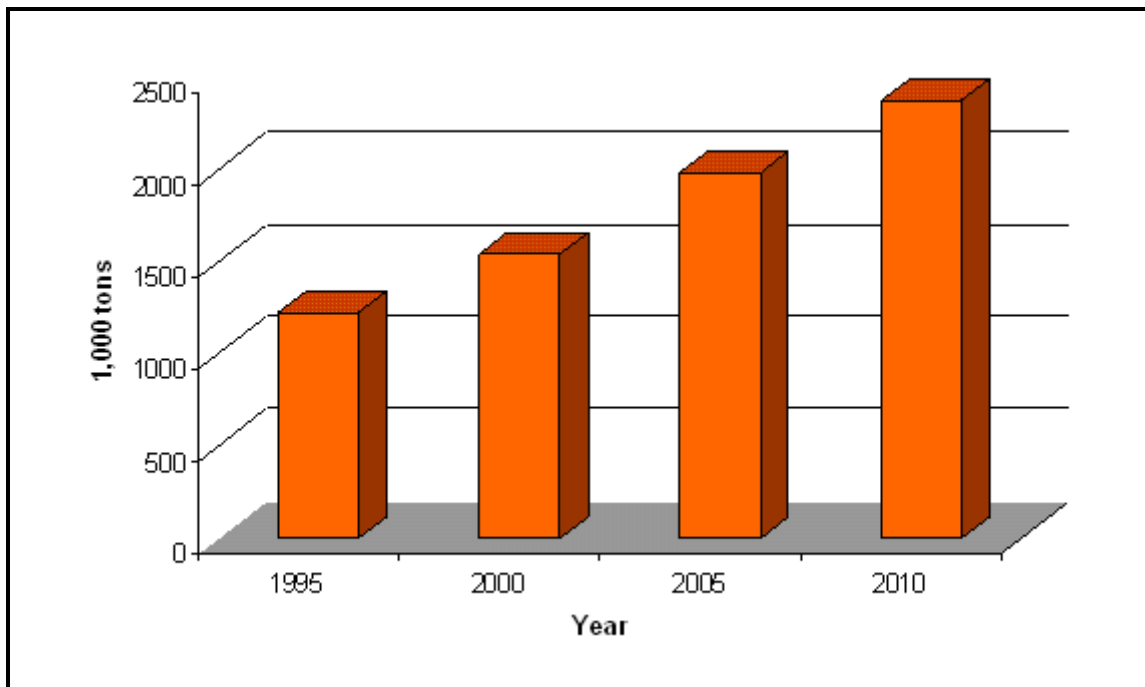


*Figure 3: Volume of world consumption of medical textiles in last 20 years [1].*

At the present time the importance of lowering the total costs per capita on post traumatic recovery is a driving force for intensive materials research oriented on surface coatings and different tissue regeneration vehicles. Both synthetic as well as the natural biopolymer systems are used. Our aim is the study of the polysaccharides

based tissue recovery enhancement devices due to their both healing as well as anti-inflammatory effects. One of the possible applications seems to be cosmetics and wound healing dressings.

Skin is the human body's largest organ. Skin has many functions, which are essential for life. It helps to regulate body temperature, forms the natural barrier against the action of physical, chemical and bacterial agents from surrounding or it is the part of the system respiratory. The nerves in skin form the special end organs for the various sensations commonly grouped as the sense of touch. These noticed functions are only the best known.

As sketched above the skin is very important for our living. On this account it must be insured against the reactive agents from surrounding environment and also against insult by serious emergency.

Unfortunately the skin is often seriously injured during car accidents, burnt up by fire or electricity, etc. Very often these are very heavy injuries with far-reaching consequences. These are affected by problems during healing. The physical, chemical and bacterial agents influence healing process; they make it slower and not so effective. The results are tedious treatments, cicatrix, burn scars, etc.

On that account an interest to make the healing process more effective is such enormous. A special tools and methods of the treatments are being developed. Synthetic as well as natural polysaccharides are biocompatible with human skin. Both have positive effect on wound healing. These materials work on as a cover. They protect the wound against bacteria, physical and chemical processes from surrounding environment and help to speed up the healing process.

Our aim is to produce special plasters from biomaterials, polysaccharides. These plasters will be applied on the injury in a liquid form. By the medium of a cross-linking agent, liquid will form a very thin film. This film will protect the wound against

aggravating factors from surrounding atmosphere. It will speed up the healing process and conserve the wound.

In a point of time the film will degrade. The wound will be clean and it will not be hurt again by painful whipping off the plasters as in the case of using the ordinary plasters. Then the wound will be prepared for other treatment or other film application.

Before the thin films will be produced, the evaluation of suitable biomaterial is required. The based material must be determined as well as its reaction on any influences.

The part of presented work is focused to evaluate and choose natural cellulose fibres, which will be suitable as matrix for wound healing articles. Three chosen polymers are investigated: OK CEL, HEC, CMC and influence of surroundings on their physical and chemical properties are evaluated as well. Investigated factors are initial polymer concentration, temperature, pH and salt concentration of surrounding solution and their influence on density, UV-VIS light absorbency, particle size diameter as well as contact angle, tensile strength.

Other investigated factor is possibility to entrap drug molecules in to the gel matrix prepared from natural polymers. This solution can speed up the healing process of wounds, without removing plasters from the wound and without bringing other suffer to the wounded tissue. That is why the drug releasing must be controlled and gradual.

To this topic other part of presented study is dedicated. We try to investigate controlled disintegration of polymer cross-linked matrix. Initial polymer concentration and its influence on this disintegration process are also taken into account. Disintegration is evaluated by physico - mechanical tests: as evaluation of rheological characteristics, measuring of free polymer particles in surrounding solution and increasing osmotic pressure of degrading matrix. Two natural polymers were investigated dex-HEMA and PEG-HEMA.

Next investigated issue is covering of fibre surface with inorganic compounds to protect them against harmful factors from surrounding environment. This study is performed on natural fibres which are covered by silica and titanium.

Such produced inorganic/ organic compounds are nanocomposites; then can be taken as base for building silver metal particles on their surface. Silver metal particles bring antibacterial characteristic to these nanocomposites. Antibacteriability and high sterility is one of the demanded factors for medical devices.

## List of references

- [1] CZAJKA, R. Development of Medical Textile Market. *Fibres & textiles in eastern Europe*. 2005, vol. 13, no. 1.
- [2] YUDANOVA, T.N., RESHETOV, I.V. Drug synthesis methods and manufacturing technology. *Pharmaceutical Chemistry Journal*. 2006, Vol. 40, no. 2, 8.



# 1 EVALUATION OF DEX-HEMA FOR CONTROLLED DRUG DELIVERY

In the 1970's polymeric systems came into existence as potentially efficient antigen-releasing carriers designed to provide "single-step" or "single-shot" immunization. World Health Organization supports this development in immunization techniques as a way to improve immunization coverage as well as to reduce vaccination costs [1.5].

Recently, there is a growing interest to study biodegradable hydrogels for drug delivery applications [1.7], because of their several beneficial properties. They consist mainly of water, which ensures a good compability with body proteins. They possess a good biocompatibility and have a low interfacial free energy in contact with body fluids, which results in a low tendency for proteins and cells to adhere to those surfaces. And finally the release of molecules (drugs, proteins) from the hydrogel matrix can be controlled and manipulated by the characteristics of the hydrogel; such as water content and cross-link density of the gel [1.8].

This project is part of a research to design exploding microparticles, which consist of a degrading hydrogel core surrounded by a lipid membrane. This membrane should be ruptured by the osmotic pressure of the degraded gel and it should keep entrapped drug molecules and gel degradation products inside until the moment of explosion.

There are many ways to encapsulate hydrogels into a lipid coat. For example the method of Sergey Kazakov: the hydrogel-forming components are encapsulated into liposomes. The outside solution is diluted to prevent polymerization and afterwards UV exposure is used to initiate a free radical polymerization [1.9].

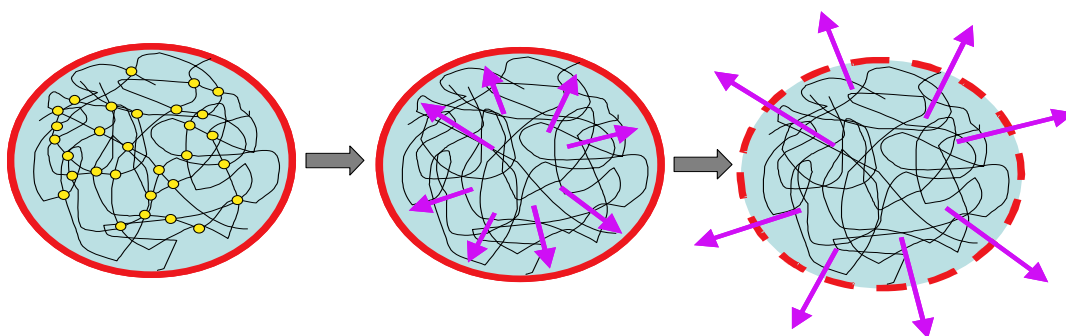


*Figure 1.1: Schematic picture of a gel particle surrounded by a semi permeable membrane, during degradation of polymer chains. Chains are connected into a three-dimensional network by chemical cross-links → at the end of degradation process polymer solution is inside the semi permeable membrane → after swelling pressure exceeds the tensile strength of the membrane, it ruptures and drug molecules are released [1.8].*

Another way can be preparation according to the method of Kiser and Needham. First hydrogel microspheres are produced and afterwards the microgels are sedimented by centrifugation on lipid film [1.10].

The lipid membrane allows transport of small molecules (water, ions) between gel and surrounding solution and also prevents large molecules from leaving the gel.

Each membrane has a tensile strength. Swelling pressure of the gel increases because of degradation. When the swelling pressure exceeds the tensile strength of the membrane, it ruptures and the drug molecules are completely released.

In earlier studies the behaviour of a methacrylated dextran (dex-HEMA) was studied for understanding thermodynamic and kinetic properties of hydrogel matrix. The degradation of the gel is caused by the hydrolysis of the carbonate ester link formed between the methacrylate group and dextran molecule.

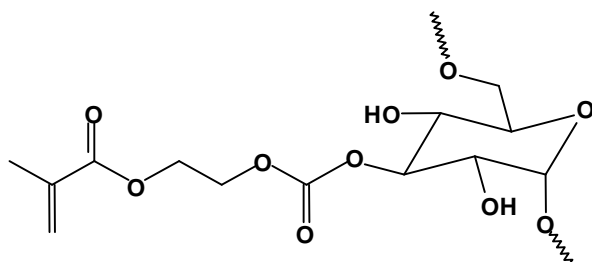


*Figure 1.2: Chemical structure dex-HEMA, that is glucose substituted with HEMA.*

*Degradation of dex-HEMA is caused by hydrolysis of HEMA cross-links and free dextran and HEMA chains are produced.*

The kinetics of the gel degradation can be influenced by degree of substitution (DS, the amount of HEMA groups per 100 glucose units) and concentration. In recent studies these influences were tested. Studies were performed on dex-HEMA gel, with molecular weight ( $M_w$ ) 19 000 and 40 000g.mol<sup>-1</sup>.

Recent studies found out that increase of swelling pressure is gradual and slow during first days of degradation. But close to the end swelling pressure suddenly increases and reaches the limit of the tensile strength of the membrane.

This study tries to compare pressure and release behaviour of the gel, which is prepared from dex-HEMA with the molecular weight 5 000g.mol<sup>-1</sup>. The reason why we examine another molecular weights is that is has to be difficult to coat microspheres of dex-HEMA with molecular weight 19 000g.mol<sup>-1</sup>. We used dex-HEMA with the same value of DS for preparation of gel and tried to investigate the other influence factor, which is initial concentration. We prepared gels with different concentrations and we expected that concentrations of cross-links grow with increasing amount dex-HEMA.

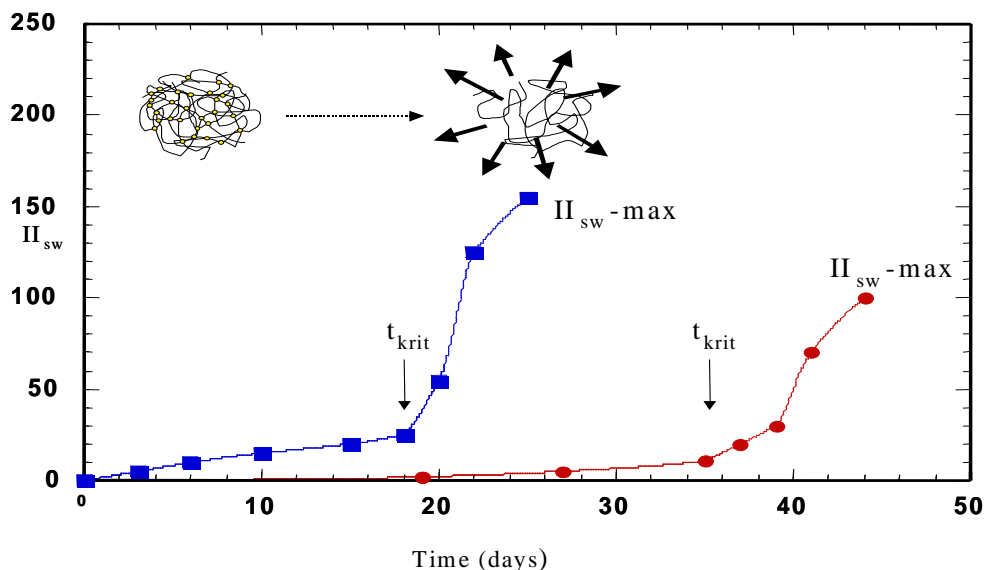


Figure 1.3: Sudden increase of swelling pressure per time. The two curves represent hydrogels with different DS.

This will be reflected in the kinetics of the degradation. The gel was prepared by UV and chemical polymerization. We expected that the polymerization type does not influence degrading behaviour of this gel.

Kinetics of the degradation process is reflected in swelling pressure of the degraded gel. Increase of the swelling pressure depends on elastic and osmotic pressure of the gel. Both values can be measured during degradation time. We measured regularly elastic modulus of the gel.

During degradation process free dextran chains are produced and leave the gel structure. The increasing amount of free dextran was also measured.

We also studied the degradation process of PEG-HEMA. The degradation was realized in buffer with different pH. We predicted that degrading process would be faster with increasing pH of the buffer. Osmotic deswelling pressure measurement was carried out after different time of degradation.

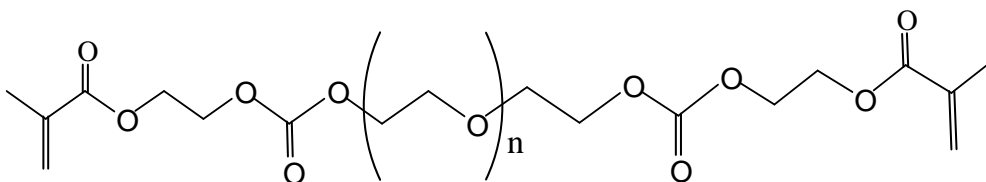


*Figure 1.4: Chemical structure of PEG-HEMA, what is poly (ethylene glycol) substituted with HEMA. Degradation PEG-HEMA is caused by hydrolysis of HEMA cross-links and free PEG chains are produced.*

The knowledge of variation of swelling pressure during gel degradation can help to design pulsed delivery system with tailored swelling pressure profile.

## **1.1 Aim of project**

This study is performed to investigate possibility of usage of natural polymers for pulsed drug delivery systems. Two different natural polymers are used as investigates materials in our study; dex-HEMA and PEG-HEMA. This study should describe different ways of polymerization and their influence on degradation process. Also other factors; as molecular weight, initial concentration of monomer or pH of diluting surrounding solution; which can influence the degradation process of prepared gel were studied.

Degradation of polymer is investigated by different measurements. Refractometric measurement evaluates free dissolved rests of polymer in dissolving solution. On the other hand rheological measurement investigates elastic modulus of degrading slices of polymer gel. Another series of measurement will be performed on home made osmotic pressure measurement device. The predicted increasing osmotic pressure will be

investigated by this device with usage of two different standardized semi permeable membranes.

Results will be presented in charts, which will be prepared from calculated values by using presented and described equations.

Investigated decision about using evaluated substances for pulsed drug deliveries systems will be concluded at the very end of this first part of presented work.

## **1.2 Materials and methods**

### **1.2.1 Synthesis of dextran derivatized with hydroxyethyl methacrylate (Dex-HEMA)**

#### *Chemicals*

Dextran (from *Leuconostoc mesenteroides*, T40,  $M_w = 5\,000\text{g}\cdot\text{mol}^{-1}$ , as determined by GPC analysis, lot.n° 2528), dimethyl sulfoxide (DMSO, <0.01% water), 2-hydroxyethyl methacrylate (HEMA,  $M_w = 145, 3\text{g}\cdot\text{mol}^{-1} > 97\%$  GC, lot.n° 4519711) and dichloromethane (DCM, no alcohol as stabiliser, 99.9%,  $M_w = 84, 93\text{g}\cdot\text{mol}^{-1}$ , lot.n° K32082944 325) were obtained from Fluka Chemie AG, Busch, Switzerland. 4-N, N-dimethylaminopyridine (DMAP, 99%,  $M_w = 122, 17\text{g}\cdot\text{mol}^{-1}$ ) and 1, 1'-carbonyldiimidazole (CDI, 98%,  $M_w = 162, 15\text{g}\cdot\text{mol}^{-1}$ ) were from Acros Chimica, Geel, Belgium. Concentrated HCl (37%, 12,5M) is from Vel, Leuven, Belgium. Sicapent with Indicator (P2O5 on carrier) and magnesium sulphate ( $\text{MgSO}_4$ ) were obtained from Merck, Darmstadt, Germany. Deuterated chloroform ( $\text{CDCl}_3$ ) Deuterium oxide ( $\text{D}_2\text{O}$ ) was delivered by Isotope Laboratories Cambridge. Water was purified by reversed osmosis. Liquid nitrogen was used to force out oxygen.

**Materials and apparatus**

Vacuum oven with a Petri dish with Sicapent, 500 ml one-necked round bottom flask, nipple, stirring bar, rotation film evaporator (rotavap), 1l three-necked round bottomed flask, septa, 300ml conical flask, long metal needle, needle with tube connection, cellulose dialysis tubes (Spectra/Por®, size 7 and molecular weight cut off 2000 D) from Spectrum Laboratories, Rancho Dominguez USA, 5l beaker, freeze dryer, 1l 1-necked round bottom flasks of high quality glass, magnetic stirrer and Pasteur pipette were used during synthesis.

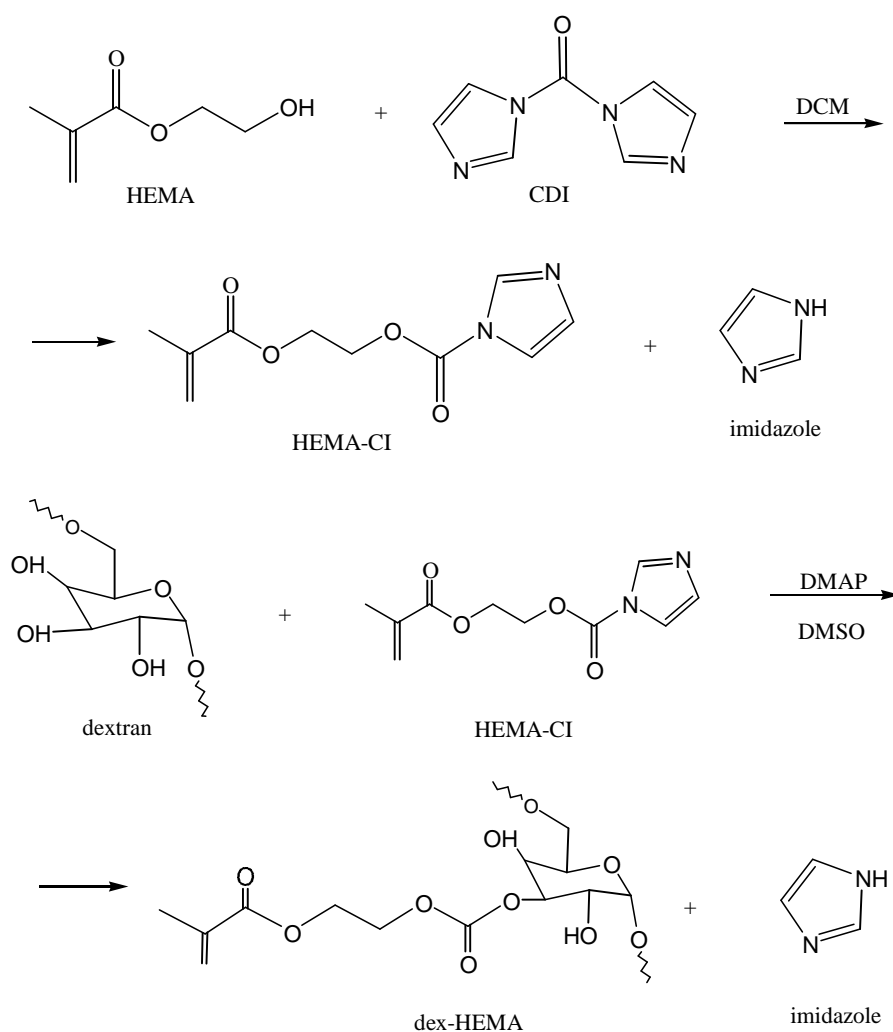


Figure 1.5: Reaction schema of dex-HEMA synthesis.

### ***Procedure***

11 3-necked and 500 ml 1-neck round bottomed flasks, stoppers, nipples and stirring bars were dried with a heat gun while flushing with N<sub>2</sub> (g) to remove water because this is an inhibitor in these synthesis. Dextran in a 300 ml conical flask was dried in a vacuum oven at 40°C on Sicapent.

For useful coupling of HEMA to dextran, the terminal hydroxyl group of HEMA has to be activated, using CDI. Activated HEMA (HEMA-CI) was obtained by the following procedure. The 500 ml one-necked round-bottomed flask was allowed to reach room temperature under nitrogen. About 250 ml DCM was poured into the flask under nitrogen stream. 14,59g CDI (0,09mol, 2eq.) was poured into this flask under nitrogen atmosphere, while mixing very gently. It was difficult to dissolve. Then 5,81g HEMA (0,04mol, 1eq.) was added drop by drop using a Pasteur pipette while stirring vigorously until the solution became clear. The solution was mixed vigorously for one hour at room temperature under nitrogen.

DCM was washed with an equal amount of water. This was poured in a conical flask with MgSO<sub>4</sub> as a drying agent. It was firmly shaken. Afterwards a spatula tip hydroquinone monomethylether was added to inhibit the polymerization of the HEMA groups. The DCM was evaporated using a rotavap with the water bath no higher than 30°C. The activated HEMA (HEMA-CI) was obtained as a slightly yellow liquid. It was stored in the freezer for later use.

Putting 3-neck flask under low nitrogen pressure started synthesis of dex-HEMA. This flask was filled with 450ml DMSO by a transfer needle. Magnetic stirrer was turned on and 50g-dried dextran was added under nitrogen flow. Dextran was completely dissolved next day.

The activated HEMA is coupled to dextran in dimethyl sulfoxide in the presence of the catalyst DMAP. 10g DMAP (0,09mol, 2eq.) was crushed and added to dissolve



## Evaluation of dex-HEMA for controlled drug delivery

completely. Then 2,03g activated HEMA-Cl (0,01mol, 0,25eq.) was dropped into this solution. Mixture was stirred for 4 days at room temperature under nitrogen flow.

Concentrated HCl was added to the reaction mixture and mixed well to adjust to neutral pH.

The dialysis tubes were cut and washed for at least 10 minutes in RO-water. One side of the tube was closed and dialysis tube was filled. The volume of the solution can grow up due to osmotic pressure, so 2/3 of dialysis tube was filled and the rest was left empty without air bubbles.

The dialysis took place in RO-water at 4°C during 7 days, while stirring gently. Water was refreshed two times first day and than once every other day.

After dialysis the solution was clear and poured into plastic Petri dishes and filled half to prevent breaking the dishes during freezing.

The product was characterized by <sup>1</sup>H-NMR (dissolve in 2H<sub>2</sub>O). The degree of substitution was calculated by <sup>1</sup>H-NMR.

### *Freeze-drying*

Freeze-drying or lyophilization is the process in which water is removed from a product. The main principle is sublimation; this is converting ice, in this case to vapour under vacuum conditions. Water sublimates when the molecules have enough energy to break free but the conditions aren't good enough to form a liquid.

The process of sublimation depends on the relationship between temperature and pressure.

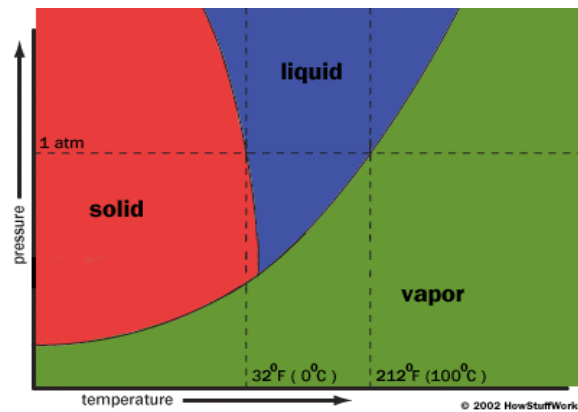


*Figure 1.6: Pressure and temperature relationship necessary for different water phases*

This process is performed in lyophilization equipment, which consists of a freeze-drying chamber with several temperature-controlled shelves; a freezing coil connected to a refrigerator compressor, a vacuum pump to reduce the pressure in the chamber and a control system.

Lyophilization has three phases: freezing, primary drying – sublimation and secondary drying – desorption.

The samples are placed onto the unfrozen shelves. Lowering the temperature in the chamber freezes the mobile water. In the primary drying phase the vacuum pump forces out air from the chamber and lowers the pressure below 0,6atm. Temperature is lower under these nearby vacuum conditions causing the ice to sublime. The water vapor flows out of the chamber and condenses onto the freezing coil in solid ice.

In the second drying phase the temperature can be increased again under the maximum vacuum to desorb bound water and it can be dried by the same drying process.

This process is mild enough not to change the composition and material structure. The main advantage of this process is that the product is completely dry and ready for storage, but it is not broken down.

Water is removed by freeze-drying. Under these conditions: frozen to 228K over a time period of 2,55h at pressure 1000mbar. The primary drying was performed at 258K and pressure varying between 0,8 and 1mbar during 13h followed by the secondary drying performed at elevated temperature 283K and reduces pressure between 0,1 and 0,2mbar for 7h.

### *Nuclear magnetic resonance spectroscopy*

NMR –spectroscopy is based on magnetic field. A proton is in fact a spinning positive charge, so it can be compared with a small magnetic bar.

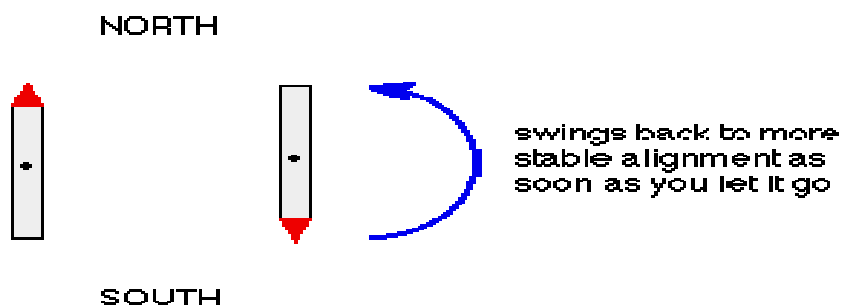


*Figure 1.7: Small magnetic bar in external magnetic field*

When a small magnet is placed in the field of a larger magnet, there are two possibilities: the small magnet will be aligned with the external field ( $\alpha$ -spin), it has the lowest energetic level, positioning in the opposite direction ( $\beta$ -spin) has the highest energetic level.

The amount of energy between these two levels is not large and when the right amount of energy is added, the proton can flip from one state to the other. A nucleus is in resonance when it is irradiated with radio-frequency photons having energy equal to the energy difference between the spin states.

But protons are surrounded with electrons. The electrons circulate and they induce a magnetic field that is opposite to the external magnetic field. So the magnetic field that is observed by the proton is smaller than the external field. It can be said that the nucleus is shielded. If hydrogen is in the neighbourhood of a more electronegative atom, than the electron density around the hydrogen atom is lower, so the observed field is higher than without the electronegative atom. It is called that the hydrogen is deshielded.

So each structure has its own effect of electrons and surrounding atoms and it results in a spectrum of magnetic fields and it is shown on a horizontal scale as chemical shift relative to a zero point that is defined by TMS (tetramethylsilane).

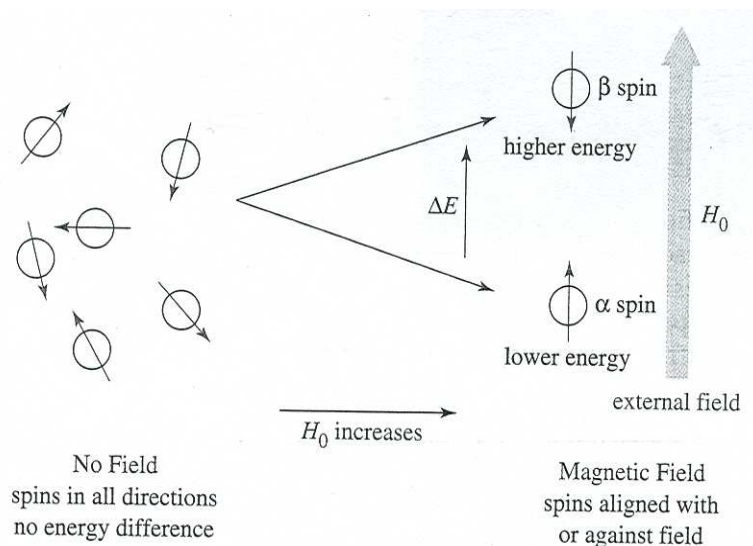


Figure 1.8: Picture shows orientation of protons without and with external magnetic field.

In TMS every hydrogen atom has the same behaviour, so they produce a single peak. The chemical shift is measured in ppm. The area under a peak is proportional to the number of chemically equivalent protons. This means that the protons have identical chemical environment with the same shielding. From combination of the place of the peak (i.e. chemical environment) and the area of the peak (i.e. number of protons) one can find the structure of a given molecule.

### **1.2.2 Preparation of buffer**

Phosphate buffer (PB) was prepared at pH 7, 10 mM. 10mM NaH<sub>2</sub>PO<sub>4</sub>·2H<sub>2</sub>O (M<sub>w</sub> = 156.01 g.mol<sup>-1</sup>, Vel, Leuven, lot. n° 98020029) and 10mM Na<sub>2</sub>HPO<sub>4</sub> (M<sub>w</sub> = 141.96 g.mol<sup>-1</sup>, UCB, lot. n° 94020029), were dissolved in distilled aqua and mixed together till pH 7. pH was measured by Multi-Channel analyzer Consort C831. NaOH was added to increase alkaline of the buffer until pH 8.5.

The Advanced<sup>TM</sup> Micro Osmometer was used to measure osmotic pressure of the buffer. The osmotic pressure of the buffer was 28 mOsm.

9.44 g/l of Na<sub>2</sub>HPO<sub>4</sub> (M<sub>w</sub> = 141.96 g.mol<sup>-1</sup>, UCB, lot. n° 94020029) was mixed with 10.3 g.l<sup>-1</sup> of citric acid and 0.2g.l<sup>-1</sup> of NaN<sub>3</sub> (M<sub>w</sub> = 65.01 g.mol<sup>-1</sup>, Sigma Chemicals, Steinheim, lot. n° 58H2504) to prepare citric buffer with pH 4.4.

### **1.2.3 Preparation of PEG-solution**

PEG solution was prepared in different concentrations. PEG (M<sub>w</sub>=20 000g.mol<sup>-1</sup>, Merk, Hohenbrunn, lot. n° S29595 945) was mixed with citrate buffer. Concentration of the PEG varied between 0 and 30 g. (100 ml)<sup>-1</sup>.

### **1.2.4 Preparation of gel**

Dex-HEMA (M<sub>w</sub> = 5 000g.mol<sup>-1</sup>, DS = 3.2) and PEG-HEMA (M<sub>w</sub> = 4 000g.mol<sup>-1</sup>) hydrogels were prepared by UV polymerization of aqueous polymer solutions.

Calculated amount of dex-HEMA or PEG-HEMA for each concentration was dissolved in equivalent volume of phosphate buffer.

Photoinitiator, Irgacure 2959 (2-hydroxy-4-hydroxyethoxy-2-methylpropiophenon, CIBA Speciality Chemicals, lot. n° 0098752S) was used in concentration 0.02%. 0.1g was dissolved in 2 ml phosphate buffer. Precise amount of this solution was added under nitrogen atmosphere into the aqueous solution of dex-HEMA or PEG-HEMA and it was mixed very gently. Than this mixture was poured into a quartz tube and let to polymerize under UV light source (365 nm) for 470 s in nitrogen atmosphere. Hydrogel samples used for rheological measurements (diameter 2.2cm) and for deswelling and dextran or PEG release measurements (diameter 1.5cm) were cut by thin wire to cylindrical slices.

Dex-HEMA hydrogels were also prepared by chemical polymerization. Solution was prepared by dissolving dex-HEMA in phosphate buffer. Polymerization reagents were N,N,N',N'-tetramethyl-ethylenediamine as a catalyst (TEMED,  $M_w = 116,2 \text{ g.mol}^{-1}$ , Sigma Chemicals, Steinheim, lot. n° 88H1181) and potassium peroxydisulfate as an initiator (KPS,  $M_w = 270,33 \text{ g.mol}^{-1}$ , Merck, Darmstadt, lot. n° 231-781-8). The initiator KPS reacts with TEMED and they produce TEMED radical and bisulphate radical. These radicals are used to initiate polymerization.

100  $\mu\text{g}$  of KPS was dissolved in 2 ml of PB and 100  $\mu\text{l}$  of TEMED was mixed with 200  $\mu\text{l}$  of PB and 200  $\mu\text{l}$  HCl. Polymer solution was poured into the glass tube. 50  $\mu\text{l}$  of TEMED solution per 1 g of polymer solution was added and mixed gently to homogenise. Afterwards 90  $\mu\text{l}$  of KPS mixture per 1 g of polymer solution were added to the system to initiate gelation process. It was let to polymerise at 4 °C for 1 hour 30 minutes. Samples for every measurement were cut by thin wire on 3mm thin slices.

Swelling pressure during degradation is investigated in this study. The swelling pressure can be express by equation:

$$\pi_{sw} = \pi_{osm} - \pi_{el} \quad (1.1)$$

Two types of deswelling measurement determined swelling pressure: by pressure device and osmotic deswelling measurement.

Elastic pressure was measured by rheology and afterwards osmotic pressure could be calculated from that equation.

### 1.2.5 Pressure device

The  $\pi_{sw}$  was measured by a home made pressure device. This device consists of a sample chamber (4,5ml) and a buffer chamber (11ml). These two chambers are separated by a semi permeable membrane (Spectra/Por®, Cellulose Ester Membrane, Molecular weight cut of 500g.mol<sup>-1</sup>). The membrane is supported by a porous Bekipor frame, which is further supported by a Teflon perforated cylinder. The membrane is permeable for small molecules (ex. water molecules). They can go through the membrane into the sample chamber. The sample start to degrade in the chamber, but large free dextran or PEG free molecules can't go out; it results in an increase of the swelling pressure.

The chambers are surrounded by water channels; they are connected with a water bath to provide heating or cooling of the chambers. Measurement was done at 37°C, temperature of the degradation.

The sample chamber can be connected with UV source (365nm, Honle UV technology bluepoint 2.1) to polymerize the sample directly in the chamber and after that pressure changes can be monitored.

Chamber pressure transducer is placed on one side of the sample. The transducer is connected with a Fluka 189 true RMS Multimeter. This multimeter measures the pressure in mV, it can be recalculate via this relation: 1mV is 6.8948 kPa.

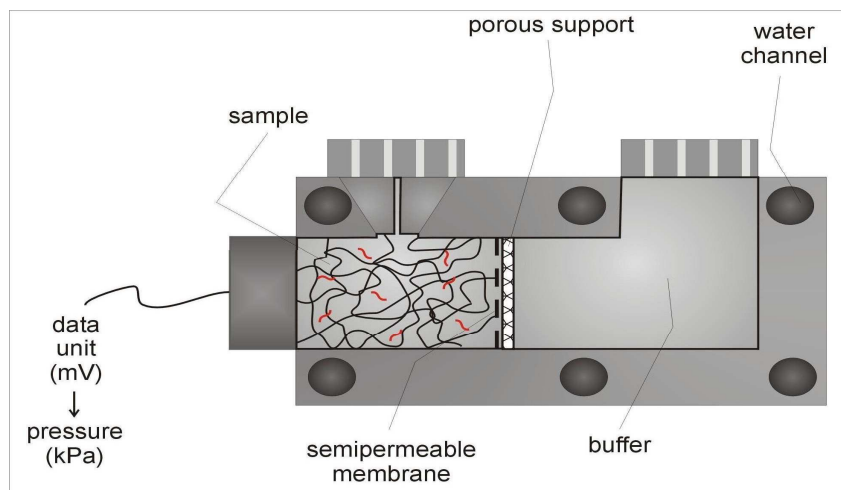


Figure 1.9: Schema of the home made pressure device

### ***Osmotic deswelling measurement***

The  $\pi_{sw}$  was also measured by osmotic deswelling measurements. It was performed on degrading PEG-HEMA gels according to a method described by Horkay and Zrinyi 16. Gel samples (PB, pH 7; 8.5) were put into semi permeable membrane (Spectra/Por®, Cellulose Ester Membrane, Molecular weight cut of  $500\text{g}\cdot\text{mol}^{-1}$ ) and dipped into PB with appropriate pH. The samples were let to degrade in  $37^\circ\text{C}$  for different time intervals (0 and 3 days). After degradation PB was removed and replaced by PEG solution in concentration range 15-30%. Samples were equilibrated in PEG solution for 7 days at  $4^\circ\text{C}$  to prevent degradation. Than samples were weighted (Mettler H45) and put into a vacuum oven to dry at  $50^\circ\text{C}$ . Samples were weighted again after two days of drying.

During equilibrium water from the gel goes through the membrane and PEG solution is diluted. 1ml of PEG solution from each concentration was dried in the



## Evaluation of dex-HEMA for controlled drug delivery

vacuum oven, weighted before and after the drying process. Then the exact pressure caused by PEG solution could be calculated by formula (1.2).

At equilibrium the  $\pi_{sw}$  of the gel is equal to the  $\pi_{osm}$  of PEG solution. The  $\pi_{osm}$  of PEG solution can be express by this formula:

$$\pi_{PEG} = \left[ \frac{1}{M_w} + A_2 \cdot c + A_3 \cdot c^2 \right] \cdot cRT \cdot 10 \quad (1.2)$$

Where R is the gas constant, T is absolute temperature, c is the PEG solution concentration ( $\text{g} \cdot (100\text{ml})^{-1}$ ),  $A_2$  and  $A_3$  are second and third virial coefficients. According to the data reported by Edmond and Ogston<sup>17</sup> for PEG ( $M_w = 20\,000 \text{ g} \cdot \text{mol}^{-1}$ )  $A_2 = 2.59 \cdot 10^{-5} (\text{mol} \cdot 10^{-2} \text{ml}) / \text{g}^{-2}$  and  $A_3 = 1.35 \cdot 10^{-6} (\text{mol} \cdot 10^4 \text{ml}) \cdot \text{g}^{-3}$ .

For calculation of the PEG-HEMA concentration was used this equation:

$$c = \frac{w_{PEG-HEMA}}{w_{PEG-HEMA} \cdot v_1 + \frac{w_{gel} - w_{PEG-HEMA}}{\rho}} \cdot 100 \quad (1.3)$$

Where  $w_{gel}$  is the weight of PEG-HEMA gel,  $w_{PEG-HEMA}$  is weight of PEG-HEMA determined after two days of drying the gel in a vacuum oven at  $50^\circ\text{C}$ .  $\rho$  is density of phosphate buffer ( $1,07 \text{ g} \cdot \text{ml}^{-1}$ ) and  $v_1 = 0,86 \text{ ml} \cdot \text{g}^{-1}$  and it is the specific volume of PEG-HEMA.

The polymer volume fraction of the gel was calculated from equation (4):

$$\phi = c \cdot v_1 \quad (1.4)$$

where c is the concentration of PEG-HEMA and  $v_1$  is its specific volume.

Calculated amount of PEG for concentration dissolved in phosphate buffer was used for osmotic deswelling measurement to mimic completely dissolved PEG-HEMA gel. The solution was put into the semi-permeable membrane (Spectra/Por®, Cellulose Ester Membrane, Molecular weight cut of  $500\text{g}\cdot\text{mol}^{-1}$ ) and surrounded by PEG solution in the same concentration range as PEG-HEMA gels. PEG solution was equilibrated at  $4\text{ }^{\circ}\text{C}$  for 7 days. Afterwards solution was weighted and dried in a vacuum oven for two days. Afterwards the samples were weighted again. Values were used to calculate concentration and volume fraction. The concentration of PEG solution was also checked as in the previous case.

### **1.2.6 Rheological Characterisation of Hydrogels**

Rheology studies the deformation and flow behaviour of the materials in liquid, melt or solid form. Deformation is the reaction of a material structure to an applied force. One of the main tasks of rheology is the description and classification of materials. According to rheology basis materials can be divided into the three main groups: viscous, elastic and visco-elastic materials. Most of the polymers and hydrogels come under the group of visco-elastic materials. It means that Hook's law can be applied and rheological methods are used for measuring  $\pi_{\text{el}}$ . In this experiment the control stress test is used, this means that stress is applied and the actual behaviour of the sample is directly measured.

Viscosity is the ability of a material to deform in a permanent way. Applied energy will not come back. The Newton's law of viscosimetry describes the flow behaviour of an ideal material in equation (1.5):

$$\tau = \eta \cdot \dot{\gamma} \tag{1.5}$$

$\tau$	shear stress	[Pa]
$\eta$	dynamic viscosity	[Pa.s]
$\dot{\gamma}$	share rate	[s <sup>-1</sup> ]

Shear stress is the ratio of applied force to area on which the force is applied. It can be expressed by this equation:

$$\tau = \frac{F}{A} \tag{1.6}$$

$\tau$	shear stress	[Pa]
F	force	[N]
A	area	[m <sup>2</sup> ]

Elasticity is the ability of a material structure to resist a distorting influence or stress and return to its original size and shape, when the stress is removed. Most solids are elastic for small deformations, when the stress exceeds a certain amount known as the elastic limit a permanent deformation is produced. The elasticity of a material is expressed by Young's modulus. This modulus relates the stiffness of the solid to applied energy.

$$\sigma = E \cdot \gamma$$

(1.7)

$\sigma$       tensile stress      [Pa]

$E$       Young's modulus [Pa]

$\gamma$       strain

Forces applied may lead to tensile or shear stresses and the tensile modulus  $E$  or the shear modulus  $G$  are the correlating factors. Then the Hook's law can be rewritten into this equation:

$$\tau = G^* \cdot \gamma$$

(1.8)

$\tau$       shear stress      [Pa]

$G^*$       complex modulus [Pa]

$\gamma$       strain

Figure 1.10 demonstrates the differences between elastic, viscous and visco-elastic behaviour.

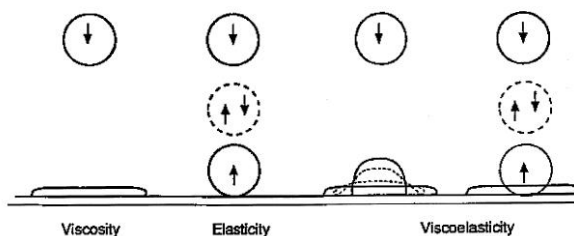


Figure 1.10: Viscous, elastic and viscoelastic behaviour.

Signals applied by a rheometer can be stepped-ramp, jump or co-sinus. Deformation of these hydrogels is measured by using oscillatory test or it can be called dynamic test. The stress is applied as sinusoidal time function.

$$\tau = \tau_0 \cdot \sin(\omega t) \quad (1.9)$$

$$\omega = 2\pi \cdot f \quad (1.10)$$

$\omega$  angular frequency [rad.s<sup>-1</sup>]

f frequency [Hz]

The oscillation mode at 1 Hz in the linear viscoelastic region of these gels was used by applying a constant strain of 0.5%. The resulting strain was measured with strain amplitude  $\gamma_0$  and the phase angle  $\delta$ . The resulting equation is:

$$\gamma = \gamma_0 \cdot \sin(\omega t + \delta) \quad (1.11)$$

Initial shear stress used as input and the result strain, which is out of phase, are shown in

Figure 1.11. Using formula (1.17) the complex modulus can be calculated from known initial stress and measured value of deformation.

Afterwards the complex modulus is used to express storage modulus  $G'$  (equation (1.12) and loss modulus  $G''$  (equation (1.13)).

$$G' = G^* \cdot \cos \delta$$

(1.12)

$$G'' = G^* \cdot \sin \delta$$

(1.13)

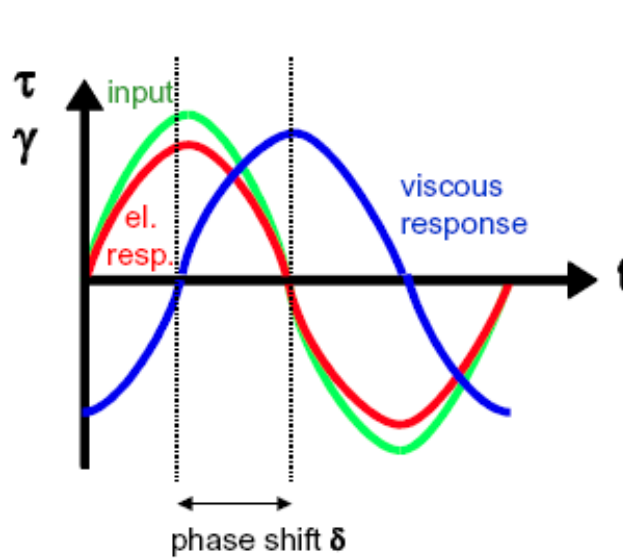


Figure 1.11: Diagram of stress and strain as a function of the time

$G'$  represents storage modulus. It shows the elastic storage of energy or how well structured the material is. If the sample is well build the storage modulus is high, but if it is being destroyed the modulus will decrease. If the sample is purely elastic the phase shift angle  $\delta$  is zero and the storage modulus can be measured.

Equation shows loss modulus. It hints at the fact that the energy, which has been used to initiate flow, is irreversibly lost having been transformed into shear heat. The

phase shift angle is  $90^\circ$  and it means that the sample is purely viscous. We transferred storage modulus to elastic pressure by using formula.

$$G' = -\pi_{el} \quad (1.14)$$

Rheological measurements were performed by an AR 1000-N controlled stress rheometer from TA-Instruments. Rheometer consists from an electronically controlled induction motor. Motor provides torque over a very wide range. It provides that a wide variety of materials can be measured from very low viscosity materials to polymer melts and solids. The air bearing uses air as a lubricating medium. This allows virtually friction-free application of torque. Even turbulent flow in the assembly is sufficient to make the bearing rotate.

The Peltier plate is temperature controlled. It ensures via thermo-electric effect the rapid and accurate control of heating and cooling. This bottom plate was covered with a Plexiglas plate with roughened surface. Water is used as a temperature controlled external fluid reservoir for heating and cooling. Next part is the geometry. Parallel plate, cone or concentric cylinders are geometries that can be chosen. The acrylic parallel top plate, with diameter 2cm, was chosen for these measurements and to avoid slippage it was covered by sandpaper.

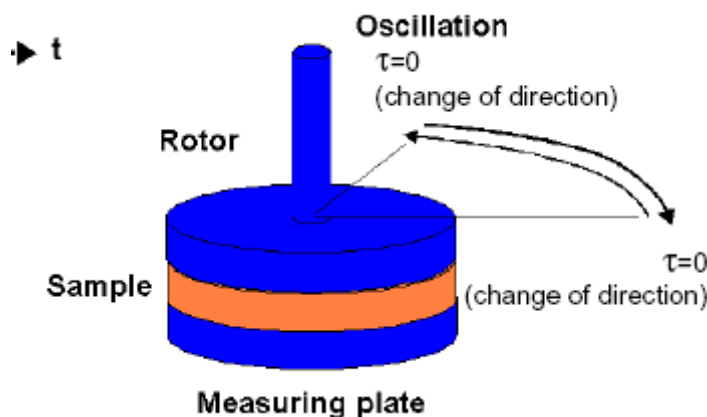


Figure 1.12: Schematic picture of oscillation rheological measurement.

### ***Refractometry***

The concentration of free dextran in dex-HEMA hydrogels was determined from a release experiment performed in phosphate buffer, pH 7 and at 37°C. 2 ml sample was taken every second day and replaced with the same amount of fresh buffer.

The amount of dextran chains in the solution was measured by differential refractive index. This measuring equipment consists of high-pressure pump (Waters 510), an injector (Waters U6K) and differential refractometer (Waters 410). Flow rate of 0.5 ml per minute was applied and 250 µl of sample was injected.

The principle of this method is based on a refractive index. The index is constant and unique characteristic of each pure compound and is defined as the ratio of the velocity of electromagnetic radiation in a vacuum to its velocity in the medium of interest. It is known as a Snell's law.

$$n = \frac{\Phi_v}{\Phi_m} = \frac{\sin i}{\sin r} \tag{1.15}$$

The rays of the light pass from one medium with refractive index  $n_1$  to second one with refractive index  $n_2$ . The extent of the deflection is a function of each medium refractive index and the refractive index depends on the solutes concentration in the solvent. Results are shown in the chromatogram. Peak height is shown in function of time. The dex-HEMA concentration is calculated from a calibration curve. Dextran concentration is between 0 and 0,09.



### 1.3 Results and discussion

It is necessary to activate HEMA with CDI to couple HEMA with dextrane. Activated HEMA (HEMA-Cl) was determined by NMR (Varian Mercury 300 NMR Spectrometer with an Oxford Instruments Ltd. superconducting magnet, a 300 MHz NMR spectrometer and a Sun Ultra 5 workstation). Data from NMR spectroscopy charts were used to calculate purity and activation of HEMA-Cl.

Activation (a) was calculated from 
$$a = \frac{(H_c + H_d)/4}{(H_{a'} + H_{a''} + H_b)/5}$$

(1.16):

$$a = \frac{(H_c + H_d)/4}{(H_{a'} + H_{a''} + H_b)/5} \tag{1.16}$$

Where  $H_x$  are stands for the area under the peak of an appropriate proton. It was calculated by integration.

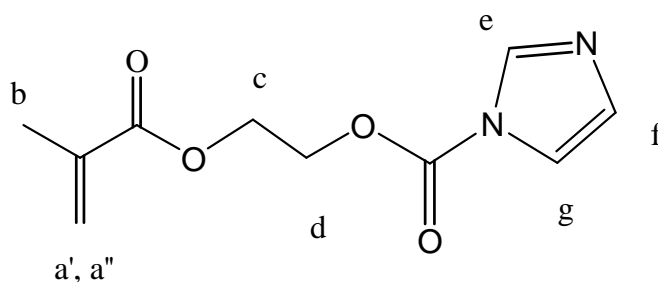


Figure 1.13: Molecule of HEMA-Cl with identified protons.

Each proton in a molecule has a specific chemical shift. Protons are identified according Figure 1.13 and relevant values were found in NMR spectrum for HEMA-

CI. The peaks of the appropriate protons can be found in the spectrum under the following values:  $H_{a'}$  at 6.11 ppm;  $H_{a''}$  5.6 ppm;  $H_b$  1.92 ppm;  $H_c$  4.48 ppm and  $H_d$  4.64 ppm. The integrated values of the peaks were used to calculate activity by equation

(1.16).

$$a = \frac{(13.31 + 13.05) / 4}{(5.93 + 6.11 + 17.42) / 5} = 1.12$$

Activation (a) for HEMA-CI was 1.12.

Possible impurities in HEMA-CI might be DCM and imidazole, coming from the synthesis. These impurities have to be taken into account for further calculations.

Purity (p) was calculated from equation (1.17):

$$p = \frac{((H_{a'} + H_{a''}) / 2) \cdot 224.2}{((H_{a'} + H_{a''}) / 2) \cdot 224.2 + H_{(imidazole)} \cdot 93 + (H_{(DCM)} / 2) \cdot 84.93} \cdot a \quad (1.17)$$

The values of the  $H_x$  for purity calculation were also identified according to Figure 1.13. Chemical shift for imidazole and DCM are respectively  $H_{imidazole}$  7,1 and 7,7ppm and  $H_{DCM}$  at 5,3ppm.

$$p = \frac{((5.93 + 6.11) / 2) \cdot 224.2}{((5.93 + 6.11) / 2) \cdot 224.2 + (0.28 + 1.21) \cdot 93 + (0.53 / 2) \cdot 84.93} \cdot 1.12 = 1$$

Purity of HEMA-CI was 1 it means 100 %.

HEMA-CI was weighted to calculate efficiency of activation of HEMA by CDI. 5.81 g (44.66 mmol) of HEMA was added to activate. Weight of HEMA-CI was 8,23g (36.71mmol). Efficiency of activation was calculated from:

$$\varepsilon = \frac{n_{HEMA-CI}}{n_{HEMA}} \quad (1.18)$$

$$\varepsilon = \frac{36.71}{44.66} = 0.82$$

Efficiency of activation reaction was 0.82, it is 82 %.

Purity was needed to calculate the exact amount of HEMA-CI, which was added to react with 50g of dextran. Calculating the weight of HEMA-CI was done by using equation (1.19) :

$$w_{HEMA-CI} = \frac{w_{dextran}}{M_{w,glucose}} \cdot \frac{DS}{100} \cdot M_{w,HEMA-CI} \cdot \frac{1}{p} \cdot \frac{1}{\varepsilon} \quad (1.19)$$

p          purity

ε          efficiency of coupling HEMA-CI with dextran. Efficiency is known and the value is 85 %.

$$w_{HEMA-CI} = \frac{50}{162} \cdot \frac{2.5}{100} \cdot 224.2 \cdot \frac{1}{1} \cdot \frac{1}{0.85} = 2.034g$$

2,034 g of activated HEMA was added to react with 50 g of dextran. Small amount of produced dex-HEMA was dissolved in  $_2H_2O$  and determined by  $1H-NMR$ . The integral values of areas under the peaks were taken from NMR spectrum of dex-HEMA Figure (19) and assigned to relevant protons according Figure 1.14.

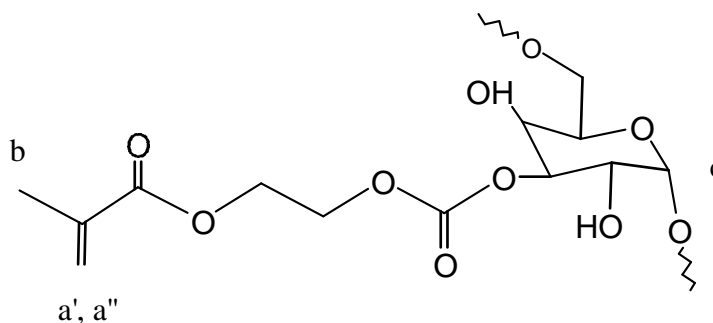


Figure 1.14: Molecule dex-HEMA with identified protons.

These values were used to calculate DS of dex-HEMA. DS was calculated by using formula (1.5):

$$DS = \frac{(H_{a'} + H_{a''})/2}{0.96 \cdot H_c} \cdot 100 \quad (1.20)$$

The value 0.96 is a correction coefficient for 4 % present -1,4-cross-links, which can make nicks on the chains in polymer structure. Integrals of the area under the peak for protons in dex-HEMA molecule can be found on the chemical shift scale under these values: Ha' 5.75 ppm and Ha'' 6.2 ppm and H<sub>c</sub> 5 ppm.

$$DS = \frac{(0.09 + 0.09)/2}{0.96 \cdot 5.74} \cdot 100 = 1,63$$

Synthesised dex-HEMA has DS 1,63. This value of DS is too low, it means that there are not enough HEMA groups to make cross-links and the product does not polymerise.

Two reasons can be found for this low value of DS. At first, during stirring for four days, complete absence of water, coming from surrounding air could not be guaranteed. The reason for this was a failing nitrogen system, so water could come in. Water is in competition with HEMA-Cl for coupling with dextrane. So when water is present the coupling of HEMA-Cl to dextrane is lower as expected. The second reason

## Evaluation of dex-HEMA for controlled drug delivery

was that the reaction mixture was brought to pH 7 at the end of the reaction after 4 days. Used pH should be between 2 and 5. The reason for this is that decoupling shows a minimum at pH 4 and is ten times higher at pH 7. So during dialysis the conditions were good to decouple HEMA from dextrane. The DS of produced dex-HEMA is lower than expected DS. Expected DS 2.5 was on the border of interval DS which can be synthesized.

Samples of dex-HEMA were investigated by rheology.  $G'$  was regularly measured during degradation time. Effect of different factor was study: way of polymerisation, Mw of dex-HEMA and concentration of dex-HEMA in the gel.

Samples (20%, dex-HEMA,  $5000\text{g}\cdot\text{mol}^{-1}$ ) were prepared by UV and chemical polymerisation. Their  $G'$  was measured during 60 days and data are presented in Figure 1.15, where two curves represent variation of the  $G'$  during degradation time and as one can see there is not different in measured  $G'$ .

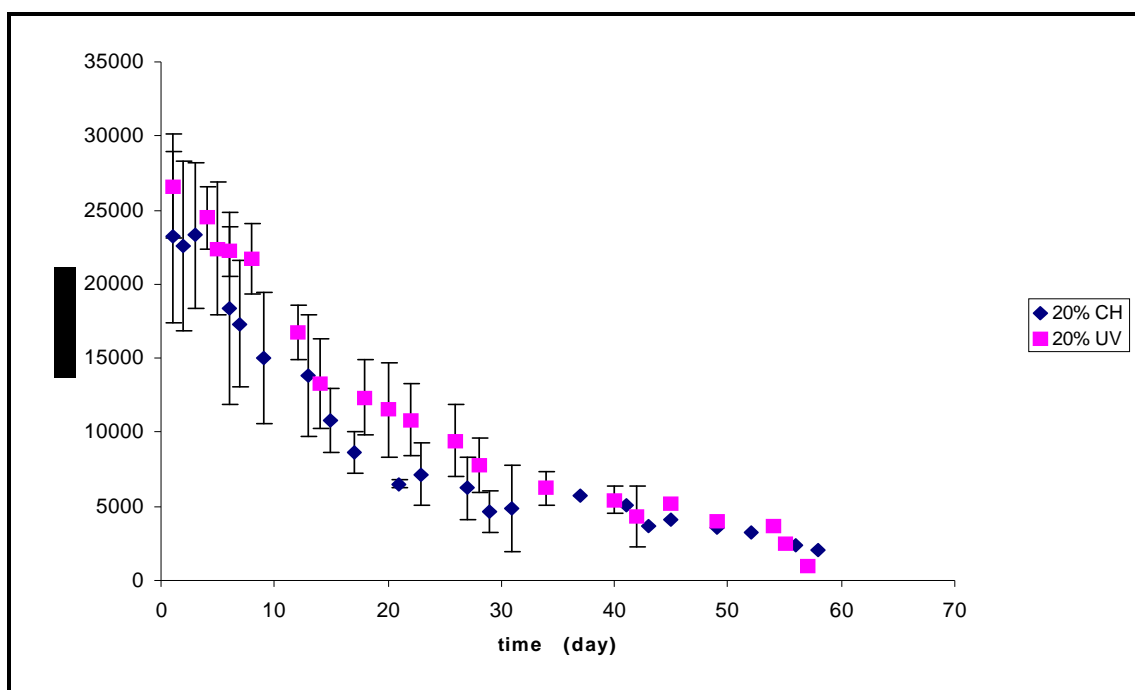


Figure 1.15:  $G'$  during degradation time. Two curves represent different way of polymerisation

Photoinitiator Irgacure 2959 is biocompatible with fibroblast cells. Study shows that photoinitiator Irgacure 2959 is biocompatible in concentrations lower than 0.5%<sup>15</sup>. In pursuance of these results it was decided to use UV polymerisation for preparation other samples.

The influence of the polymerisation type was also study by following dextran release. 20% dex-HEMA gels were prepared by both described ways of polymerisation and let to degrade in PB (pH 7) and at 37°C. During the degradation process free dextran molecules leave the gel structure into the surrounded buffer. The concentration of free dextran molecules in buffer was measured.

The dex-HEMA concentration was calculated from the height of the peak using a calibration curve. The height of the peak was corrected by a linear function, which goes through the last and lowest point in the curve. Concentration for standard curves was between 0 and 0.09g. (100 ml)<sup>-1</sup>. The reproducibility of this measurement in this concentration range, which is presented here is very good, the correlations coefficient for linear regression exceeds 0.98 for each standard curve. Standard curves are presented in Figure 1.16 as peak height as a function of concentration.

When the sample for dextran release was taken (2 ml), fresh buffer was added into the cup. It means that real concentration was diluted. Measured concentrations had to be recalculated by equation (1.21). Real concentrations are shown as a function of degradation time in Figure 1.16.

$$C_r = C_b + \left(1 - \frac{4}{5}\right)C_m \tag{1.21}$$

$C_r$  real concentration [g.(100 ml)<sup>-1</sup>]

## Evaluation of dex-HEMA for controlled drug delivery

$C_b$  concentration of the sample before [g.(100 ml)<sup>-1</sup>]

$C_m$  measured concentration [g.(100 ml)<sup>-1</sup>]

As one can see there is no difference between these two curves, which represent different types of polymerisation, so the samples did not show difference in dextran release and it can be concluded that the way of polymerisation does not influence the structure of the gel. In both types polymerisation, free dextran molecules can release by some way and in the same time.

Both  $G'$  and dextrane release show that the way of polymerisation does not influence degradation process of the dex-HEMA gels.

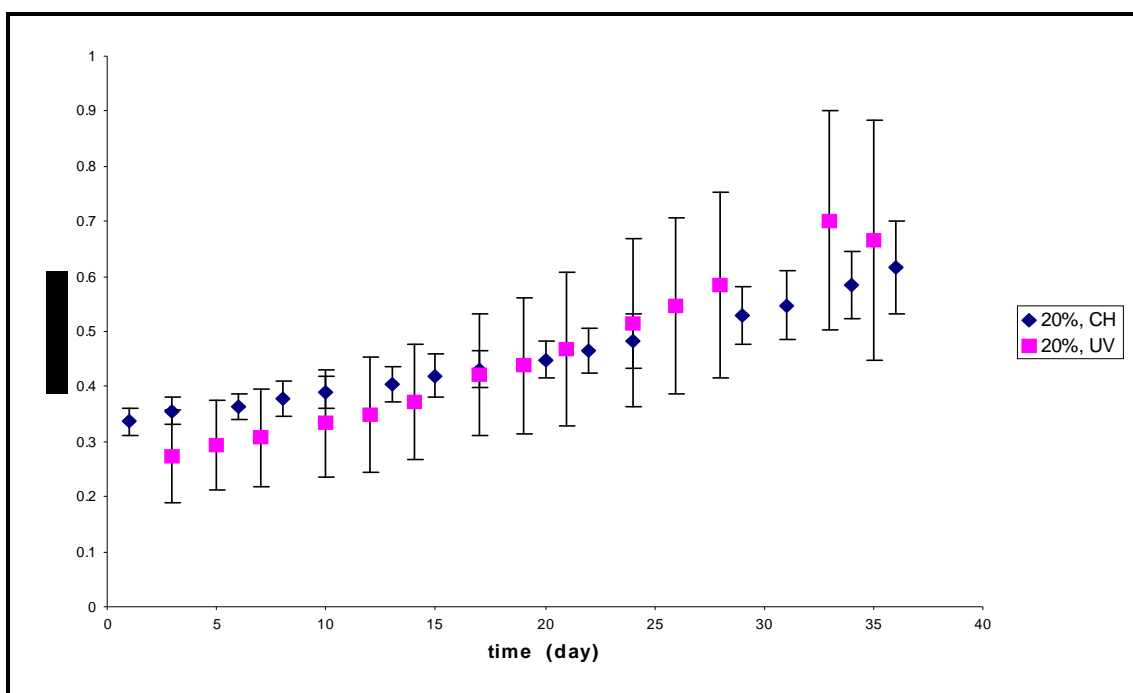


*Figure 1.16: Concentration of free dextran molecules in surrounded PB as a function of degradation time. Two curves represent different way of polymerisation and its influent on degradation process.*

Influence of molecular weight was investigated on 25 % dex-HEMA gels. Dex-HEMA gels with molecular weight  $5\,000\text{g.mol}^{-1}$  and  $19\,000\text{g.mol}^{-1}$  were compared. Figure 1.17 presents the variation of  $G'$  of these gels obtained from rheological measurement as a function of degradation time.

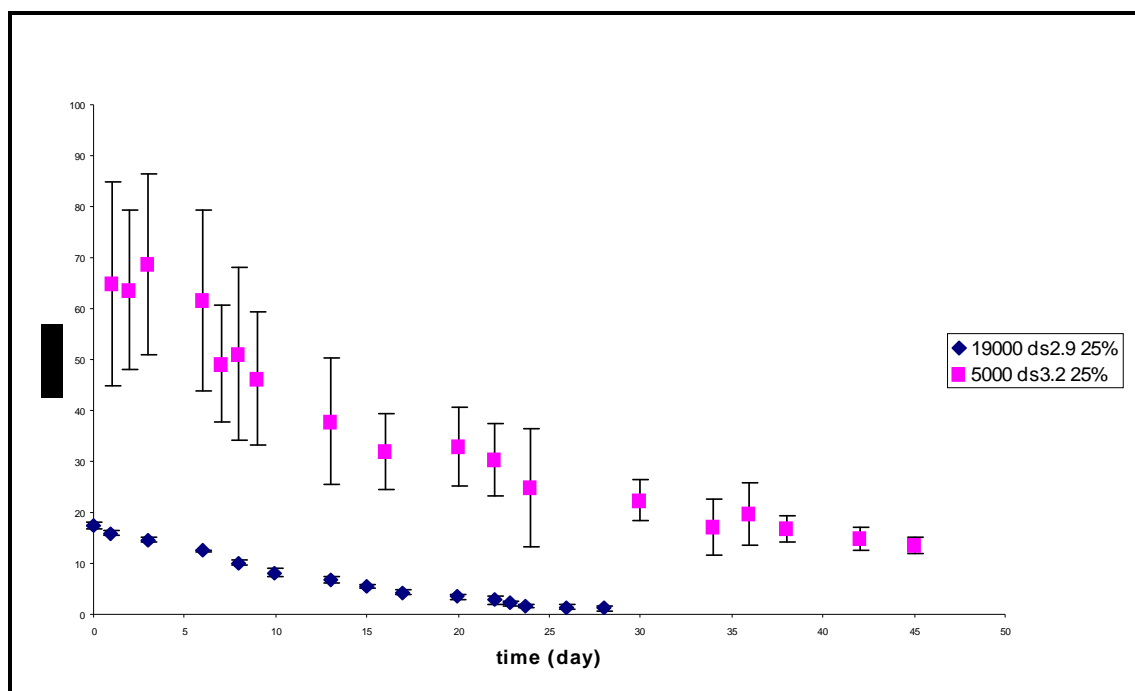


Figure 1.17: Variation of  $G'$  is presented as a function of degradation time. Two curves represent dex-HEMA gels with different molecular weight: dex-HEMA  $5\,000\text{g.mol}^{-1}$  and dex-HEMA  $19\,000\text{g.mol}^{-1}$ .

Values of  $G'$  obtained from measuring dex-HEMA with  $M_w\,5000\text{g.mol}^{-1}$  are almost four times higher than the values from measuring dex-HEMA  $19\,000\text{g.mol}^{-1}$ . When molecular weights are compared the ratio is also about four.

Reason can be found in non-ideal structure of polymer network. In real networks solfraction, loose ends and loops can be found. These irregularities of network are not elastic and do not influence the elastic behaviour of the whole network. So molecular weight must be corrected for this “non-elastic” fraction.  $c'$  is the elastic network



## Evaluation of dex-HEMA for controlled drug delivery

concentration. This means the total concentration without the polymer concentration of the non-elastic polymer parts. Elastic network concentration is calculated by formula:

$$c'' = (1 - w_s)c \left[ 1 - \frac{2M_c}{M} \right] \quad (1.22)$$

$1-w_s$	correction for sol fraction	
$c$	total polymer concentration	[g.(100 ml) <sup>-1</sup> ]
$1 - \frac{2M_c}{M}$	correction for loose ends	

A network can have too extreme types of behaviour: affine and phantom. If the cross-links in network do not move any more after applying an external force, than the behaviour is completely elastic and it is called affine and  $G'$  can be calculated by formula (1.23):

$$G' = uRT \quad (1.23)$$

$u$	mol network strands per volume unit,	$u = \frac{c''}{M_c}$ [mol.ml <sup>-1</sup> ]
$R$	gas constant	[g.mol <sup>-1</sup> .K <sup>-1</sup> ]
$T$	absolute temperature	[K]

The second extreme behaviour is when cross-links and molecules can move after applying the external force, the behaviour becomes more viscous and it is called phantom behaviour. Equation (1.24) shows  $G'$  for hydrogels with extreme phantom behaviour:

$$G' = uRT - \mu RT = (u - \mu)RT = \left(1 - \frac{2}{f}\right)uRT \quad (1.24)$$

$\mu$  mol cross-links per volume unit

$f$  functionality, this means the number of strand leaving from one cross link.

$$\mu = \frac{2}{f}u \quad (1.25)$$

Every real network is something between these two possibilities. When applied force is lower, network behaves as affine, but when applied force is higher, than real network behaves as phantom. Formula (1.23) for  $G'$  can be correct again to formula (1.26):

$$G' = \left(1 - \frac{2h}{f}\right)uRT \quad (1.26)$$

$$u = \frac{c''}{M_c} \quad (1.27)$$

$$G' = \left(1 - \frac{2h}{f}\right)\frac{c''}{M_c}RT \quad (1.28)$$

Based on these results Flory's formula can be use to explain influence of molecular weigh.

$$G' = \left(1 - \frac{2h}{f}\right) \frac{c(1 - w_s) \left[1 - \frac{2M_c}{M}\right]}{M_c} RT \quad (1.29)$$

This formula can be used only in case, if the functionality is 4. So this formula is extended by Te Nijenhuis.

The Nijenhuis states that  $M_n''$  should be used in stead of  $M_n$ .  $M_n''$  is larger than  $M_n$  because his theory is that larger polymers will take place in the network more easy than smaller polymers. Smaller polymers have bigger chance to come in the solfraction. There is fractionation of the polymer chains. It is difficult to calculate  $M_n''$  and it is based on statistics.  $M_n''$  and  $M_c$  were calculated in function of solfraction by Te Nijenhuis. This gives the final formula:

$$G_e = \left(1 - h \frac{2}{f}\right) \frac{c(1 - w_s^{0.5}) \left[ \frac{1 - w_s^{0.5f}}{1 - w_s^{0.5f-1}} \cdot w_s^{-0.5} \cdot \frac{f-2}{f} - 1 \right]}{M_n} RT \quad (1.30)$$

As one can see, molecular weight is in denominator of this equation. If molecular weight of dex-HEMA 5000 is almost four times lower than in case of dex-HEMA 19 000 it can be expected that  $G'$  of dex-HEMA 5000 should be four times higher than  $G'$  of second one and this is shown in . It is not clear whether this theory completely explains our findings. More research is needed.

Influence of molecular weight was also study by refractometry. 25% dex-HEMA gels were prepared by UV polymerisation and again let to degrade in PB (pH 7) at 37°C. Afterwards the concentration of free dextran chains in surrounded buffer was

measured by Refractometer. Real concentration were calculated from peak height and recalculated from the measured concentration, like it is explained before. Data were shown in Figure 1.18 as a function of degradation time.

As one can see there is almost no other dextran release than solfraction. There is just little linear increase in comparison with dex-HEMA 19000. This can also be seen in the structure of dex-HEMA 5000 hydrogels. After 50 days it is still in one piece, while dex-HEMA is completely dissolved within 30 days. The reason for this slower release/degradation is still yet not clear for us.

The last investigated factor, which can influence degradation process of dex-HEMA gel, is concentration. Gel samples prepared in three different concentrations were studied (20%, 25% and 30% of dex-HEMA). Samples were prepared by UV polymerisation and tested rheologically during the degradation process. In Figure 1.19 the variation of  $G'$  is presented as a function of degradation time. Three curves represent influence of concentration dex-HEMA in gel.

The Figure 1.19 shows that the higher dex-HEMA concentration the higher  $G'$  can be measured.

The cross-links are carbon ester links formed between the methacrylate group and the dextran molecule. The initial concentration influences the density of cross-links, the higher initial dex-HEMA concentration, and the higher density of cross-links. The degradation process is caused by hydrolysis of these links. The degradation process is gradual and slow. If the link is destroyed it does not mean that the molecule is free, it can be attached on another end in the network or it can be closed in a structure of the other bounded molecules. The denser structure is resulted in the higher initial value of  $G'$ , because the structure is harder and it is more resistant to the applied stress. The degradation process of the gel with higher initial concentration is longer and decrease of  $G'$  is slower than in the case of the gel with lower concentration of dex-HEMA.

## Evaluation of dex-HEMA for controlled drug delivery

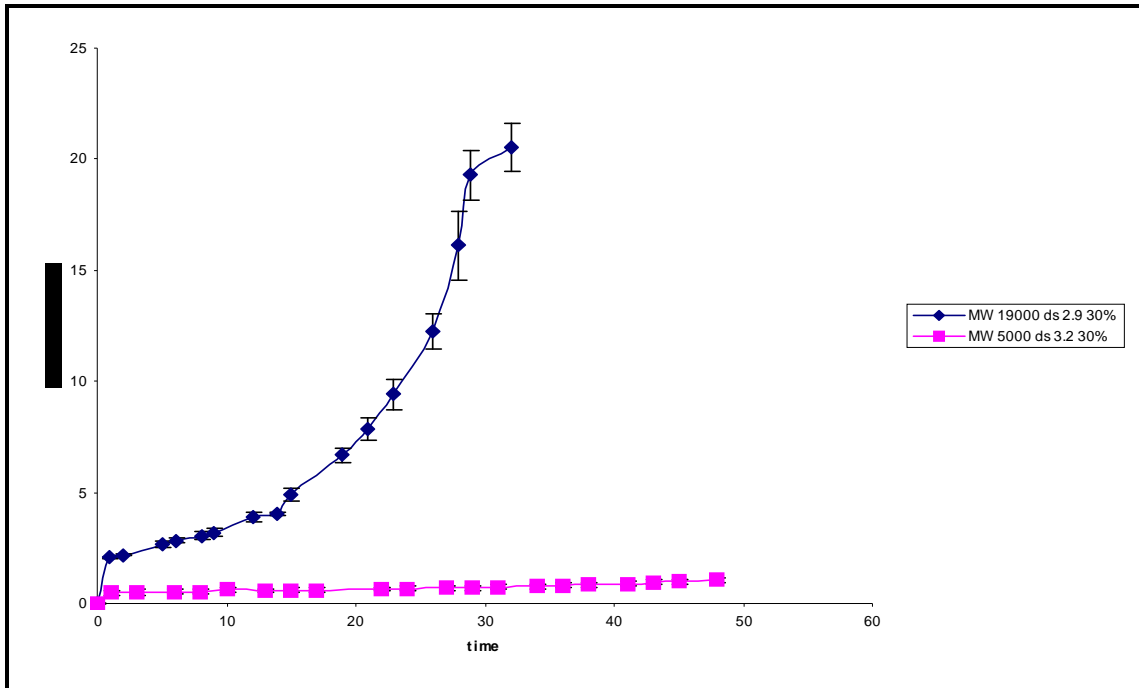


Figure 1.18: Concentration of free dextran chains in surrounded PB as a function of degradation time. Two curves represent gels with different molecular weight.

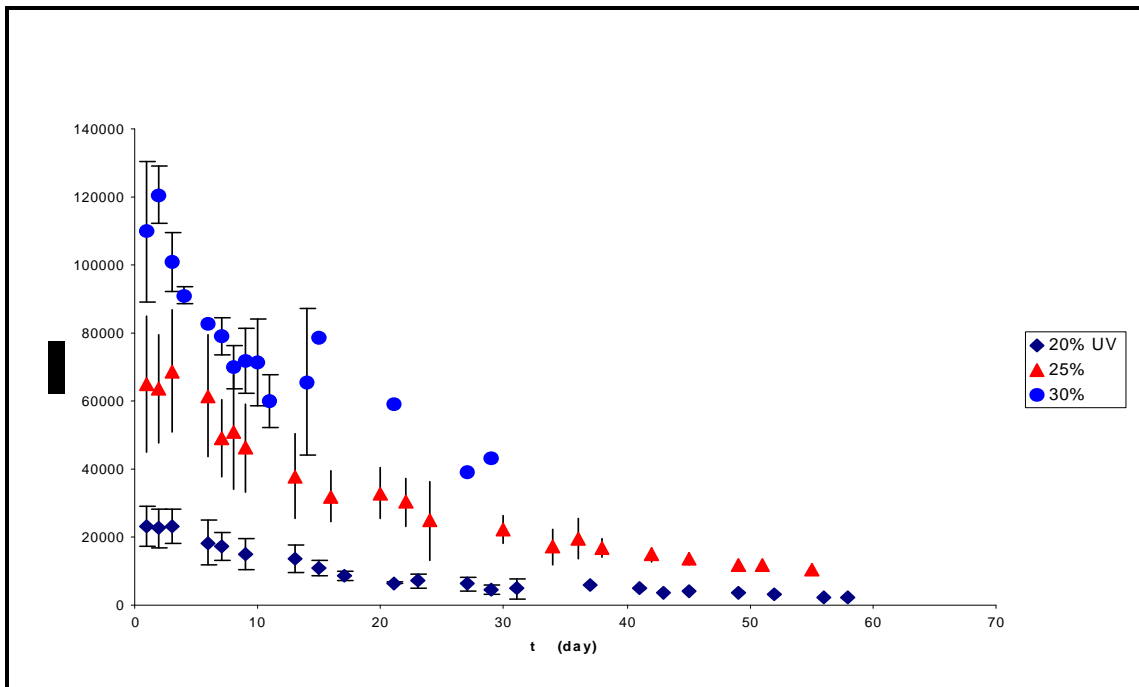


Figure 1.19:  $G'$  as a function of degradation time. Three curves represent different initial dex-HEMA concentration and its influence on  $G'$ .

The fact that the initial concentration influences the degradation process was also measured by dextran release measurement. The described process of measuring dextran release and calculation of concentration was followed again and real concentrations are presented in Figure 1.20 as a function of degradation time.

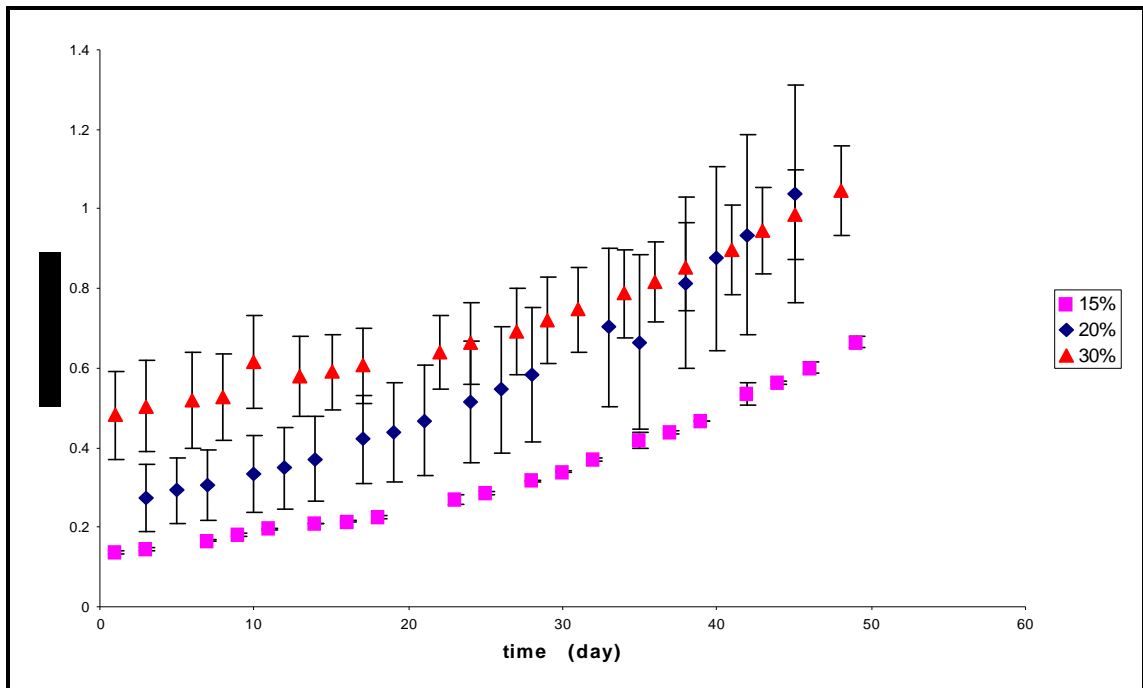


Figure 1.20: Concentration of free dextran molecules in surrounded buffer as a function of degradation time. Curves represent different initial concentration of dex-HEMA.

From Figure 1.20 one can derive that the hydrogels are not completely degraded after 50 days. Even not close to complete degradation. We know this, because in the end, the final concentration of dextran in the surrounding medium should be equal to the initial concentration of polymer solution before polymerisation. You can see this because the samples for dextran release are still intact.

Measured initial concentration of free dextran chains in surrounded buffer is higher with higher initial concentration of dex-HEMA in the gel. When the initial concentration of dex-HEMA is higher there is a higher possibility of present

solfraction, it is not attached in molecule structure, and can go immediately out of the gel structure into surrounding buffer.

Afterwards release of free dextran chains starts. We expect that dextran release from the gels with higher concentration takes longer time, because of the stronger molecular structure of the gel. Before starting the measurement in the pressure device, it is better to check the membrane, whether it is impermeable for free PEG molecules. Normally one uses a molecular weight which is half of the value of the molecular weight of produced molecules.

The membrane (Spectra/Por®, size 7 and molecular weight cut off 2000 D) was checked with a 15% PEG solution ( $M_w = 4\,000\text{g}\cdot\text{mol}^{-1}$ ). Pressure was measured in pressure device for 18 days. Pressure values were shown in Figure 1.21 as a function of time. It is shown that pressure is lowering during this time; it means that this membrane is permeable for free PEG molecules; they can pass the membrane and leave the sample chamber.

Afterwards membrane (Spectra/Por®, size 7 and molecular weight cut off 500 D) was checked. As one can also see in Figure 1.21 after initial increase the pressure is constant for the following 40 hours. Free molecules of PEG can not go through the membrane and stay in the sample chamber.

According this results, the membrane with molecular weight cut off  $500\text{g}\cdot\text{mol}^{-1}$  was used for following measurements with PEG-HEMA ( $M_w = 4\,000\text{g}\cdot\text{mol}^{-1}$ ).

25% PEG-HEMA ( $M_w = 4\,000\text{g}\cdot\text{mol}^{-1}$ ) was prepared by UV polymerisation at pH 8,5 in the sample chamber of the pressure device. Swelling pressure during degradation process was investigated by pressure device.

Recent studies investigated that the swelling pressure slightly increase during the first days of degradation but close to the end of the degradation process sudden increase of the pressure was noticed.

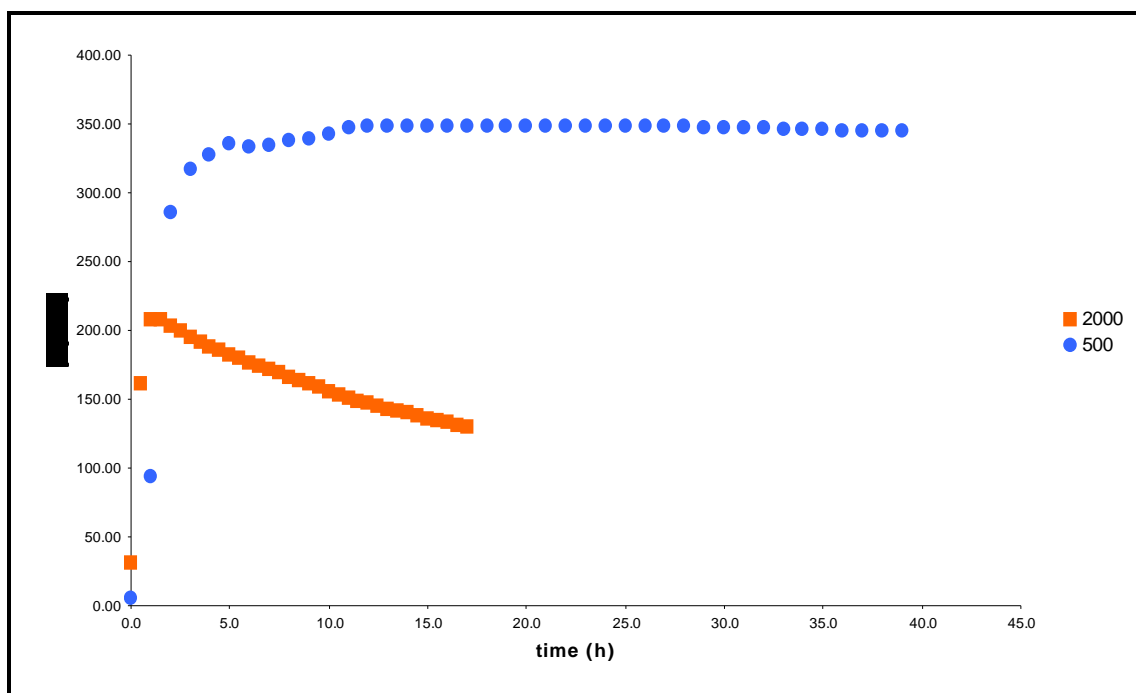


Figure 1.21: Pressure as a function of time. Two curves represent pressure device measurement with two membranes: membrane with molecular weight cut off 2000 and 500g.mol<sup>-1</sup>.

The same behaviour was expected in the case of 25% PEG-HEMA gel. Measurement takes ten days now and as one can see in the Figure 1.22 after initial increase the pressure is nearly constant for these ten days. We expect a sudden increase of the swelling pressure in following days.

The influence of pH on degradation process was investigated on 25% PEG-HEMA gels by osmotic deswelling. PEG-HEMA was dissolved in PB pH 7 or 8.5 and let to polymerise by UV. Samples were let to degrade in corresponding buffer at 37°C. The degradation process was done at different time of degradation (0 and 3 days). Fully degraded PEG-HEMA was also investigated and data were compared. The polymer volume fraction and corresponding swelling pressure were calculated by formulas (1.2, 3 and 4) and the swelling pressure is shown in the **Chyba! Nenalezen zdroj odkazů.** as a function of polymer fraction  $\varphi$ .



## Evaluation of dex-HEMA for controlled drug delivery

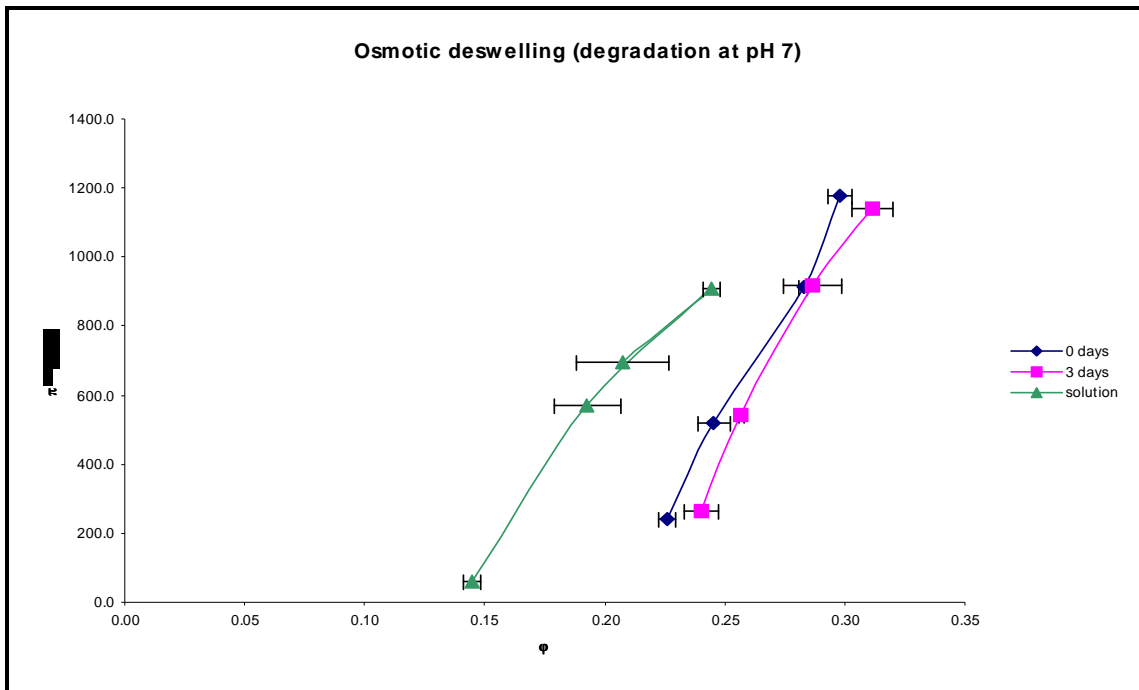


Figure 1.22: Pressure of degrading PEG-HEMA gel as a function of time, measured by pressure device.

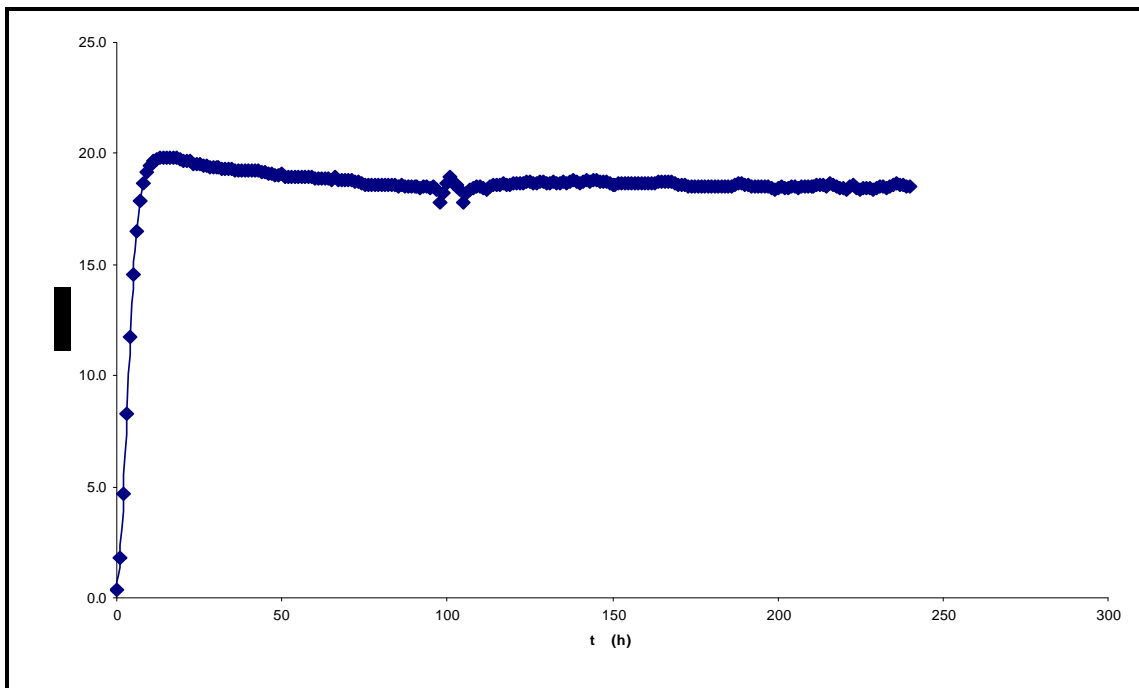


Figure 1.23: Swelling pressure as a function of polymer fraction. Graf shows influence of buffer pH (7 and 8.5) as a function of degradation time.

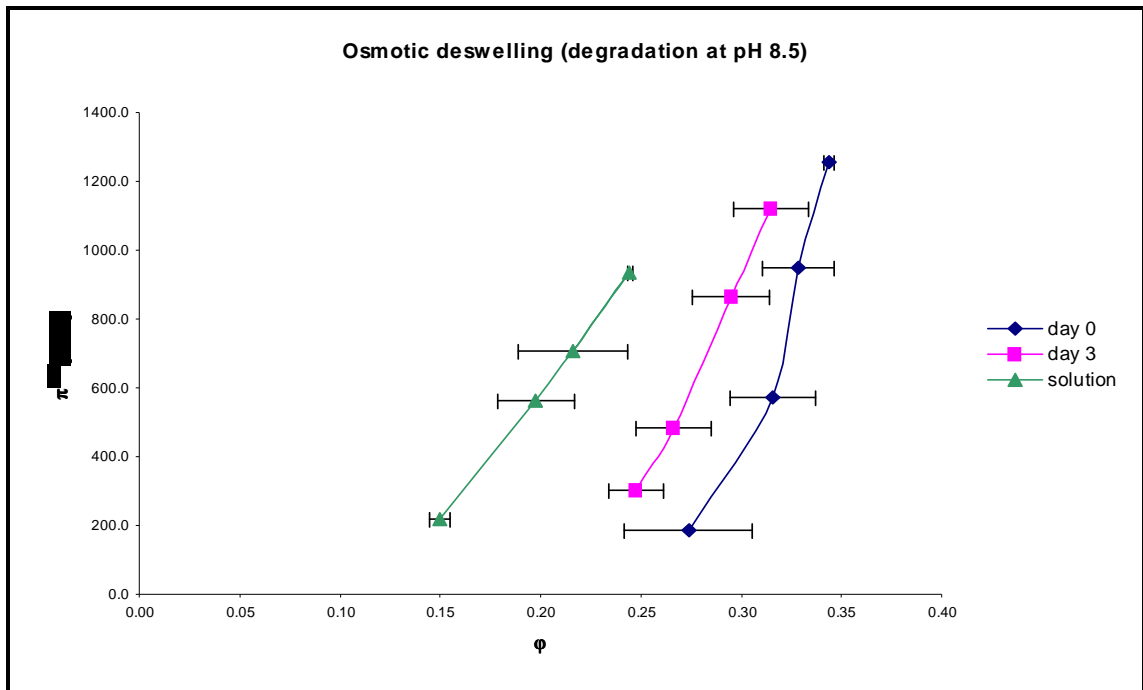


Figure 1.24: Swelling pressure as a function of polymer fraction. Graf shows influence of buffer pH (7 and 8.5) as a function of degradation time.

In Figure 1.24, results from osmotic deswelling experiments are shown as function of degradation time and degradation pH. One should look at constant  $\phi$  and compare pressure at different degradation times.

One can see that swelling pressure growing up during degradation of the gel. That is what we expect. The swelling pressure depends on the osmotic pressure according formula (1.1) and the osmotic pressure depends on the number of molecules by formula (1.2). In the beginning the hydrogel can be seen as one molecule, so the osmotic pressure is the lowest. During degradation free molecules are produced and molecule structure of the gel becomes destroyed, it results in increasing osmotic pressure. It can be seen after 3 days of degradation.

When the free molecules are produced, interactions between polymer molecules and between polymer/solution molecules are changed during degradation. This influences

equation (1.2), because virial coefficients which represent solvent/polymer interactions change.

The second conclusion is that at pH 8.5 degradation process is faster and osmotic pressure increases quicker. This was expected and reason can be found that HO-groups mediate hydrolysis of cross-links in hydrogel structure. This process is shown in Figure 1.25.

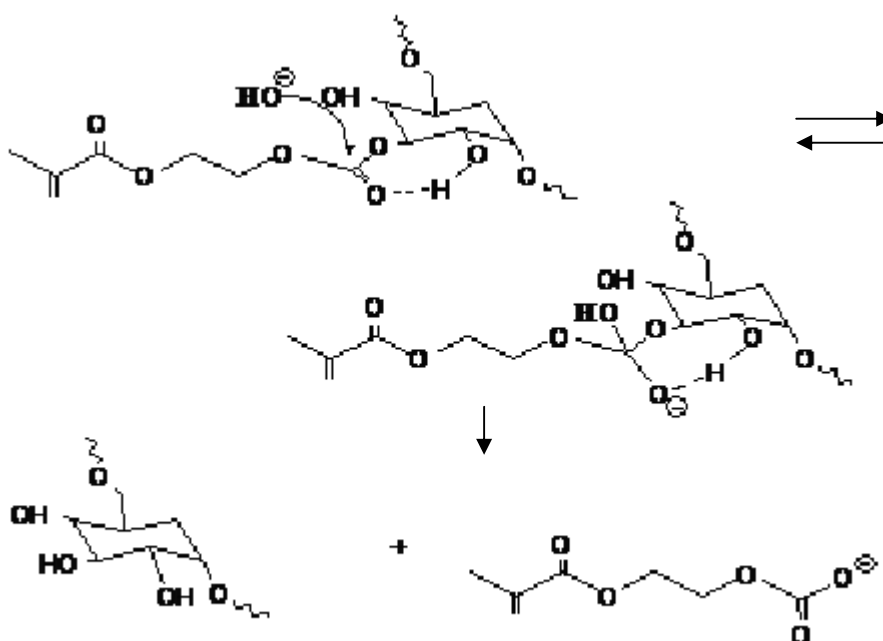


Figure 1.25: Reaction mechanism for alkaline hydrolysis of dex-HEMA.

## 1.4 Conclusions

Reaction of synthesis dex-HEMA has to be carried out under completely nitrogen atmosphere to avoid coupling with water from surrounded air.

Expected and calculated values of DS have to be higher than value 2.5, which is on the lowest border. Suitable pH of the reaction mixture on the end of reaction process should be between 2 and 5.

This study was performed to investigate effect of different factors (way of polymerisation, molecular weight, initial concentration of dex-HEMA and pH) on the swelling pressure of dex-HEMA or PEG-HEMA gels during degradation process.

Cross-links in dex-HEMA network are hydrolysable carbonate ester bonds between methacrylate groups and dextran molecules. It is demonstrate by rheological and dextran release measurements that polymerisation type does not influence the degradation process of dex-HEMA hydrogels. Based on the fact that the photoinitiator of the photo polymerisation reaction is biocompatible in concentrations lower than 0.5% (it was used 0.02%), it was decided to use UV polymerisation for following preparations.

Molecular weight of dex-HEMA influences degradation process. It was investigate by rheology measurement. The almost four times higher molecular weight results in four time lower initial value of  $G'$ . Also influence of molecular weight on dextran release from hydrogel structure was investigated. Reasons were found in non-ideal structure of polymer network, which contains non-elastic parts. Flory's and Te Nijenhuis theories were used to understand this influence, but it is not clear whether these theories completely explain our findings. More research in this problematic is need.

Third investigated factor, initial dex-HEMA concentration was study by rheology and dextran release. The higher initial concentration results in stronger structure of the gel, so  $G'$  is higher. But higher initial concentration brings higher concentration of sol fraction, it was investigated by dextran release, and it results in higher initial concentration free dextran chains in surrounded buffer. Afterwards release of free

dextran molecules, which were attached in network, is harder from the denser structure of the gel and it takes longer time to complete degradation.

The influence of pH on the osmotic pressure during degradation was studied on PEG-HEMA gel, prepared by UV polymerisation. We can conclude that at higher pH more hydrolysis take place of cross-links between PEG and hydroxy-methacrylate groups and the increase of the osmotic pressure is faster during the degradation process in higher pH.

Degradation process was also performed at different time intervals. It was found out that during the degradation process, the osmotic pressure increases.

From our investigations we can conclude that dex-HEMA and PEG-HEMA are possible hydrogels for pulsed drug delivery systems. Following investigations must come to prepare and construct drug releasing from dex-HEMA and PEG-HEMA.

## 1.5 List of abbreviations

a	activation
A	area
$A_2$	second virial coefficient
$A_3$	third virial coefficient
c	total polymer concentration
$c''$	concentration of elastic network
$C_r$	real concentration of dextran chains in buffer
$C_m$	measured concentration of dextran chains in buffer
$C_b$	concentration of dextran chains in buffer from sample before

## Evaluation of dex-HEMA for controlled drug delivery

CDI	1.1'-carbonyldiimidazole
CDCl <sub>3</sub>	deuterated chloroform
D	g.mol <sup>-1</sup>
dex-HEMA	hydroxyethyl methacrylate derivatized dextran
DCM	dichloromethane
DMAP	4-N, N-dimethylaminopyridine
DMSO	dimethyl sulfoxide
D <sub>2</sub> O	deuterium water
DR	dextran release
DS	degree of substitution
E	Young's modulus
f	functionality, number of strands leaving one cross-link
f	frequency
F	force
G'	elastic modulus
G*	complex modulus
h	factor varied between 0 (affine) and 1(phantom)
H <sub>x</sub>	stand for the area under a peak, (NMR)
HEMA	hydroxyethyl methacrylate
HEMA-CI	hydroxyethyl methacrylate activated by carbonylimidazole
HCl	hydroxy chloride
KPS	potassium peroxodisulphate

## Evaluation of dex-HEMA for controlled drug delivery

$M_c$	average of $M_w$ of networkstrands
$M_w$	molecular weight ( $\text{g}\cdot\text{mol}^{-1}$ )
$n$	refractive index; number of mols
NMR	nuclear magnetic resonance
$p$	purity
PB	phosphate buffer
PEG	poly(ethylene)glycol
PEG-HEMA	hydroxyethyl methacrylate derivatized poly(ethylen)glycol
pH	hydroxyl exponent ( $\text{mol}\cdot\text{l}^{-1}$ )
ppm	parts per million, unit of chemical shift
$R$	gas constant
$t$	time
$T$	absolute temperature
TEMED	N,N,N',N'-tetramethyl-ethylenediamine
TMS	tetramethylsilane
$u$	mol network strands per volume unit
UV	ultraviolet
$v_1$	specific volume
$w$	weight
$\varepsilon$	efficiency
$\eta$	dynamic viscosity
$\Phi$	angel

$\rho$	density
$\gamma$	shear rate
$\delta$	phase
$\phi$	polymer volume fraction
$\sigma$	tensile stress
$\tau$	shear stress
$\omega$	angular frequency
$\pi_{el}$	elastic pressure
$\pi_{osm}$	osmotic pressure
$\pi_{sw}$	swelling pressure

## 1.6 List of references

- [1.1] G. Schramm, et al. A Practical Approach to Rheology and Rheometry, Gebueder HAAKE GmbH Karlsruhe, 1994.
- [1.2] Thermo electron corporation, Viscoelasticity, Seminar of rheology.
- [1.3] TA instruments, The Rheolyst Series AR 1000 Rheometer-Hardware Manual, Thermal Analysis& Rheology, New Castle, 1996.
- [1.4] TA instruments, Oscillation for CSL- The Theory of Oscillation, Thermal Analysis& Rheology, New Castle, 1996.
- [1.5] A. Sanchez, Pulsed Controlled Release System for Potential Use in Vaccine Delivery, Journal of Pharmaceutical Sciences, June 1996, USA.



- [1.6] B.G. Stubbe, et al., Tailoring the Swelling Pressure of Degrading Dextran Hydroxyethyl Methacrylate Hydrogels, *Biomacromolecules*, 4 (2003) 691-695.
- [1.7] B.G. Stubbe, et al., Swelling Pressure Observations on Degrading Dex-HEMA Hydrogels, *Macromolecules*, 35 (2002) 2501-2505.
- [1.8] W.N.E. van Dijk-Wolthuis, Biodegradable dextran hydrogels for pharmaceutical applications, Thesis University Utrecht, Utrecht University, 1997.
- [1.9] S. Kazakov, et al., UV-Induced Gelation on Nanometer Scale Using Liposome Reactors, *Macromolecules*, 35 (2002) 1911-1920.
- [1.10] P.F. Kiser, et al., Lipid-coated microgels for the triggered release of doxorubicin, *Journal of Controlled Release*, 68 (2000) 9-22.
- [1.11] L.G. Wade, jr., *Organic Chemistry*, Chapter 13 Nuclear magnetic resonance spectroscopy, New Jersey, 1999.
- [1.12] P.J. Flory, *In Principles of Polymer Chemistry*, Cornell University Press, London, 1953.
- [1.13] K. Te Nijenhuis, Calculation of Network Parameters During Crosslinking of Uniform and Non-Uniform Polymer with Crosslinks of Various Functionalities, *International Conference on Crosslinked Polymers*, Luzern, 1991.
- [1.14] S. De Smedt, De invloed van het netwerk in hyaluronzuur-oplossingen en dextraan-glycidylmethacrylaat-hydrogelen op de diffusie van macromoleculen, Universiteit Gent, 1995.
- [1.15] S.J. Bryant, et al., Cytocompatibility of UV and visible light photoinitiating systems on cultured NIH/3T3 fibroblasts in vitro, University of Colorado Boulder, USA, 1999.

- [1.16] F. Horkay, M. Zrinyi, Studies on the mechanical and swelling behaviour of polymer networks based on the scaling concept. 4. Extension of the scaling approach to gels swollen to equilibrium in a diluent of arbitrary activity *Macromolecules*; 1982, 15(5), 1306-1310.
- [1.17] E. Edmond, A. G. Ogston, An approach to the study of phase separation ternary aqueous systems, *Biochemical journal*, 1968, 109-569.

## **2 PREPARATION OF INORGANIC/ ORGANIC NANOCOMPOSITES**

### **2.1 Aim of project**

The aim of this part of project is to produce inorganic/ organic nanocomposites from natural biopolymers. Selected inorganic compounds are silica and titanium. These materials cover fibre surface to protect them against influences from surroundings.

Next step is building up silver metal particles on nanocomposites surface to arrange antibacterially and sterility of fibres which will be further used as construction material for wound healing dressing. In this application the antibacterial functionality is extremely demanded.

### **2.2 Materials and methods**

#### **2.2.1 Chemicals**

Tetraethyl ortosilicate (TEOS) - 98%, obtained Aldrich,  $(C_2H_5O)_4Si$  with molecular weight 208,33 is clear, colourless liquid with alcohol odour. Ammonia - a chemical compound with chemical formula  $NH_4OH$  with molecular weight 35,05. It was used as 25% solution in water as obtained by Merck.

Ethanol (99%, Panreac) - Aldrich. It is also known as ethyl alcohol or grain alcohol, is a flammable, colourless chemical compound, one of the alcohols that is most often found in alcoholic beverages. In common parlance, it is often referred to simply as alcohol. Its molecular formula is  $C_2H_6O$ , variously represented as EtOH,  $C_2H_5OH$  or as its empirical formula  $C_2H_6O$  and molecular mass 46.07.

Urea (Panreac) is an organic compound of carbon, nitrogen, oxygen and hydrogen, with the formula  $(NH_2)_2CO$  and molecular weight 60.07.

## Preparation of inorganic/ organic nanocomposites

Titanium tetrachloride (98%, Fluka) - a chemical compound with chemical formula  $\text{TiCl}_4$  and molecular mass 189.71. It is an important intermediate in the separation of titanium from its ores and in the production of titanium as well as many chemicals. This chemical compound is remarkable in many ways, not the least of which is that it is an unusual example of a liquid metal halide and it fumes spectacularly in air.  $\text{TiCl}_4$  is a dense, colourless (or pale yellow) distillable liquid, although crude samples can be reddish-brown. It is one of the rare transition metal chlorides, that is liquid at room temperature. This distinctive property arises from the fact that  $\text{TiCl}_4$  is molecular, that is each  $\text{TiCl}_4$  behaves independently. Most metal chlorides are polymers, where the chloride atoms bridge between the metals. The attraction between the individual  $\text{TiCl}_4$  molecules is weak, primarily van der Waals forces, and these weak interactions result in low melting and boiling points akin to that for  $\text{CCl}_4$ .

Silver nitrate (Aldrich) - a chemical compound with chemical formula  $\text{AgNO}_3$ . This nitrate of silver is a light-sensitive ingredient in photographic film and is a poisonous, corrosive compound. Silver nitrate crystals can be produced by dissolving silver in nitric acid and evaporating the solution. The compound notably stains skin a greyish or black colour that is made visible after exposure to sunlight.

Sodium diethyldithiocarbamate trihydrate (Aldrich)  $\text{Na}(\text{dtc})$  - a chemical compound with chemical formula  $(\text{C}_2\text{H}_5)_2\text{NCS}_2\text{Na} \cdot 3\text{H}_2\text{O}$  and molecular weight 225, 31  $\text{g}\cdot\text{mol}^{-1}$

Potassium chloride - a chemical compound ( $\text{KCl}$ ) is a metal halide composed of potassium and chlorine. In its pure state it is odourless. It has a white or colourless vitreous crystal, with a face-centred cubic structure that cleaves easily in three directions. It is also commonly known as "Muriate of Potash". Potash varies in colour from pink or red to white depending on the mining and recovery process used. White potash, sometimes referred to as soluble potash, is usually higher in analysis and is used primarily for making liquid starter fertilizers.  $\text{KCl}$  is used in medicine, scientific applications, food processing and in judicial execution through lethal injection. It

## Preparation of inorganic/ organic nanocomposites

occurs naturally as the mineral sylvite and in combination with sodium chloride as sylvinite. Its molecular mass is  $74,55 \text{ g}\cdot\text{mol}^{-1}$ .

Titanium(IV) ethoxide - a chemical compound with chemical formula  $\text{Ti}(\text{OC}_2\text{H}_5)_4$  and molecular mass  $228 \text{ g}\cdot\text{mol}^{-1}$ . It is incompatible with strong oxidizing agents and strong acids. It is irritant and it is necessary to use it under the nitrogen atmosphere.

Sodium borohydride (Aldrich) - also known as sodium tetrahydridoborate, has the chemical formula  $\text{NaBH}_4$ . It is a selective specialty reducing agent used in the manufacture of pharmaceuticals, intermediates and fine chemicals. It is a white solid with molecular weight  $37,89 \text{ g}\cdot\text{mol}^{-1}$ , usually encountered as a powder or confectioned into pills. It melts at  $36^\circ\text{C}$  ( $97^\circ\text{F}$ ) and is stable (when dry) up to approximately  $300^\circ\text{C}$  ( $570^\circ\text{F}$ ). It is soluble in methanol and cold water, but reacts with hot water.

Acetone (98%, Aldrich) - a colourless mobile flammable liquid with melting point at  $-95,4^\circ\text{C}$  and boiling point at  $56,53^\circ\text{C}$ . It has a relative density of 0,819 (at  $0^\circ\text{C}$ ). It is readily soluble in water, ethanol, ether, etc., and itself serves as an important solvent. The most familiar household use of acetone is as the active ingredient in nail polish remover. Acetone is also used to make plastic, fibres, drugs, and other chemicals. Its molecular weight  $58,09 \text{ g}\cdot\text{mol}^{-1}$ .

1,2-diaminopropan (Aldrich) - a chemical compound with formula  $\text{C}_3\text{H}_{10}\text{N}_2$ . It is stable, flammable and incompatible with strong oxidizing agents, acids, acid chlorides, acid anhydrides.

All reactants were used as received without any purification.

Wood cellulose fibres (Eucalyptus globulus. ECF bleached craft pulp), composed essentially of cellulose ( $\sim 85\%$ , and humidity about  $40\%$ ).

Glucuronoxylan ( $\sim 15\%$ ) supplied by Portucel (Portugal) was disintegrated and washed with distilled water before use.

### 2.2.2 Synthesis

#### *In situ synthesis of SiO<sub>2</sub> nanoparticles in the presence of cellulose fibres I)*

To prepare the SiO<sub>2</sub>/cellulose nanocomposites a Stöber method with experimental conditions similar to synthesis of pure SiO<sub>2</sub> particles was used [1]. In a typical synthesis, cellulose fibres were added to a mixture of ethanol, distilled water and ammonia under moderate stirring (1% consistency) followed by addition of TEOS, at room temperature for about 24 hours. The final fibres were then collected by filtering and thoroughly washed with distilled water and finally dried in an oven at 50°C.

Ethanol (1 740 ml) + H<sub>2</sub>O (180 ml) mix well for 2 minutes

Add right amount of fibres (humidity=recalculation) in this case: humidity is about 40%. For 20g dry cellulose fibres the weighted amount is 33g.

Mix for 40-60 minutes

Add NH<sub>4</sub>OH (20 ml)

Add TEOS (60 ml)

Whole mixture mixed very well under moderate stirring for 24 hours

Filtrate

Dry in the oven in 50 °C

Test by SEM, TG, RAMAN, X-ray and Calcination

#### *In situ synthesis of TiO<sub>2</sub>/ SiO<sub>2</sub>/cellulose nanocomposites IIa)*

The method of nanocomposites preparation by TiCl<sub>4</sub> hydrolysis in the presence of urea was used [2]. In a typical synthesis right amount of urea to produce anatase crystalline form on the surface of SiO<sub>2</sub>/cellulose nanocomposites, was dissolved in 50 ml of ice-cold solvent water or (water: propan-1-ol in ration 1:4) under vigorous

## Preparation of inorganic/ organic nanocomposites

stirring. Subsequently 1 ml of  $\text{TiCl}_4$  was added in the homogeneous solution. The solution was mixed for about 1 hour. Cellulose fibres (in ration 1:100 to whole volume of mixture, 0,5g) were added to this solution and the mixture was heated at  $70^\circ\text{C}$  during 24 hours. It is necessary to use condenser. Afterwards the nanocomposite fibres were collected by filtering, thoroughly washed with distilled water and dried in the oven at about  $50^\circ\text{C}$  over 3, 6 and 24 hours.

Mix water and popan-1-ol and put it into ice bath (1:4, 10 ml:40ml)

Gradually add exact amount of  $\text{TiCl}_4$  without bubbles (1 ml)

Add hybrid fibres (0,5 g)

Mix for 24 hours

Filltrate

Dry in oven in about  $40^\circ\text{C}$  for 24 hours

Test by SEM, Raman, TG, X-ray analysis and Calcination

### ***In situ synthesis of nanocomposites prepared by hydrolysis of $\text{Ti}(\text{OC}_2\text{H}_5)_4$ I Ib***

There is another way to prepare nanocomposites of  $\text{TiO}_2/\text{SiO}_2$ /cellulose by using titanium ethoxide.

In 100 ml of ethanol 0,4 ml of 0.1M KCl is dissolved

Into the clear solution 0,5 g of fibres, normally the weight of substrate is 1% (1:100) of solution, if the solvent is water. But in the case, that the solvent is ethanol, propanol or something different than water, it is not easy to disperse the substrate than it is better to use substrate in ration 1:200.

This mixture is mixed very well for about one hour.

Than 1,7 ml of  $\text{Ti}(\text{OC}_2\text{H}_5)_4$  is added under the  $\text{N}_2$  atmosphere.

## Preparation of inorganic/ organic nanocomposites

In case without fibres: mix the solution till it turns white. It is about 120 minutes. Then let it grow the crystals for 24 hours.

In case with fibres: mix the solution whole time of aging to provide the growth of titanium particles on whole fibres surface.

After aging the pigment is cleaned two times by ethanol and two times by water by using the centrifuge and dried in the oven.

The final product is tested by Raman, SEM and X-Ray analysis.

### ***Growth of silver sulfide nanocrystals on TiO<sub>2</sub>/SiO<sub>2</sub>/cellulose nanocomposites surface III)***

TiO<sub>2</sub>/SiO<sub>2</sub>/cellulose nanocomposites were used as prepared. As Ag<sub>2</sub>S precursor silver diethyldithiocarbamate (Ag(dtc)) was used. Ag(dtc) was prepared by mixing of 100 ml of 0,1 M silver nitrate (Ag(NO<sub>3</sub>)) with 100 ml of 0,1M sodium diethyldithiocarbamate (Na(dtc)) for 1 hour under moderate stirring. Afterwards solution was filtrate, thoroughly washed with distilled water and at the last time with acetone and let to dry in a desiccator over silica gel.

All the nanocomposite particles were prepared by adding 1,2-diaminoproapn (1 ml) drop-wise to an acetone solution (20 ml) containing 0.03 g of Ag(dtc) and 0.1 g of TiO<sub>2</sub>/SiO<sub>2</sub>/cellulose nanocomposites. The suspension was then refluxed with stirring, under a N<sub>2</sub> stream, inside a well-ventilated fume-cupboard. Samples were collected by filtering and washed thoroughly with acetone. All obtained amount was dried at room temperature in the desiccator over silica gel.



***Preparation of Ag metal nanocrystals on the surface of TiO<sub>2</sub>/SiO<sub>2</sub>/cellulose nanocomposites IV)***

TiO<sub>2</sub>/SiO<sub>2</sub>/cellulose nanocomposites with Ag<sub>2</sub>S nanoparticles were used as prepared. Ag metal nanoparticles are prepared by removing sulphur from Ag<sub>2</sub>S nanocrystals by reaction with sodium borohydride (BH<sub>4</sub>Na). 100 ml of BH<sub>4</sub>Na is prepared and 0,1 g of TiO<sub>2</sub>/SiO<sub>2</sub>/cellulose nanocomposites with Ag<sub>2</sub>S nanoparticles is added and let to mix for. Fibres are collected by filtering, thoroughly washed with distilled water and dried in the desiccator over silica gel.

## **2.3 Result and discussion**

### **2.3.1 List of prepared substances**

***SiO<sub>2</sub>/cell***

Cellulose fibres covered by compact SiO<sub>2</sub> film, produced by process I).

***TiO<sub>2</sub>/cell.***

Cellulose fibres covered by compact TiO<sub>2</sub> film, produced by process II), by adding clear cellulose fibres.

***TiO<sub>2</sub>+SiO<sub>2</sub>/cell. (w, 24)***

Cellulose fibres covered by compact SiO<sub>2</sub> film, produced by process I) and recovered by TiO<sub>2</sub> particles or film, according the process II), where solvent was distilled water and reaction time was 24 hours.

***TiO<sub>2</sub>+SiO<sub>2</sub>/cell. (w:p, 6)***

Cellulose fibres covered by compact SiO<sub>2</sub> film, produced by process I) and recovered by TiO<sub>2</sub> particles or film, according the process II), where solvent was distilled water and propan-1-ol (ration 1:4) and reaction time was 6 hours.

***TiO<sub>2</sub>+SiO<sub>2</sub>/cell. (w:p, 24)***

Cellulose fibres covered by compact SiO<sub>2</sub> film, produced by process I) and recovered by TiO<sub>2</sub> particles or film, according the process II), where solvent was distilled water and propan-1-ol (ration 1:4) and reaction time was 24 hours.

***Ag(dtc)***

***AgC<sub>5</sub>H<sub>10</sub>NS<sub>2</sub>, precursor of Ag<sub>2</sub>S.*** Reaction described as process III).

***Ag<sub>2</sub>S-TiO<sub>2</sub>/SiO<sub>2</sub>/cell;***

Cellulose fibres covered by compact SiO<sub>2</sub> film, produced by process I) and recovered by TiO<sub>2</sub> particles or film, according the process II), where solvent was distilled water and propan-1-ol (ration 1:4) and reaction time was 24 hours. With nanocrystals of Ag<sub>2</sub>S on the surface, which were prepared by process III).

***TiO<sub>2</sub>/SiO<sub>2</sub>/cell; Ag<sub>2</sub>S***

Cellulose fibres covered by compact SiO<sub>2</sub> film, produced by process I) and recovered by TiO<sub>2</sub> particles or film, according the process II), where solvent was distilled water and propan-1-ol (ration 1:4) and reaction time was 24 hours. With nanocrystals of Ag<sub>2</sub>S on the surface, which were prepared by process III).

***TiO<sub>2</sub>/SiO<sub>2</sub>/cell; Ag<sub>2</sub>S-Ag, NaBH<sub>4</sub> 0.01M, 7h***

Cellulose fibres covered by compact SiO<sub>2</sub> film, produced by process I) and recovered by TiO<sub>2</sub> particles or film, according the process II), where solvent was distilled water and propan-1-ol (ration 1:4) and reaction time was 24 hours. With nanocrystals of Ag<sub>2</sub>S on the surface, which were prepared by process III). Ag<sub>2</sub>S is reduced to Ag-metal by mixing with 100 ml 0,01 M NaBH<sub>4</sub> for reaction time 7 hours.

***TiO<sub>2</sub>/SiO<sub>2</sub>/cell; Ag<sub>2</sub>S-Ag, NaBH<sub>4</sub> 0,03M, 7h***

... Ag<sub>2</sub>S is reduced to Ag-metal by mixing with 100 ml 0,03 M NaBH<sub>4</sub> for reaction time 7 hours.

***TiO<sub>2</sub>/SiO<sub>2</sub>/cell; Ag<sub>2</sub>S-Ag, NaBH<sub>4</sub> 0,05M, 7h***

... Ag<sub>2</sub>S is reduced to Ag-metal by mixing with 100 ml 0,05 M NaBH<sub>4</sub> for reaction time 7 hours.

***TiO<sub>2</sub>/SiO<sub>2</sub>/cell; Ag<sub>2</sub>S-Ag, NaBH<sub>4</sub> 0,01M, 24h***

... Ag<sub>2</sub>S is reduced to Ag-metal by mixing with 100 ml 0,01 M NaBH<sub>4</sub> for reaction time 24 hours.

***TiO<sub>2</sub>/SiO<sub>2</sub>/cell; Ag<sub>2</sub>S-Ag, NaBH<sub>4</sub> 0,03M, 24h***

... Ag<sub>2</sub>S is reduced to Ag-metal by mixing with 100 ml 0,03 M NaBH<sub>4</sub> for

***TiO<sub>2</sub>/SiO<sub>2</sub>/cell; Ag<sub>2</sub>S-Ag, NaBH<sub>4</sub> 0,05M, 24h***

... Ag<sub>2</sub>S is reduced to Ag-metal by mixing with 100 ml 0,05 M NaBH<sub>4</sub> for reaction time 24 hours.

***TiO<sub>2</sub>/SiO<sub>2</sub>/cell; Ag<sub>2</sub>S-Ag, NaBH<sub>4</sub> 0,01M, 72h***

... Ag<sub>2</sub>S is reduced to Ag-metal by mixing with 100 ml 0,01 M NaBH<sub>4</sub> for reaction time 72 hours.

***TiO<sub>2</sub>/SiO<sub>2</sub>/cell; Ag<sub>2</sub>S-Ag, NaBH<sub>4</sub> 0.01M, 72h***

... Ag<sub>2</sub>S is reduced to Ag-metal by mixing with 100 ml 0,01 M NaBH<sub>4</sub> for reaction time 72 hours.

SiO<sub>2</sub>/cellulose fibres nanocomposites were remitted to several tests. From results of these tests might be concluded that the synthesis of SiO<sub>2</sub> in the presence of cellulose fibres originated a homogeneous coating at the fibres surface.

Typically the deposited SiO<sub>2</sub> represent about 23,6% (w/w) of the nanocomposite weight as determined by TGA. UV-VIS spectroscopy analysis shows typical spectrum for SiO<sub>2</sub>. SEM analysis showed cellulose fibres fully covered with a compact silica film.

TiO<sub>2</sub>/SiO<sub>2</sub>/cellulose fibres nanocomposites were prepared by II) described synthesis in two different solvents: water and water: propan-1-ol (1:4) and for different reaction time: 3, 6, 24 hours. Nanocomposites were tested by Raman, SEM and UV-VIS analysis. Based on results from these tests it might be concluded that TiO<sub>2</sub> forms compact cover on the surface of SiO<sub>2</sub>/cellulose fibres nanocomposites. TiO<sub>2</sub> coverage strongly depends on reaction time. This conclusion might be done from all performed tests.

Results from Raman analysis showed that after six hours reaction in water: propanol solvent the coverage is not sufficient and a peak of TiO<sub>2</sub> is hardly observable. Contrary the results for samples after 24 hours reaction in water: propanol solvent shows nice peak typical for TiO<sub>2</sub> in 159,4 cm<sup>-1</sup>. The some effect of reaction time might be described from results of UV-VIS analysis. Sample treated for 6 hours in water: propanol solvent shows lower reflectance (about 65%) compared to sample treated for 24 hours in water: propanol solvent, which shows reflectance about 80% and the typical decrease of reflectance in range 320-400 cm<sup>-1</sup> is more precipitate.

Chart obtained from UV-VIS analysis was also used to calculate morphology of obtained TiO<sub>2</sub>. The inflexion point of the curve for sample treated for 24 hours in water: propanol solvent is in 375 nm, what is equal to 3.22 eV. This value refers to anatase form of TiO<sub>2</sub>.

Samples of prepared inorganic/organic hybrids were also tested by SEM. Increasing reaction time influence amount of TiO<sub>2</sub> formed coverage of the SiO<sub>2</sub>/cellulose fibre surface.

Testing by SEM also showed that TiO<sub>2</sub> forms compact film on the surface of nano-hybrids. This is showed in the Figure 2.2.

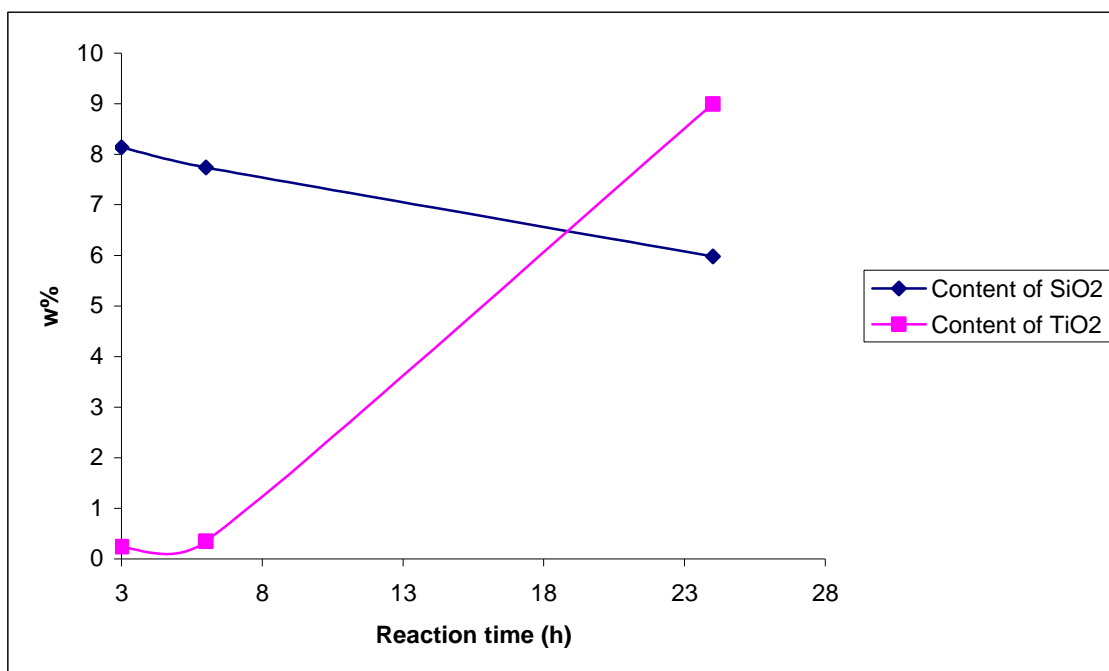


Figure 2.1: The curves represent content of SiO<sub>2</sub> or TiO<sub>2</sub> on cellulose fibres by the function of time.

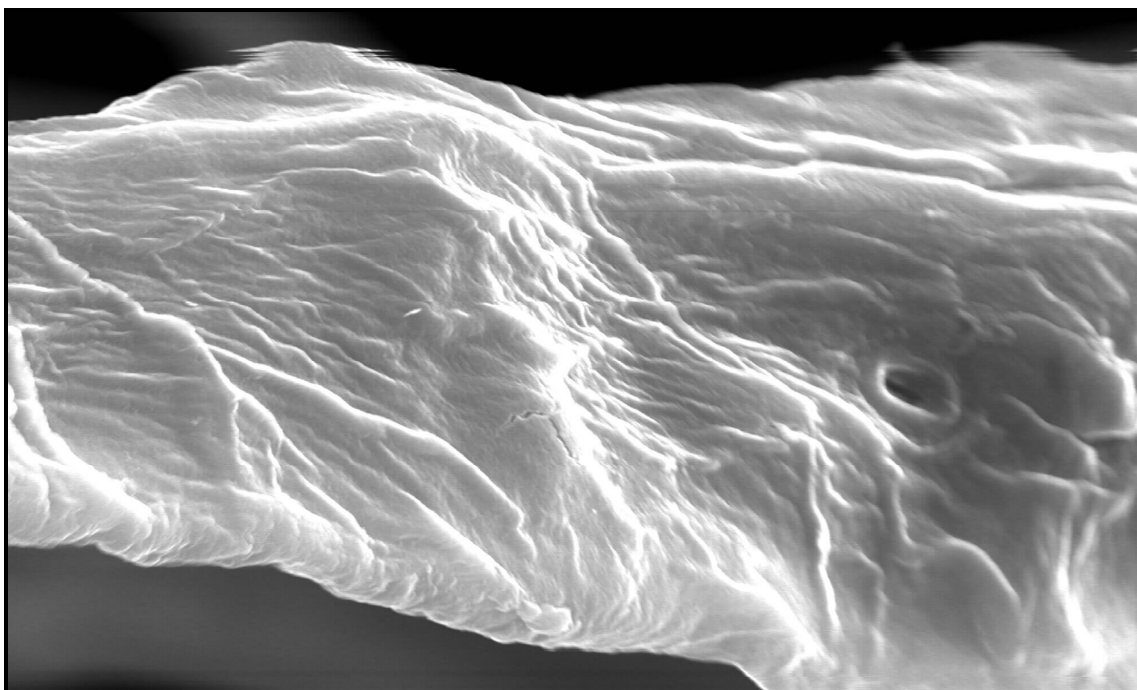


Figure 2.2: TiO<sub>2</sub>/SiO<sub>2</sub>/cellulose nanocomposite tested by SEM.

## Preparation of inorganic/ organic nanocomposites

Results were used to find optimal reactions conditions. As optimal solvent the mixture of water and propan-1-ol in ratio 1:4 was chosen and as optimal reaction time was found out 1 day.

TiO<sub>2</sub>/SiO<sub>2</sub>/cellulose fibres nanocomposites were used as substrate for growing of Ag<sub>2</sub>S.

Afterwards Ag<sub>2</sub>S was tried to reduce to Ag metal by NaBH<sub>4</sub> solution. Influence of different time and concentration of reducing solution was investigated.

With increasing concentration of NaBH<sub>4</sub> and increasing time samples changed colour from very dark grey to almost white. This visual test reflected, that Ag<sub>2</sub>S has black colour and Ag metal particles are silver, which could be visible as white. Decreasing amount of Ag<sub>2</sub>S represents in decreasing greyish colour as showed in Figure 2.3.

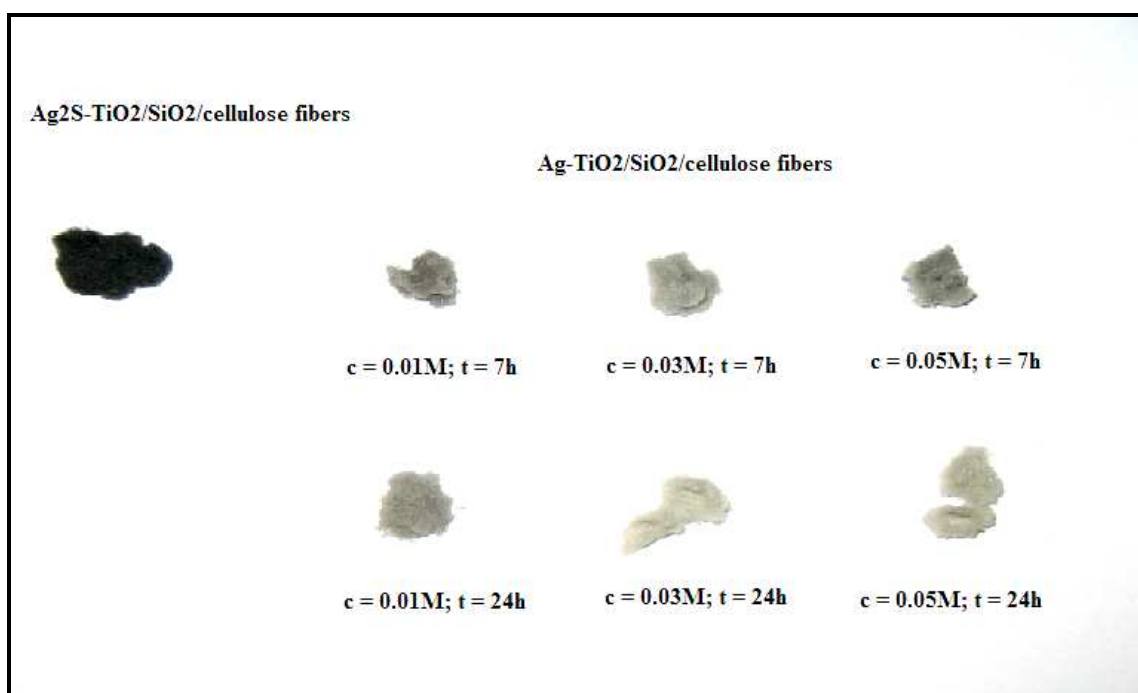


Figure 2.3: Increasing time and NaBH<sub>4</sub> concentration influence colour of samples.

## 2.4 Conclusion

Aim of this work was to prepare nanocomposites based on natural cellulose fibres. Produced inorganic/ organic hybrids were used as a base for applying silver metal on the surface of these hybrids.

The study shows possibility to coat natural polymers with inorganic material to protect those against agents from surrounding.

The other studied topic was forming of silver metal particles on prepared nanocomposites surfaces. This study was very preliminary and further investigations are necessary, this study shows possibility of preparing nanocomposites from natural fibre materials based on silica and titanium covers and also shows possibility of building further materials on its surface to raise their essential properties or build up new one.

## 2.5 List of abbreviations

M	molecular weight $\text{g}\cdot\text{mol}^{-1}$
t	time
h	hour
UV-VIS	ultraviolet - visible
TiO <sub>2</sub>	titanium oxide
SiO <sub>2</sub>	silicon oxide
SEM	scanning electron microscope
TGA	thermogravimetric analyse

## 2.6 List of references

- [2.1] TURKOVIC, A., TONEJC, A., POPOVIC, S., DUBCEK, P., IVANDA, M., MUSIC, S., GOTIC M. Transmission electron microscopz, x/ra diffraction and Raman scattering studies of nanophase TiO<sub>2</sub>. *Fizika 6*. 1997, vol. 2, p.77–88.
- [2.2] SEOK, S. I., KIM, J. H. TiO<sub>2</sub> nanoparticles formed in silica sol–gel matrix. *Materials Chemistry and Physics*. 2004, no.86, p.176–179.
- [2.3] Kwon, Ch. H., Kim, J. H., Jung, I. S., Shin, H., Yoon, K. H. Preparation and characterization of TiO<sub>2</sub>–SiO<sub>2</sub> nano-composite thin films. *Ceramics International*, 2003, no.29, p. 851–856.
- [2.4] DAOUD, W. A., XIN, J. H., ZHANG, Y.H. Surface functionalization of cellulose fibers with titanium dioxide nanoparticles and their combined bactericidal activities. *Surface Science*. 2005, no.599, p. 69–75.
- [2.5] KIM, K. D., BAE, H. J., KIM, H.T. Synthesis and growth mechanism of TiO<sub>2</sub>-coated SiO<sub>2</sub> fineparticles. *Colloids and Surfaces A: Physicochem. Eng. Aspects*, 221. 2003, p. 163- 173.
- [2.6] FANG, Ch. S., CHEN, Y. W. Preparation of titania particles by thermal hydrolysis of TiCl<sub>4</sub> in *n*-propanol solution. *Materials Chemistry and Physics* 78. 2003, p. 739–745.
- [2.7] HOCKEN, J., PIPPLIES, K., SCHULTE, K. The advantageous use of ultra fine titanium dioxide in wood coatings.
- [2.8] HANPRASOPWATTANA, A., RIEKER, T., SAULT, A. G., DATYE, A. K. Morphology of titania coatings on silica gel. *Catalysis Letters* 45. 1997, p. 165 -175.



- [2.9] Fu, X., Qutubuddin, S. Synthesis of titania-coated silica nanoparticles using a nonionic water-in-oil microemulsion. *Colloids and Surfaces A: Physicochemical and Engineering Aspects* 179. 2001, p. 65–70.
- [2.10] SONG, Ch. F., LU, M. K., YANG, P., XU, D., YUAN, D. R. Structure and photoluminescence properties of sol–gel TiO<sub>2</sub>–SiO<sub>2</sub> films. *Thin Solid Films* 413. 2002, p. 155–159.
- [2.11] LI, Y., WHITE, T.J., LIM, S.H. Low-temperature synthesis and microstructural control of titania nano-particles. *Journal of Solid State Chemistry* 177. 2004, p. 1372–1381.
- [2.12] YIN, S., LI, R., HE, Q., SATO, T. Low temperature synthesis of nanosize rutile titania crystal in liquid media. *Materials Chemistry and Physics* 75. 2002, p. 76–80.
- [2.13] FUJISHIMA, A., RAO, T. N., TRYK, D. A. Titanium dioxide photocatalysis. *Journal of Photochemistry and Photobiology C: Photochemistry Reviews* 1. 2000, p. 1–21.
- [2.14] SUI, R., RIZKALLA, A. S., CHARPENTIER, P. A. Formation of Titania Nanofibers: A Direct Sol-Gel Route in Supercritical CO<sub>2</sub>. *Langmuir*. 2005, 21, p. 6150-6153.
- [2.15] JIANG, X., WANG, T., WANG, Y. Preparation of TiO<sub>2</sub> nanoparticles on the surface of SiO<sub>2</sub> in binary liquids. *Colloids and Surfaces A: Physicochem. Eng. Aspects* 234. 2004, p. 9–15.

# **3 EVALUATION OF CELLULOSE DERIVATES FOR WOUND HEALING DRESSING**

## **3.1 Aim of this project**

The aim of this part of work is to evaluate some of basic chemical and physical properties of different selected kinds of biomaterials, polysaccharides. These polysaccharides are selected cellulose derivatives; OK CEL, HEC and CMC. They are planned to be investigated as basic construction units of mentioned special wound healing plasters.

The first of inspected chemical and physical properties is density and its dependence on solution temperature and initial solution concentration. Other evaluated factors are surface tension and contact angle of different concentrated polymer solutions and their dependence on solution temperature.

Further inspected characteristics are UV-VIS absorbency, particle size, particle size distribution and zeta potential. Influence of pH and salt concentration variation on these characteristics was also evaluated in this chapter of presented study.

## **3.2 Materials and methods**

### **3.2.1 Materials**

#### *Oxycellulose (OK CEL)*

It was obtained from Synthesia a.s. from Pardubice, Czech Republic.

### *Hydroxyethylcellulose (HEC)*

HEC was obtained from Hercules, Aqualon Division, in Alizay, France. The type 250LR, lot A-0749 with the technical name NATROSOL® was used. Molecular weight of Natrosol 250LR is about  $9,104\text{g}\cdot\text{mol}^{-1}$ .

Natrosol non-ionic, water-soluble polymer is derived from cellulose. It is used in water-based paints for its action as a rheology modifier, stabilizer and/or suspending agent. And it also plays a significant role in controlling rheology before, during, and after application.

Physically, HEC is a white, free-flowing powder that dissolves readily in hot or cold water. Available in a variety of types and grades, it can be used to produce solutions with a wide range of viscosity and pseudo-plastic rheology. Upon drying, solutions of Natrosol form clear, gel-free films.

Natrosol is compatible with pigments, binders, surfactants, and preservatives used in water-based paint systems.

Natrosol is a hydroxyethyl ether of cellulose. Each anhydroglucose unit in the cellulose molecule has three reactive hydroxyl groups. The number of hydroxyl groups substituted in any reaction is known as the degree of substitution (DS). Theoretically, all three hydroxyls can be substituted. The product from such a reaction would have a DS of 3.

Type 250 LR has low molecular weight and it is treated to provide fast dispersion and easier dissolving in water.

Solutions of Natrosol are non-Newtonian in flow, since they change in viscosity with rate of shear. Natrosol is dissolved in water; the viscosity of the aqueous solution rapidly increases with concentration. The viscosity-concentration relationship is nearly linear. The viscosity of Natrosol solutions

changes with temperature, increasing when cooled, decreasing when warmed. The viscosity of the solution is 10 Pa.s at 25 °C [3.42].

### *Carboxymethylcellulose (CMC)*

CMC was obtained from Hercules, Aqualon Division, in Alizay, France. Refined CMC type 7L, lot 20075 with the technical name BLANOSE® was used. Molecular weight of Natrosol 250LR is about 30g.mol<sup>-1</sup>.

It is purified sodium carboxymethylcellulose with minimum purity of 98%. Physically it is a light cream to white free-flowing powder or granulate, which readily dissolves in water to form clear, viscous solutions. It dissolves rapidly in cold or hot water. Refined CMC acts as a thickener, rheology control agent, binder, stabilizer, protective colloid, suspending agent and water retention aid forms films that are resistant to oils, greases and organic solvents and it is physiologically inert.

Refined CMC is cellulose ether, produced by reacting alkali cellulose with sodium monochloroacetate. The reaction is controlled in such a way that a predetermined substitution by sodium carboxymethyl groups (-CH<sub>2</sub>COONa) is obtained. This is expressed as degree of substitution (DS) or the average number of sodium carboxymethyl groups per anhydroglucose unit on the cellulose chain. The substitution necessary to achieve optimum solubility and other desirable physical properties is much less than three, for commonly used type 7, as is used for measurements in this work is substitution in range 0,65-0,90.

Varying the length of the basic cellulose chain controls the viscosity of CMC. Viscosity of type 7L is in range 25 - 50 mPa.s at 25 °C. Viscosity is the most important property of CMC aqueous solutions. These solutions have a wide tolerance for fluctuations of pH, for monovalent salts, and for water-miscible organic solvents such as methanol, ethanol and glycerine. The pH of solutions is in range 5,0 - 8,5.

The CMC aqueous solutions had pseudoplastic behaviour and thixotropy character. Generally high viscosity CMC will show a stronger thixotropy, or a lower speed of return. Both properties depend on degree of substitution of the CMC.

Refined CMC is readily soluble in water at all temperatures right up to boiling point. Under normal conditions, the effect of temperature upon viscosity is reversible and rising or lowering the temperature has no permanent effect on the viscosity characteristics of the solution. However, long periods of heating at high temperatures may degrade the sodium carboxymethylcellulose and reduce its viscosity permanently.

CMC solutions are more resistant to microbiological attack than most other water-soluble gums they are not immune. If solutions have to be stored for any prolonged period, it is important to destroy or immobilize any cellulose (hydrolytic, viscosity destroying enzymes), which may have been introduced by microbial action. [3.43], [3.44]

### ***Samples preparation***

Every measurement, in this thesis, was obtained on 2 and 4 weight % samples of each derivate (OK CEL, HEC, CMC).

Weighted amount of cellulose derivate powder was diluted in given amount of distil water. The cellulose powder was wetted by small volume of ethanol before dilution. Whole mixture was stirred till it forms clear, viscous solution. In case of OK CEL the solution was not clear but it was slightly yellowish and opalescent.

In case of particle size and zeta potential measurement prepared 2 and 4 weigh % samples were measured.

## Evaluation of cellulose derivates for wound healing dressing

Measurement of pH influence was obtained on prepared samples. These prepared samples were poured into the beaker where the special electrode for pH measurement was dipped. The small amounts of HCl or NaOH were added subsequently under gently stirring to change pH of the solution. This was done till obtaining the desired pH.

Measurement of ionic concentration influence was obtained on samples diluted by ( $1 \cdot 10^{-2}$ ,  $1 \cdot 10^{-3}$ ,  $1 \cdot 10^{-4}$ ,  $1 \cdot 10^{-5}$ ,  $1 \cdot 10^{-6}$  mol.l<sup>-1</sup>) concentrated solutions of NaCl. The dilution was in ration 1:1. 2 ml of sample were poured into the cuvette, than 2 ml of NaCl solution were added into this cuvette and whole volume was shaken very gently.

UV-VIS measurement used the same samples as zeta potential and particle size measurements. But it was also measured on 1 weight % sample, this one was made by diluting 2 weight % sample by distil water in ratio 1:1 and whole mixture was shaken.

### ***Chemicals***

sodium hydroxide (NaOH), solution (c = 1 mol.l<sup>-1</sup>)

hydrochloric acid (HCl), solution (c = 1 mol.l<sup>-1</sup>)

sodium chloride (NaCl), solutions (c =  $10^{-2}$ ;  $10^{-3}$ ;  $10^{-4}$ ;  $10^{-5}$ ;  $10^{-6}$  mol.l<sup>-1</sup>)

### ***Instruments***

***Tensiometr K12 (Krüss, Germany)***

#### ***Density measurement:***

solid tester (Krüss standard, hook for solid tester

sensitivity 0,006g; time interval 5s

#### ***Surface tension measurement:***

Wilhely method

## Evaluation of cellulose derivates for pulsed drug delivery

standard plate: platinum, width = 19,9 mm, thickness 0,2 mm

sensitivity 0,01g; immersion depth 2 mm; time interval 2s; 10 measured values

### ***Contact angle measurement:***

Ring method, dynamic

ring standard (Krüss): diameter 20 mm, thickness 0,2 mm

sensitivity 0,0005g; time interval 2s; immersion depth 3 mm, 3 measured values

Samples were poured into the glass cup and established in the tensiometer. This cup is the standard for Tensiometer K12. Consequently it was let to temper on the requested temperature for 20 minutes.

As the first the density measurement was done. The software was set up for this measurement and the empty hook was installed and let to calibrate. Then we gently added the solid tester into the hook and start the density measurement.

When this measurement was finished the measuring extender was replaced by standard plate for surface tension measurement. Software was also changed and right setting data for surface tension measurement were set up. The measurement was repeated ten times just to have enough values for calculation of correct results and their standard deviation.

Last measurement on this device was the measurement of contact angle. The standard plate was replaced by standard ring and the software and settings were set up. Three values were measured.

The measured data were elaborated into the charts. Standard deviations were calculated and they are presented in the charts also.

***Doublebeam UV-VIS spektrofotometr (Helios Alpha - Thermo Spectronic, Germany)***

wavelength range 190 - 110 nm

slot latitude 2 nm

silicon cuvette, width 1 cm

Firstly, the distilled water was poured into the two cuvettes. Both cuvettes were placed into their compartments, one into the compartment for sample and the other into the solution compartment. Then the baseline measurement was started.

The prepared samples were poured into the clean and dry silicon cuvette. Spectrophotometer settings were set up. It was set up whole wavelength range and medium smoothing.

***ZetaPlus (Brookhaven Instruments Corporation, USA)***

Zeta potential analyser with goniometry BI-9000AT, measured particle diameter is from 0,002 to 3  $\mu\text{m}$

Zeta plus and particle size software

special electrode for zeta potential measurement

special electrode for pH measurement

principle of laser-Doppler electrophoresis; particle size for electrophoresis 0.005-30  $\mu\text{m}$ ;

pH range: 2-12; sample volume: 1 ml-1.5 ml; conductive range: 0 - 700  $\text{mS}\cdot\text{m}^{-1}$ ; mobility range:  $10^{-9}$  to  $10^{-7}$   $\text{m}^2\cdot(\text{V}\cdot\text{s})^{-1}$ .

The prepared cellulose samples were poured into the clean and dry polystyrene cuvette, standard for ZetaPlus instrument. This cuvette was got inside the zeta potential analyser chest. The software for particle size



measurement was dropped on and settings, such as sample name, number of rounds (5), spell of particular round (20 s).

When the particle size measurement was finished, the cuvette with sample was taken out. The special electrode for zeta potential measurement was plugged in this cuvette. The redundant sample amount was forced out and dried by a paper serviette. The clean and dry cuvette was got inside the chest again. In zeta potential software the optimal settings were selected, such as sample name, number of rounds (5), number of measurements in one round (5), concentration of solution, measured pH and the measurement was performed.

### **3.3 Results and discussion**

#### **3.3.1 Density measurement**

The density measurement was performed, because of needs of knowledge of density values for measurement of the surface tension and the contact angle.

On the top of them the influence of concentration and temperature on density was investigated. It is significant that increasing temperature influences density of the cellulose solutions. Density decreases slowly with increasing temperature.

In Figure 3.1 the results are demonstrated for OK CEL sample how temperature and solution concentration influence polymer samples density.

Density decreasing is gradual for both concentrations of each cellulose solution. Steeper decreasing is observable only in the case of OK CEL 4 w% sample, during initial increasing of temperature.

## Evaluation of cellulose derivates for wound healing dressing

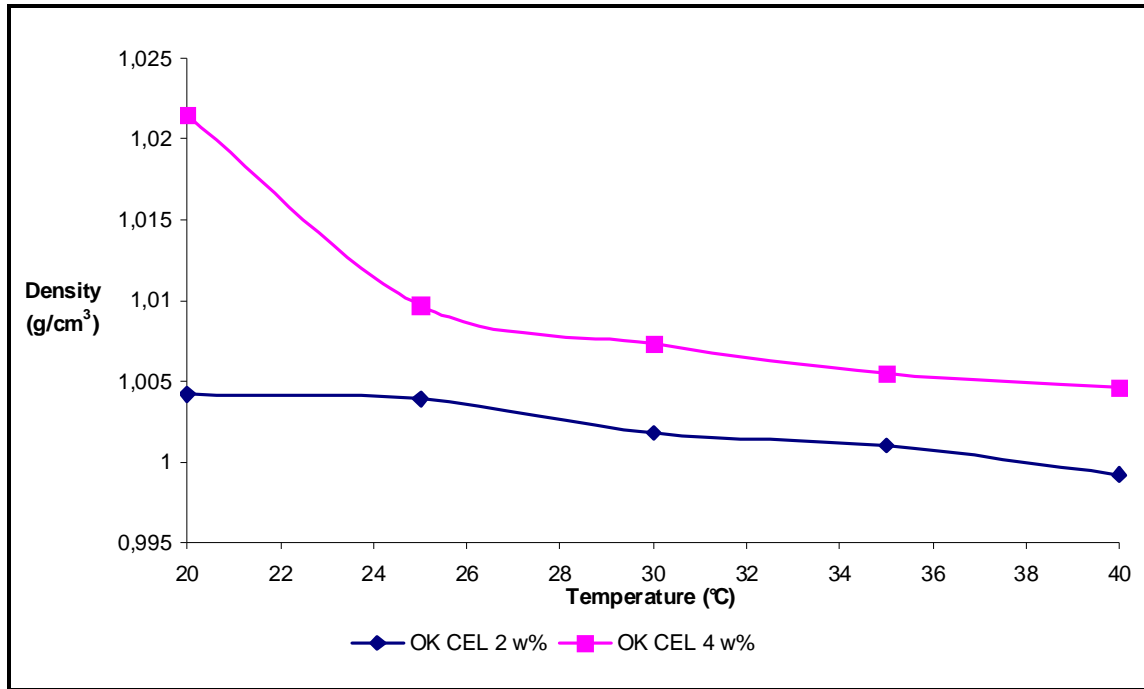


Figure 3.1: Temperature dependence of OK CEL solution density.

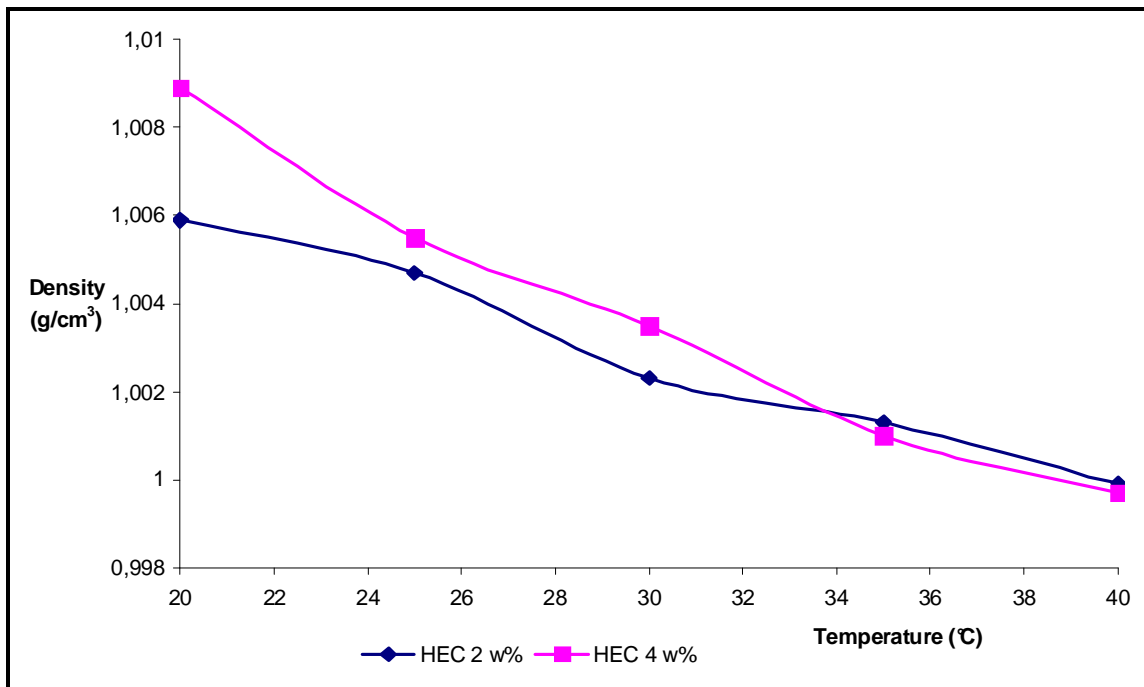


Figure 3.2: Temperature dependence of HEC solution density.

The low influence of solution concentration could be observed in case of HEC. Contrariwise, the higher influence of solution concentration is significant in case of CMC solution.

This is what was expected and the values of density are used to set up initial settings of the instrument for surface tension and contact angle measurements.

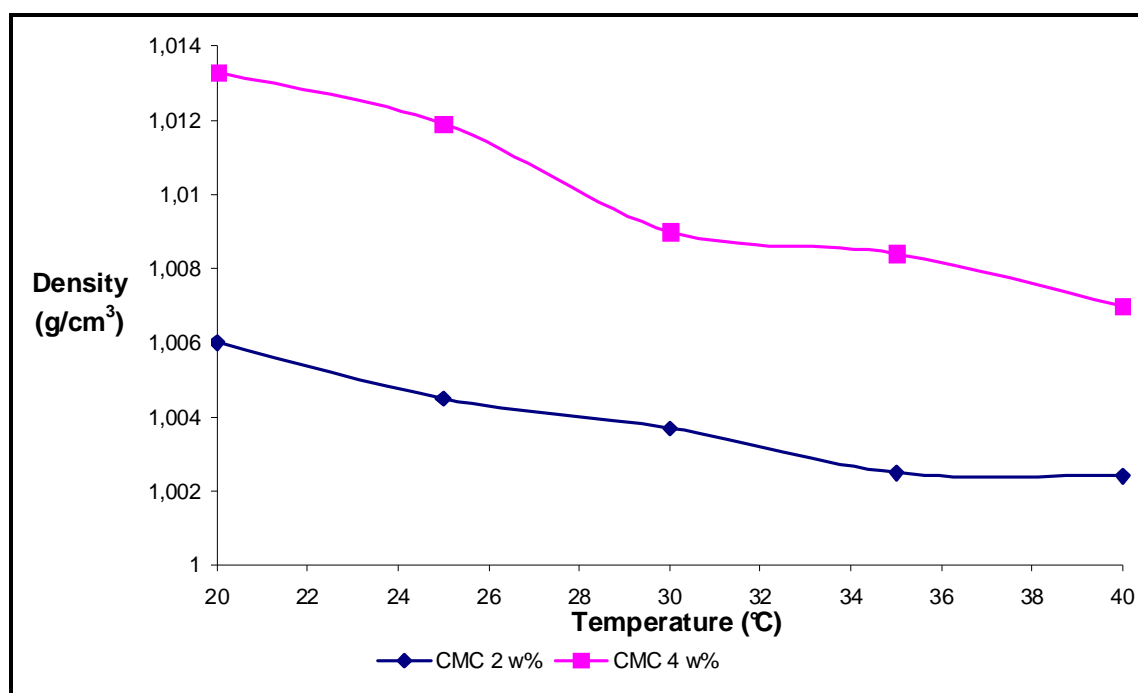


Figure 3.3: Temperature dependence of CMC solution density.

### 3.3.2 Surface tension measurement

Our imposition was to investigate surface tension of three cellulose derivate solutions OK CEL, HEC and CMC. These derivatives were investigated as different concentrated solutions (2 w%, 4 w%). The main point of this measurement was to investigate how the surface tension of these cellulose solutions reacts on increasing temperature and concentration of solutions. It was expected that surface tension could decrease with increasing temperature.

These data are also presented in more general charts on Figure 3.4, Figure 3.5, Figure 3.6. In this table and charts it is significantly shown that the surface tension has a decreasing trend with increasing temperature. The critical temperature, where the surface tension is equal to zero, was not evaluated in our measurement.

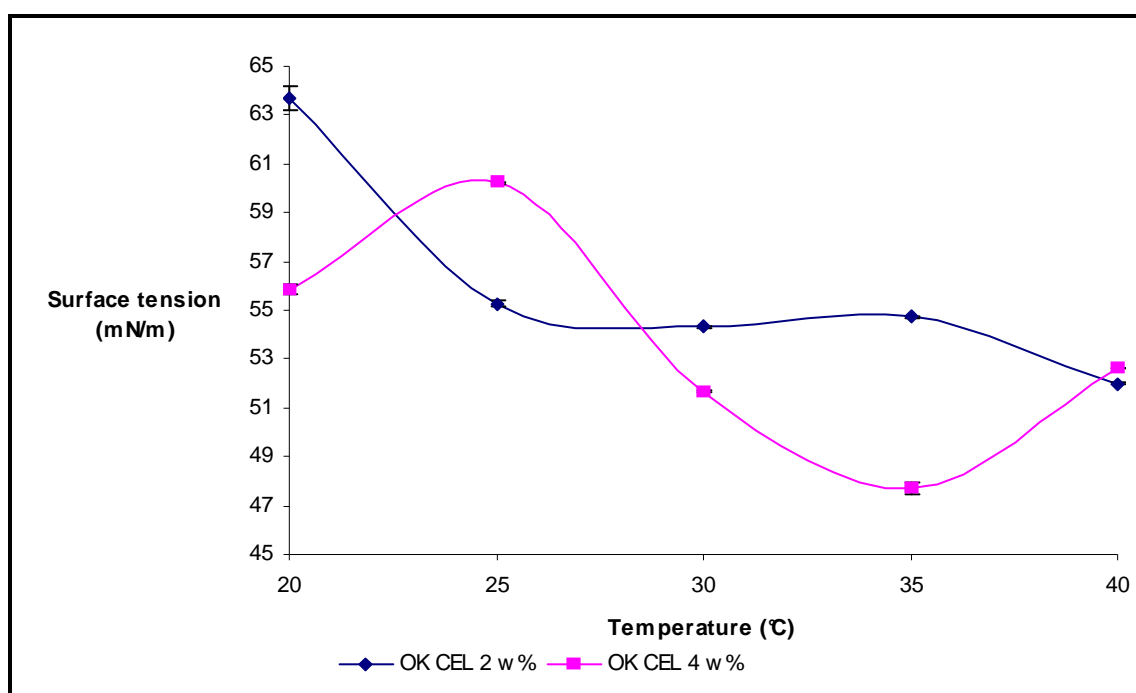


Figure 3.4: Temperature dependence of OK CEL solution surface tension.

In case of OK CEL 2 w% solution it could be sum up that there is streamer decreasing of surface tension in temperature range 20 – 25 °C. Other decreasing is slow and gradual. Surface tension of OK CEL 4 w% varies with big changes in setting temperature range. The same behaviour could be observed in the case of both concentrations of HEC solutions. The decrease of surface tension is slow and gradual.

Surface tension decrease, in case of CMC solutions, is slow in temperature range 20 – 25 °C. Than surface tension decreases suddenly and rapidly. It is

shown that values of surface tension of our investigated samples are much lower than surface tension of water.

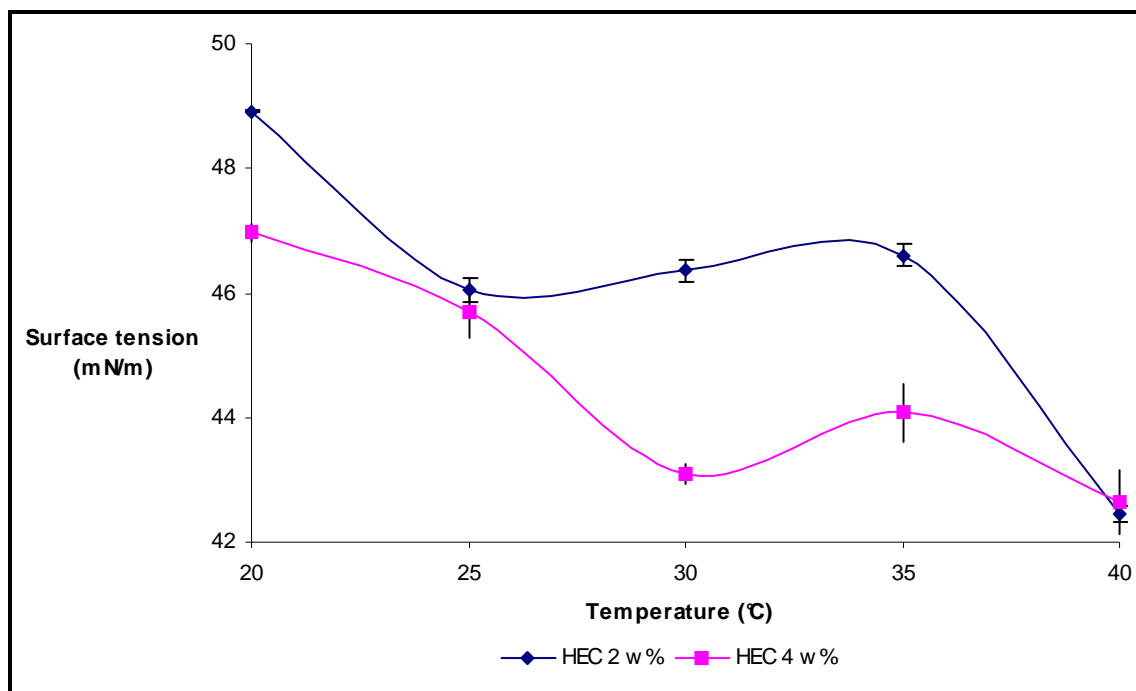


Figure 3.5: Temperature dependence of HEC solution surface tension.

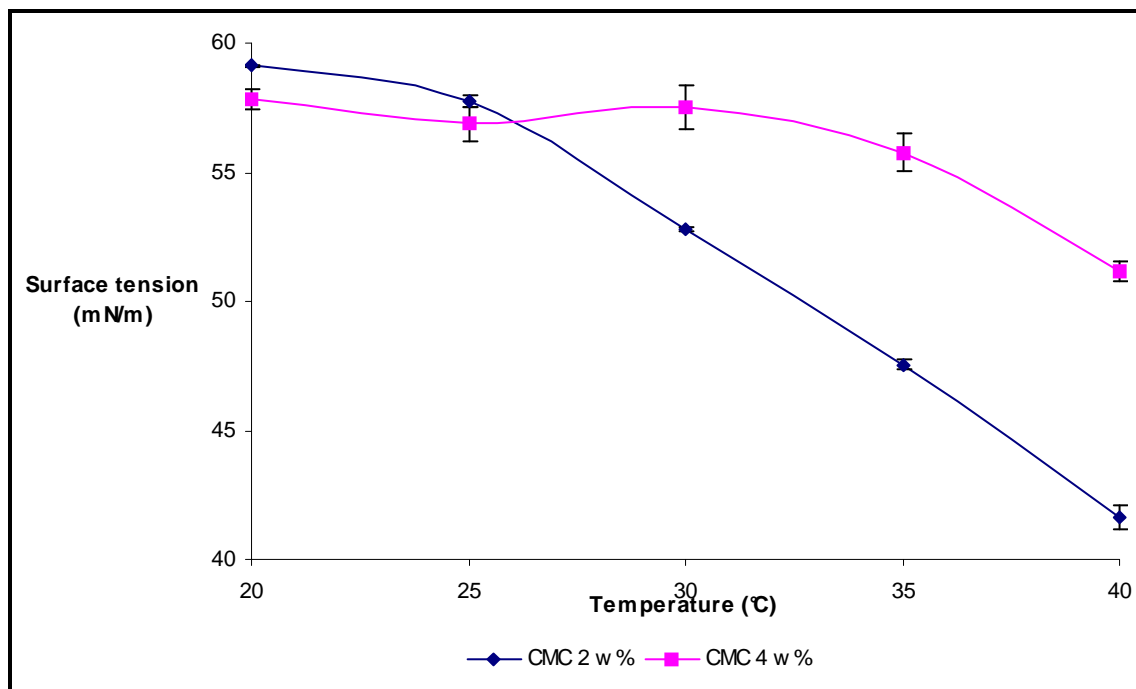


Figure 3.6: Temperature dependence of CMC solution surface tension.

The data from surface tension measurement were recalculated and results for OK CEL solution are presented in chart on Figure 3.7.

These data were elaborated by linear regression and the final equation was equaled with equation (2). The linearity data and their equations are used to calculate surface free energy. The results of this elaboration are values of surface free energy.

The highest surface free energy is observed in case of CMC 2 w% solution. Results of recalculation for HEC and CMC solutions are presented in followed diagrams presented in

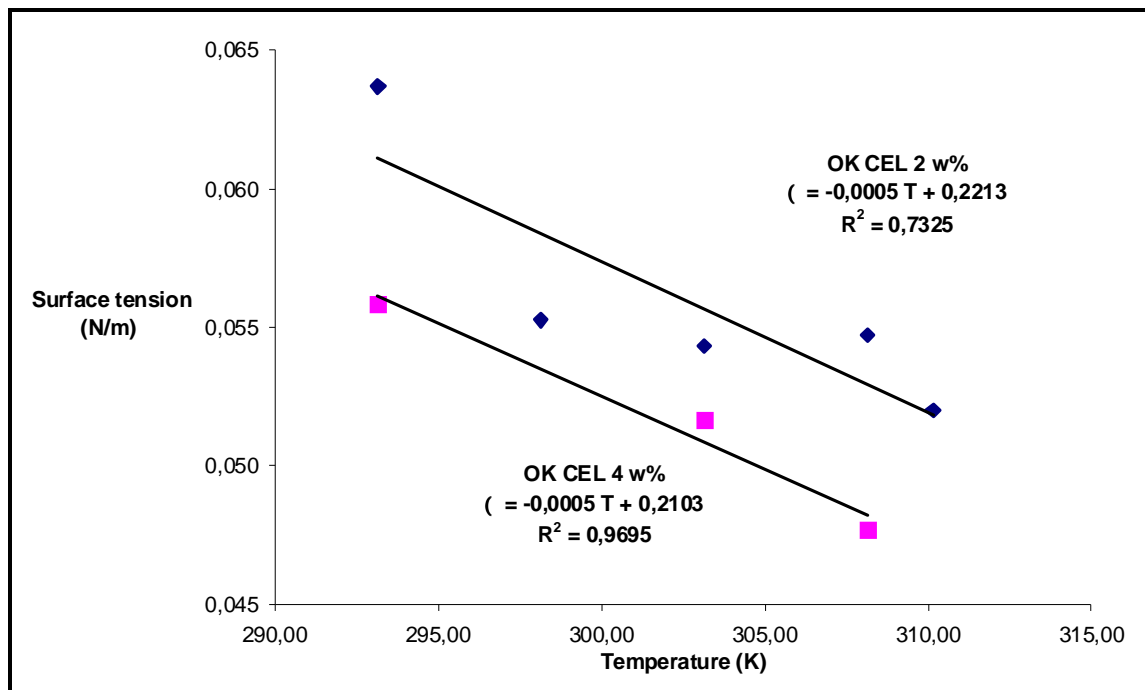


Figure 3.7: The diagram presents the OK CEL temperature relation of the surface tension. These linearity and their equations were used to calculate the surface free energy.

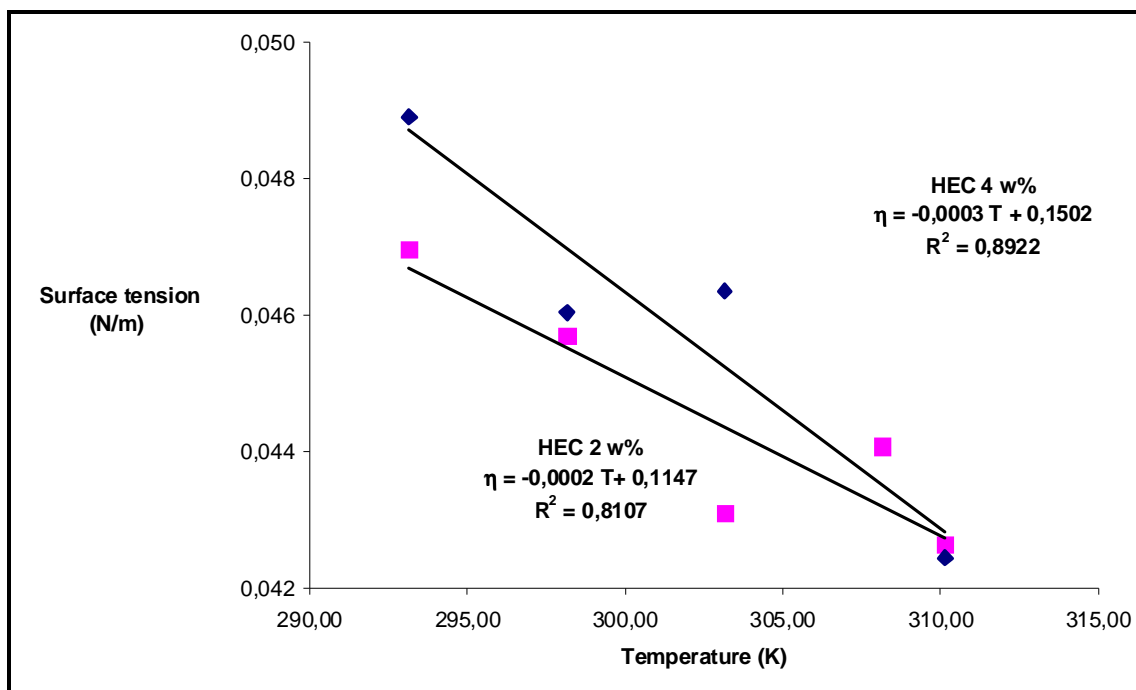


Figure 3.8: The diagram presents the HEC temperature relation of the surface tension.

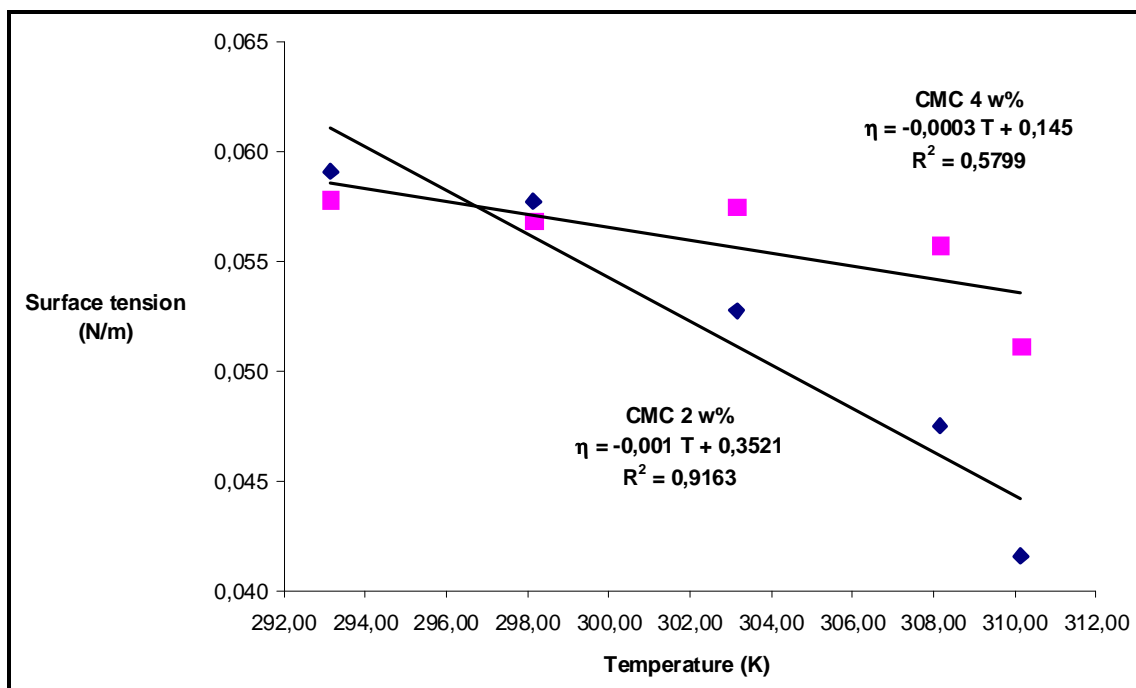


Figure 3.9: The diagram presents the CMC temperature relation of the surface tension.

### 3.3.3 Contact angle measurement

Another characteristic of cellulose derivates is their contact angle. The advancing and receding contact angle was investigated by the Ring method on the Tensiometer K12. The effect of increasing temperature on contact angle was evaluated. The measurement was done for two weight concentrations (2 w%, 4 w%) of each cellulose sample (OK CEL, HEC, CMC). The temperature subjection is digestedly demonstrated at diagrams on Figure 3.10, Figure 3.11, Figure 3.12. Here it is demonstrable shown that receding contact angle is smaller than advancing contact angle.

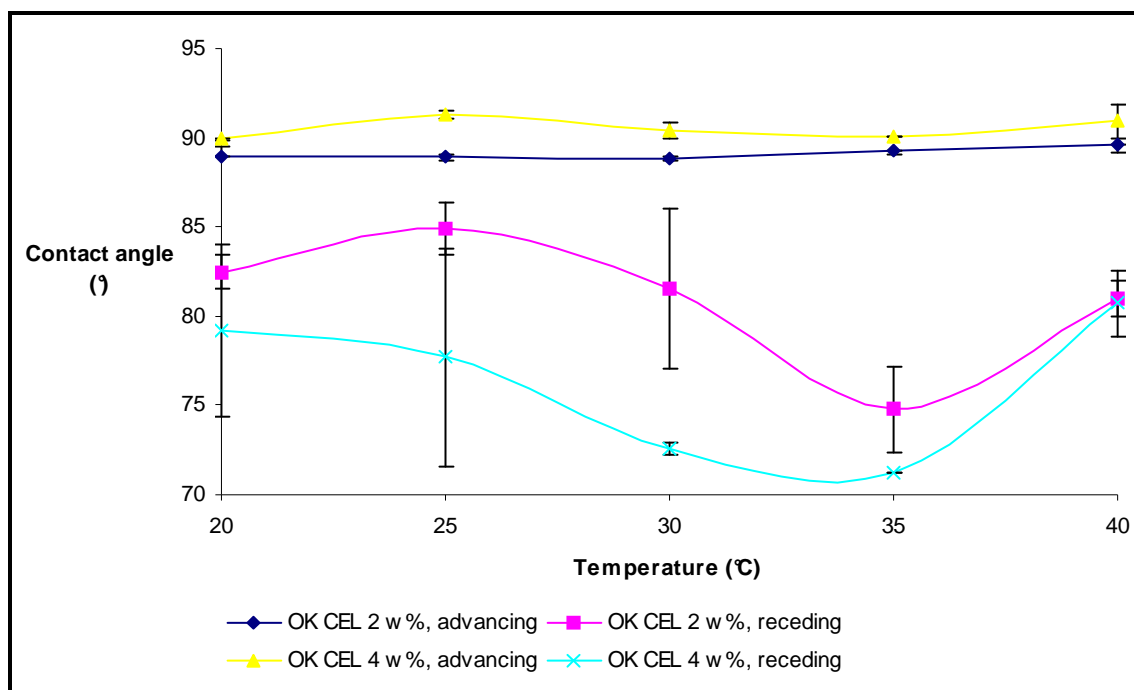


Figure 3.10: These charts show temperature dependence of advancing and receding contact angle. They also show differences cause by different weight concentration of cellulose solution.



In case of OK CEL and HEC solutions the advancing contact angle only slightly depends on increasing temperature or solution concentration. The receding angles have the same continuance. The two curves, which represent each weight concentration of one cellulose solution, slightly vary in the same range.

For every sample applies that the advancing angle is higher in case of 4 w% solutions and the receding angle is higher in case of 2 w% solutions. The great peak on advancing angle curve could be observed in case of 4 w% CMC solutions at temperature range around 30°C. It could be concluded that the solution is highly hydrophobic in this temperature point. In case of other samples it could be concluded that the wet-ability is not influenced by temperature of solution or its concentration.

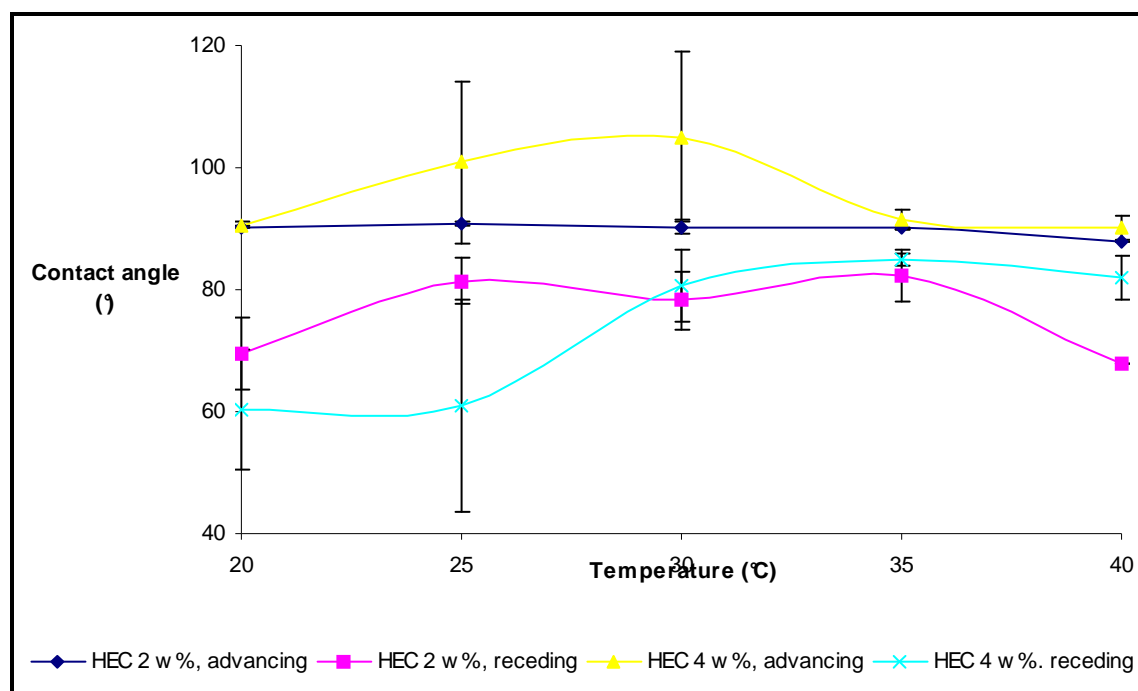


Figure 3.11: These charts show temperature dependence of advancing and receding contact angle. They also show differences cause by different weight concentration of cellulose solution.

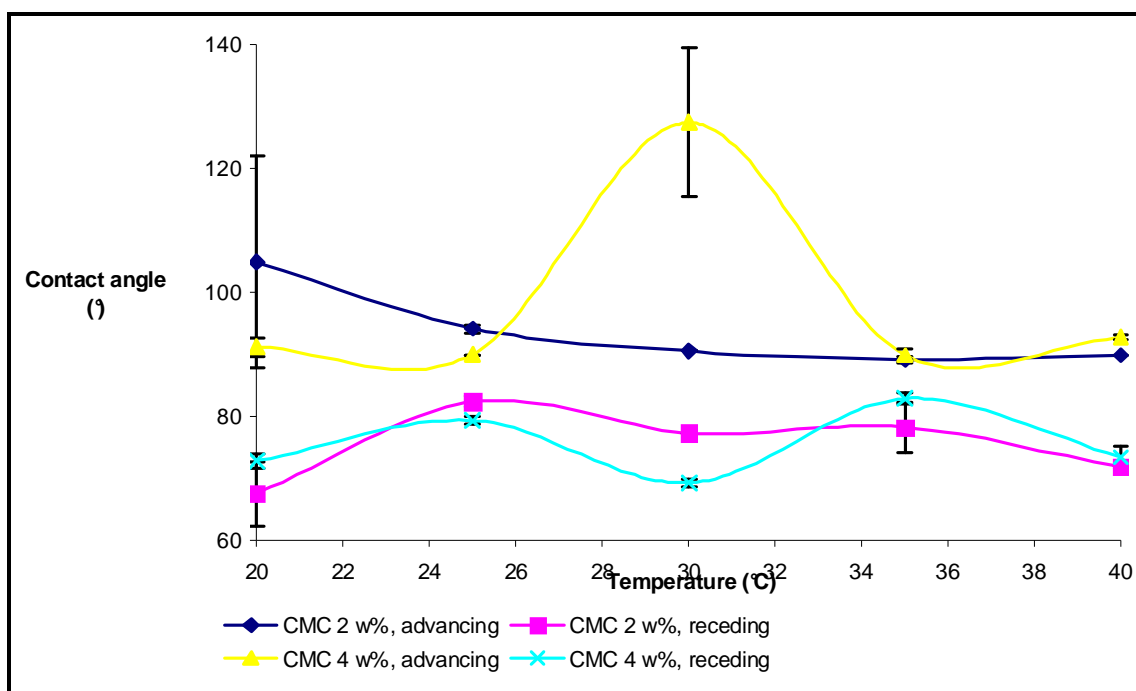
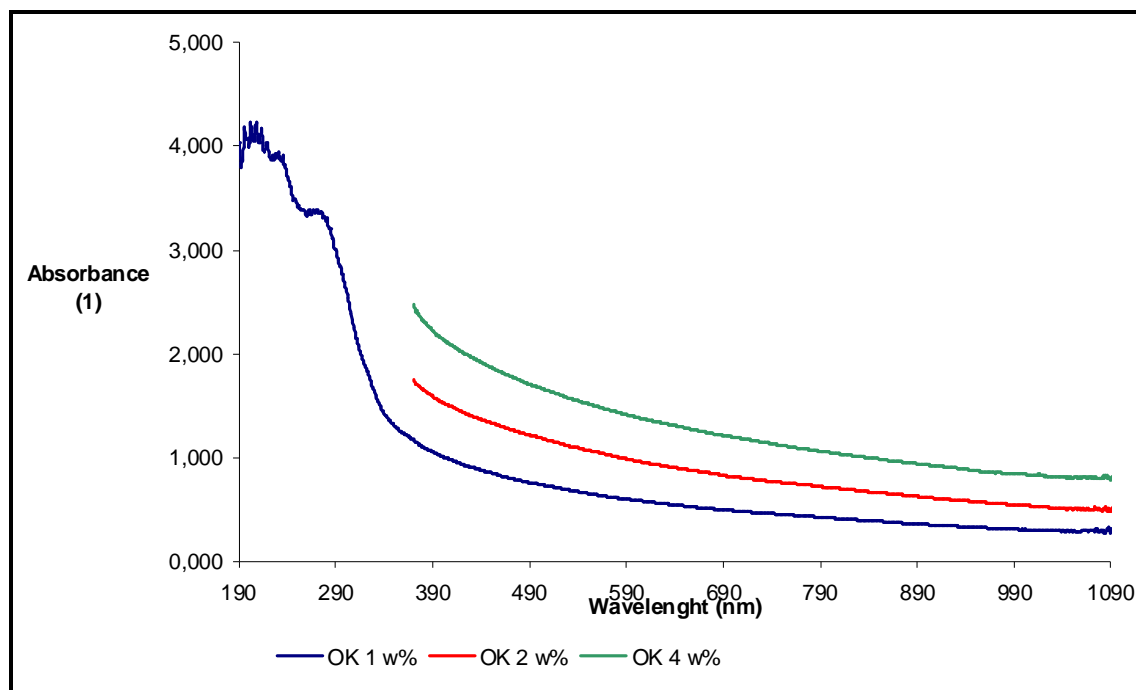


Figure 3.12: These charts show temperature dependence of advancing and receding contact angle. They also show differences cause by different weight concentration of cellulose solution.

### 3.3.4 UV-VIS spectroscopy

Another point of our work was to investigate how concentration of cellulose solution influences absorbance of ultraviolet and visible light. The measurement was done for three different weight concentrations of each derivate (1w%, 2w% and 4 w%). The data obtained by this measurement are presented for OK CEL solution in Figure 3.13.

The curves in this presented chart represent three different concentrations of cellulose solution. It is significant that the higher solution concentration the higher light absorbance.



*Figure 3.13: These graphs are obtained from absorbance measurement. They show absorbance dependence on cellulose solution concentration.*

The absorbance is much higher on case of OK CEL solutions. This is not observable on case of HEC and CMC solutions. For OK CEL it could be observe small absorbance of light in ultraviolet and the incipient phase of visible light. It could be cause by the transitions, which are observable in the wavelength, range 190 – 400 nm. And the absorbance of light in the incipient phase of visible light characterizes yellowish and opalesque character of OK CEL solution. It means that molecules in OK CEL solution refract the light beam and it causes that whole solution looks as slightly yellowish.

For HEC and CMC solutions this is not observable because they are clear. Here is also observable only the absorbance in UV part of spectrum which is cause by transitions.

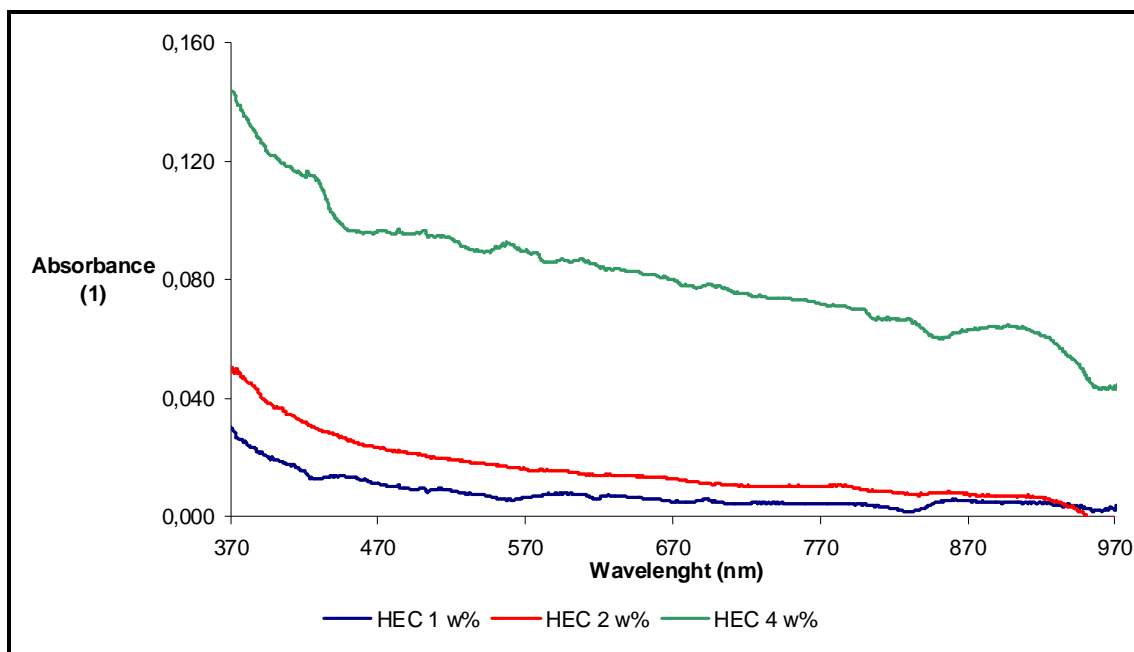


*Figure 3.14: These graphs are obtained from absorbance measurement. They show absorbance dependence on cellulose solution concentration.*

These data was elaborated for particular wavelength (400, 700 nm) to show the trend about solution concentration influence on light absorbance. These elaborated data are clearly at Figure 3.15. In these charts the linear regression is used to elaborate data. From linear regression equations the extinction coefficient are calculated for particular cellulose solution.

These charts affirm the conclusion, that absorbance increase with increasing concentration of the solution.

Extinction coefficient is the highest for OK CEL solution, and low for HEC and CMC solutions.

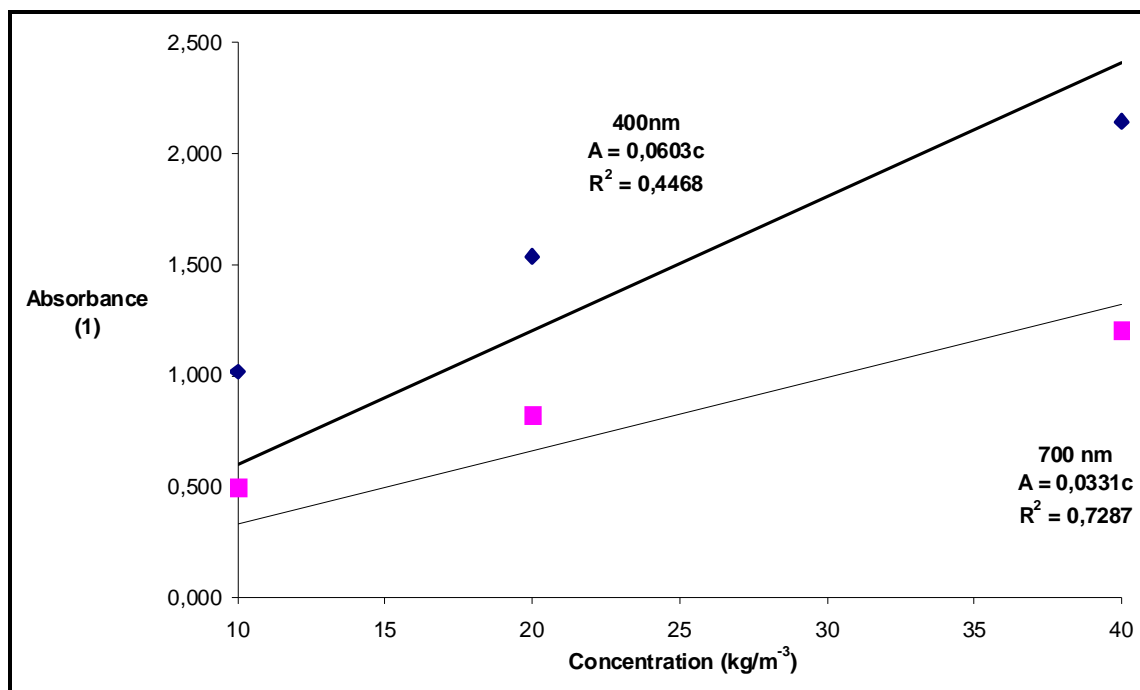


Figure 3.15: These charts show the relation between cellulose solution concentration and absorbance. The equations of linear regression were used to calculate extinction coefficient.

Other aim of UV-VIS spectroscopy was to evaluate pH influence on light absorbance. This investigation was done in pH range 2 – 12. The data obtained in this measurement are presented in Figure 3.16. In case of OK CEL solutions it could be observe that light absorbance decrease with increasing pH till pH about 5. Than suddenly increase and at the end of pH range decrease again. This behaviour is much noticeable on case of solution which 2 w% concentration.

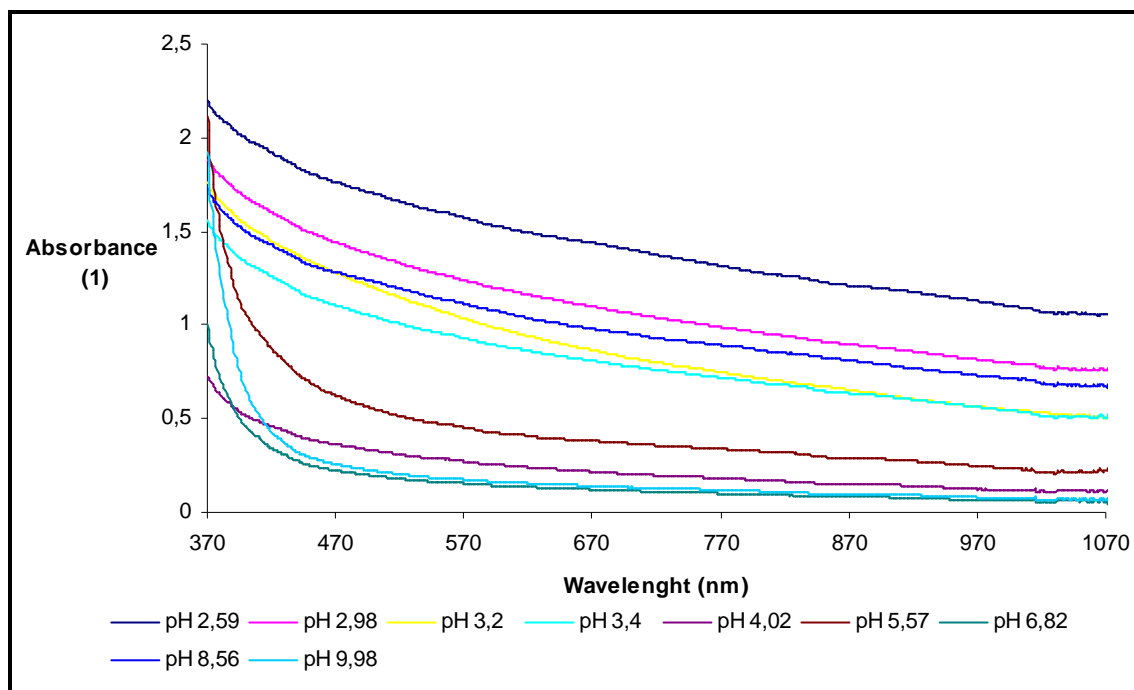


Figure 3.16: This chart shows the values of pH dependence of 2 w% OK CEL solution absorbance.

Regarding to HEC and CMC solutions, there is not any evidence of pH influence on light absorbance.

Data pertaining to wavelength 400 and 700 nm, which were obtained by this measurement, were selected and they are presented by the charts in the Figure 3.17, Figure 3.18. Here is significantly shown that for OK CEL the dependence vary in whole pH range. There is apparent sudden decrease of absorbance in pH range 2 – 5 for both weight concentrations.

Absorbance for HEC and CMC solutions is not almost subject to pH. These findings are illustrated by Figure 3.19.

The no-dependence of UV-VIS light absorbance on pH for 2 and 4 w% solution of CMC is presented here for 400nm wavelength.

## Evaluation of cellulose derivates for pulsed drug delivery

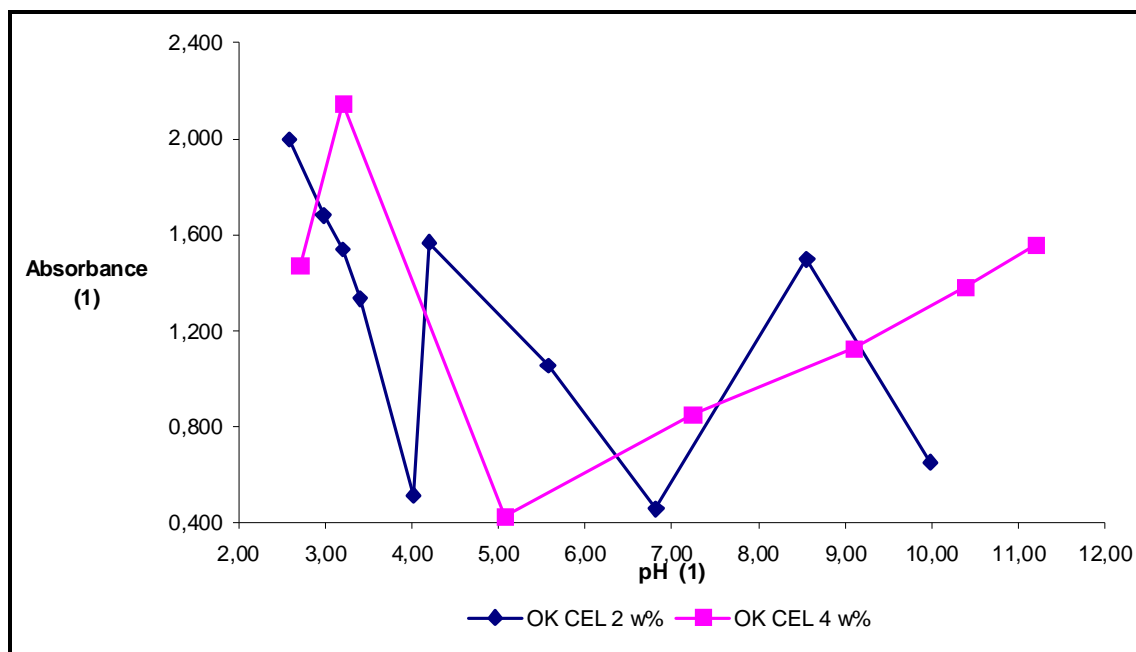


Figure 3.17: These diagrams present pH dependence of absorbance. These values belong to the wavelength 400 nm.

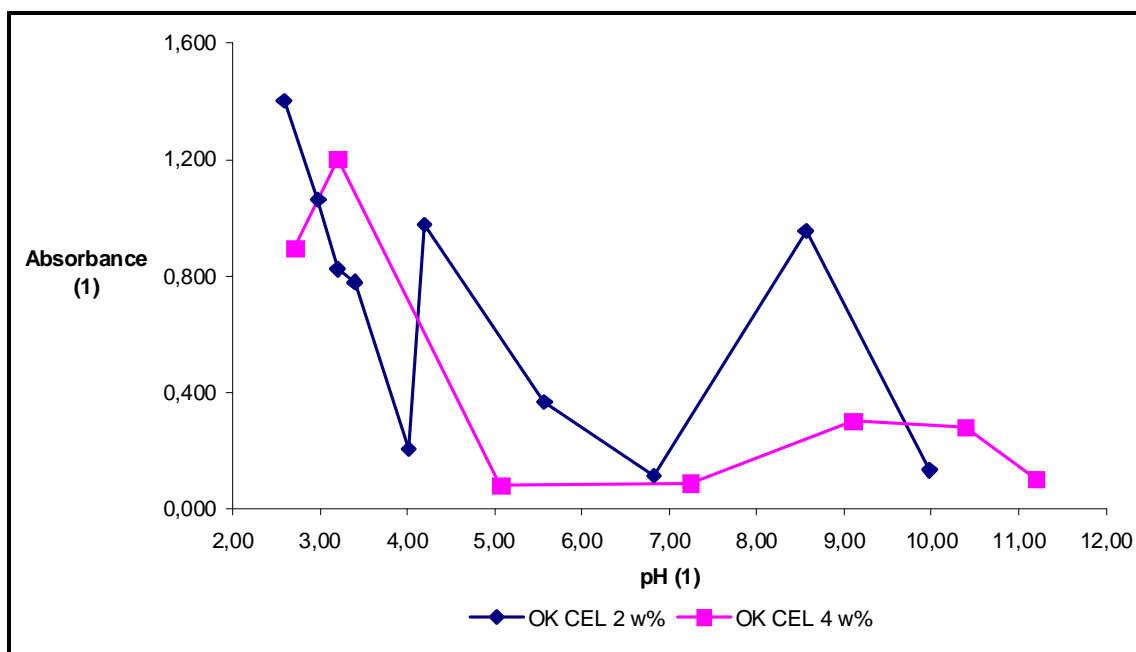


Figure 3.18: These diagrams present pH dependence of UV-VIS (700nm) absorbance. Data are presented for two solution concentrations.

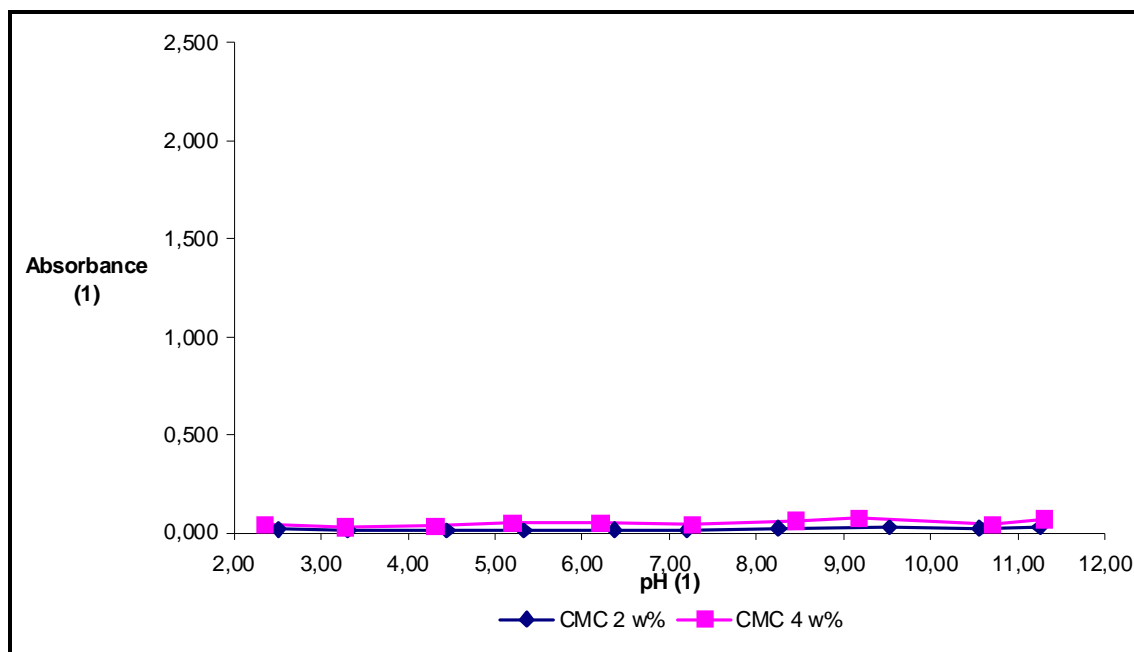
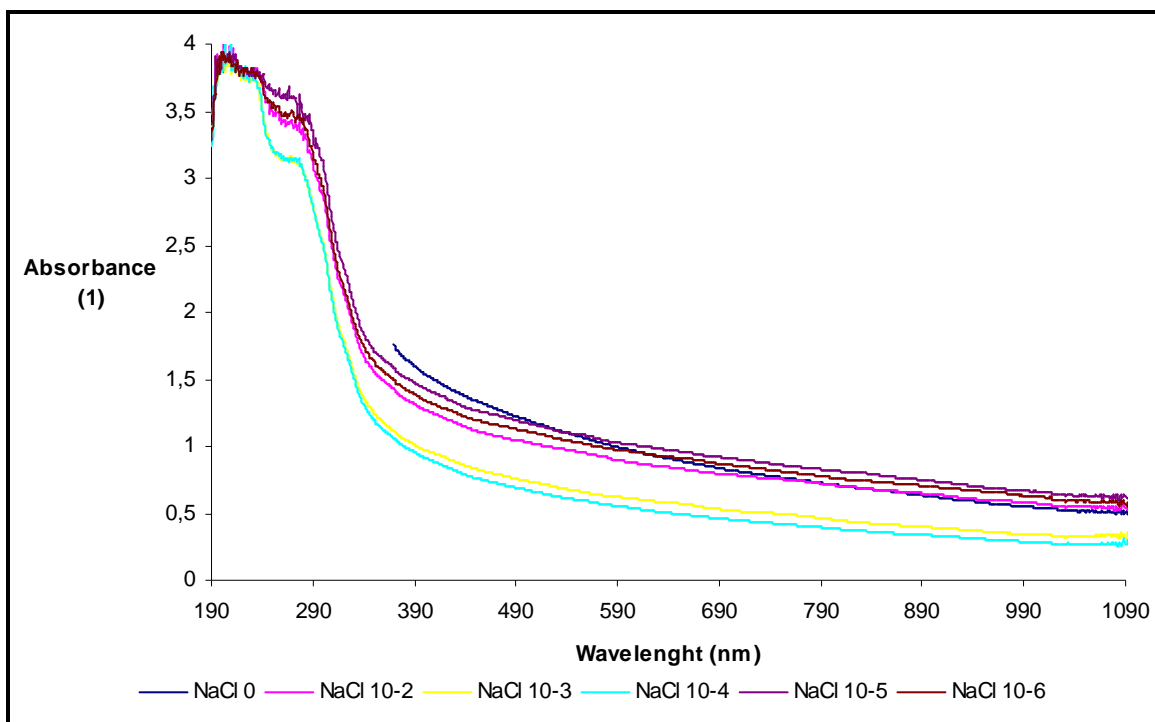


Figure 3.19: Diagram presents solution pH influence on absorbance for CMC solution for 400 nm wavelength.

Third aim for UV-VIS spectroscopy was to evaluate ionic concentration influence on light absorbance. This investigation was done for concentration 0,  $10^{-6}$ ,  $10^{-5}$ ,  $10^{-4}$ ,  $10^{-3}$ ,  $10^{-2}$  of NaCl. Cellulose solutions were diluted in ration 1:1, as described in part preparation of samples. It means that concentration of cellulose solutions is half-size (1 w%, 2 w%). The data obtained by these measurements are presented at diagrams lower.





*Figure 3.20: These curves represent relation between absorbance and increasing ionic concentration in cellulose solution. These values belong to 2w% OK CEL solution.*

For higher lucidity, data pertaining to wavelength 400 and 700 nm, were selected to show the trend of this influence. In these diagrams, when the curves represent different weight concentration, it is outward that the ionic concentration does not influence the light absorbance.

## Evaluation of cellulose derivates for wound healing dressing

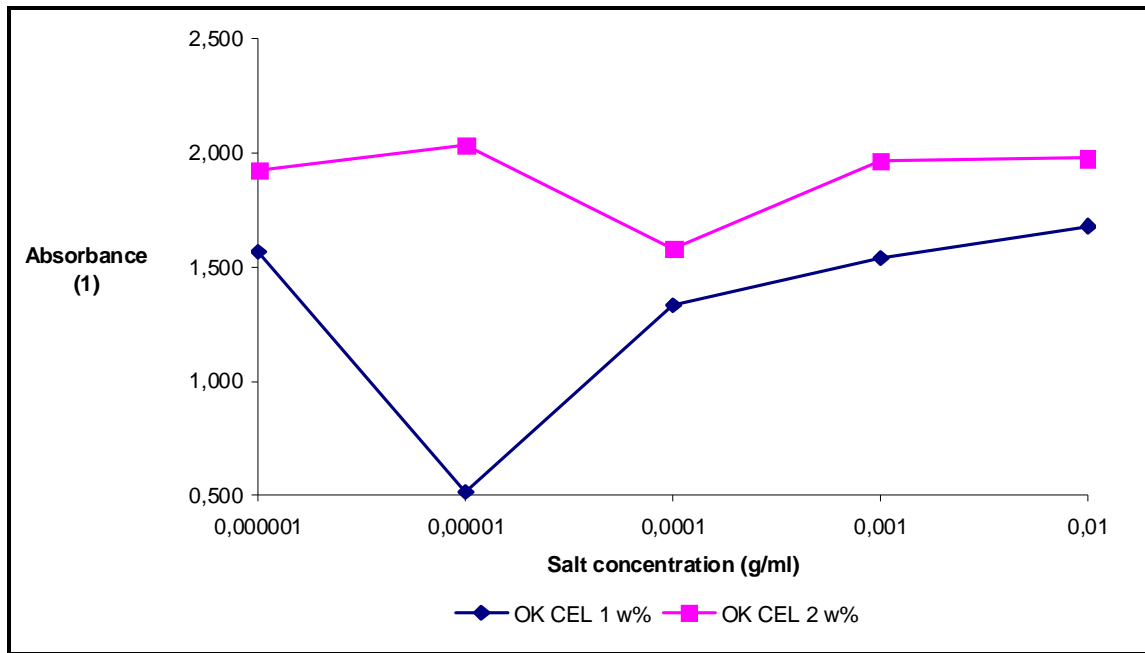


Figure 3.21: These charts present ionic concentration influence on solution UV-VIS light absorbance (400nm).

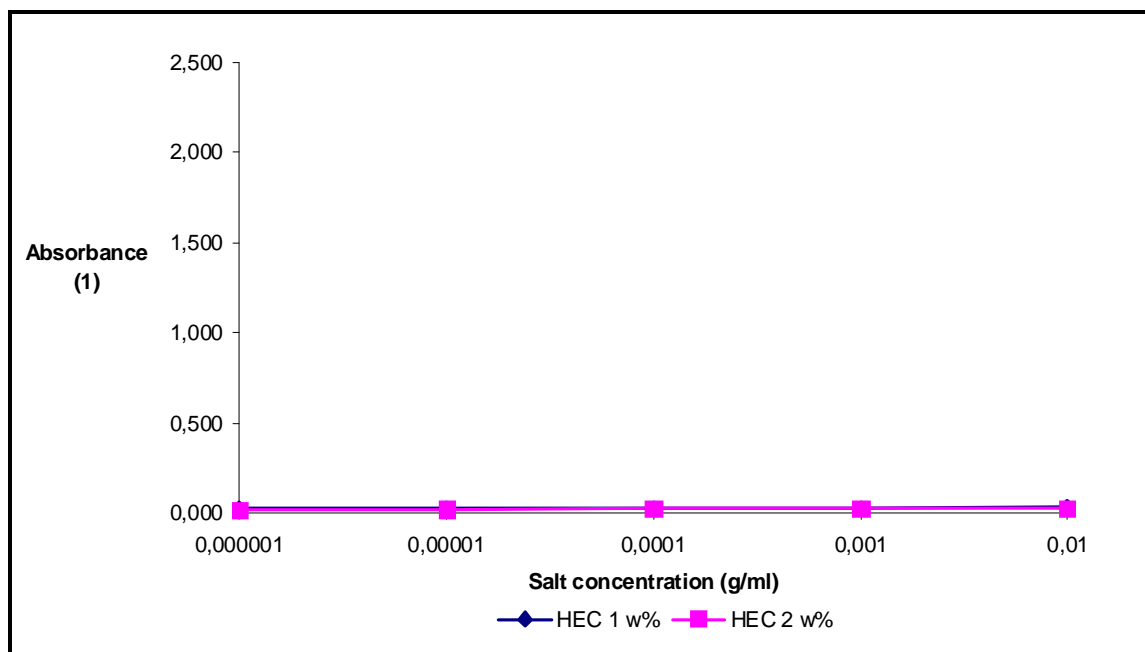


Figure 3.22: These charts present ionic concentration influence on UV-VIS light absorbance (400 nm).

## Evaluation of cellulose derivates for pulsed drug delivery

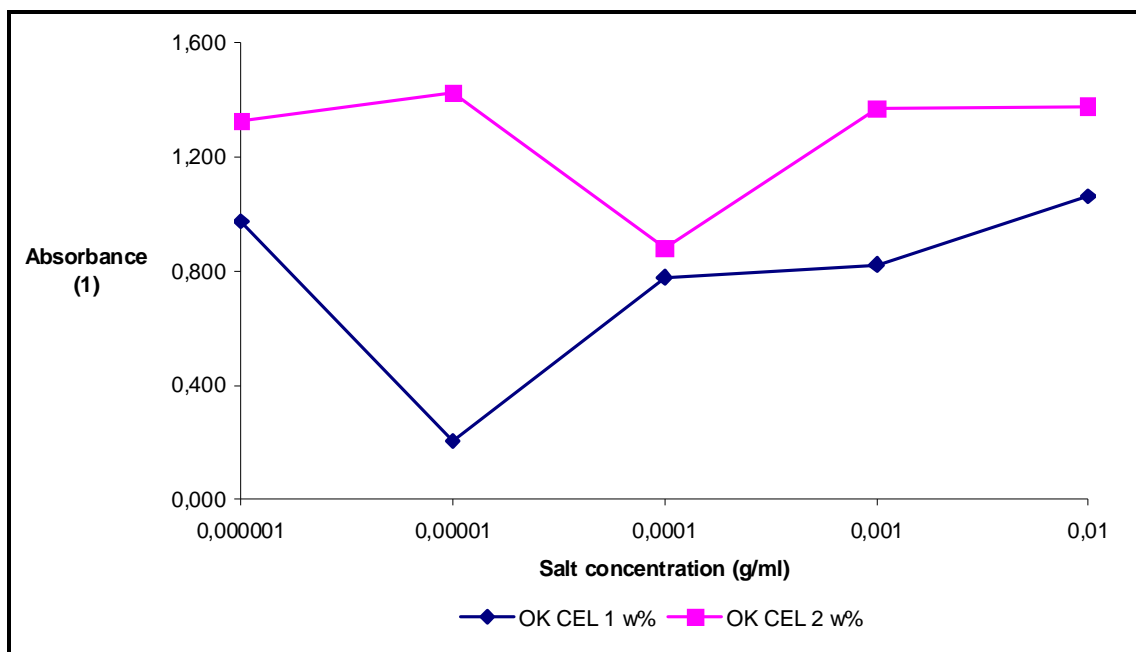


Figure 3.23: These curves present dependence of OK CEL solution UV-VIS light absorbance (700nm) on ionic concentration.

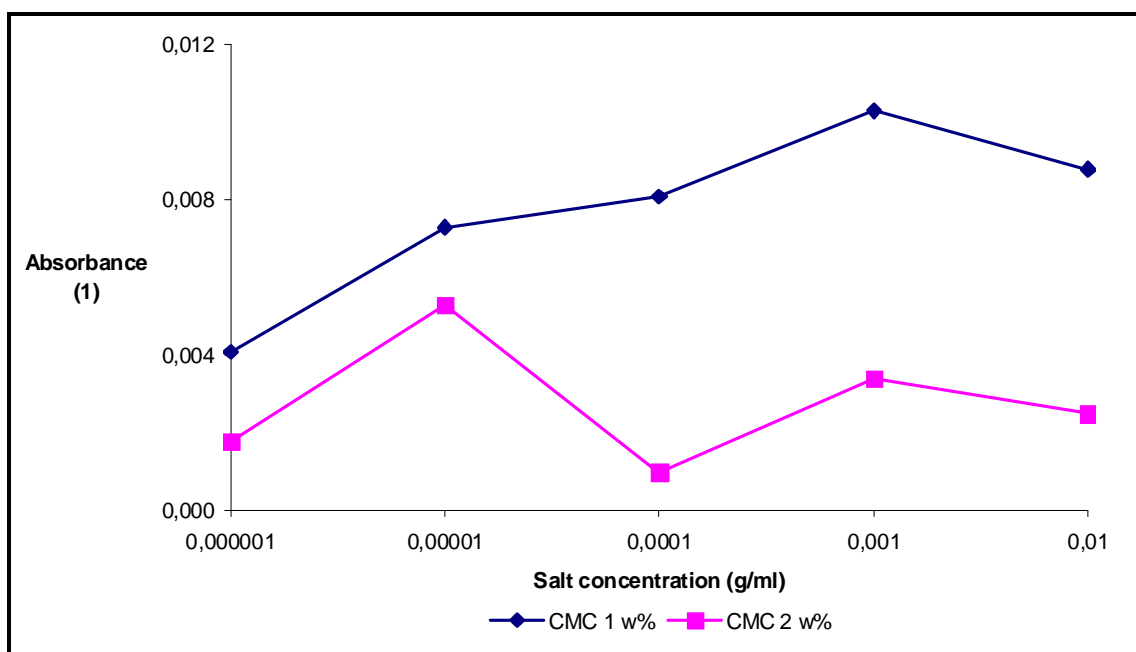


Figure 3.24: These curves present dependence of CMC solution UV-VIS light absorbance (700 nm) on ionic concentration.

### 3.3.5 Measurement of the particle diameter

The measurement of the particle size was done for two weight concentrations (2 w%, 4 w%) of each cellulose derivate sample (OK CEL, HEC, CMC). The aim of this measurement was to evaluate the influence of pH and ionic concentration on size of the colloidal particles. Data obtained by measurement of pH influence are presented and elaborated as curves at Figure 3.27.

For OK CEL solution is significantly observable that particle sizes are consists in variable cellulose solution pH. The particles diameter of in 2w% solution is slightly contingent. But the particle diameter in 4 w% solution decreases again at the pH range 2 – 4. The ability of molecules to swell is the lowest for pH about 4. From this point the diameter increases gradually.

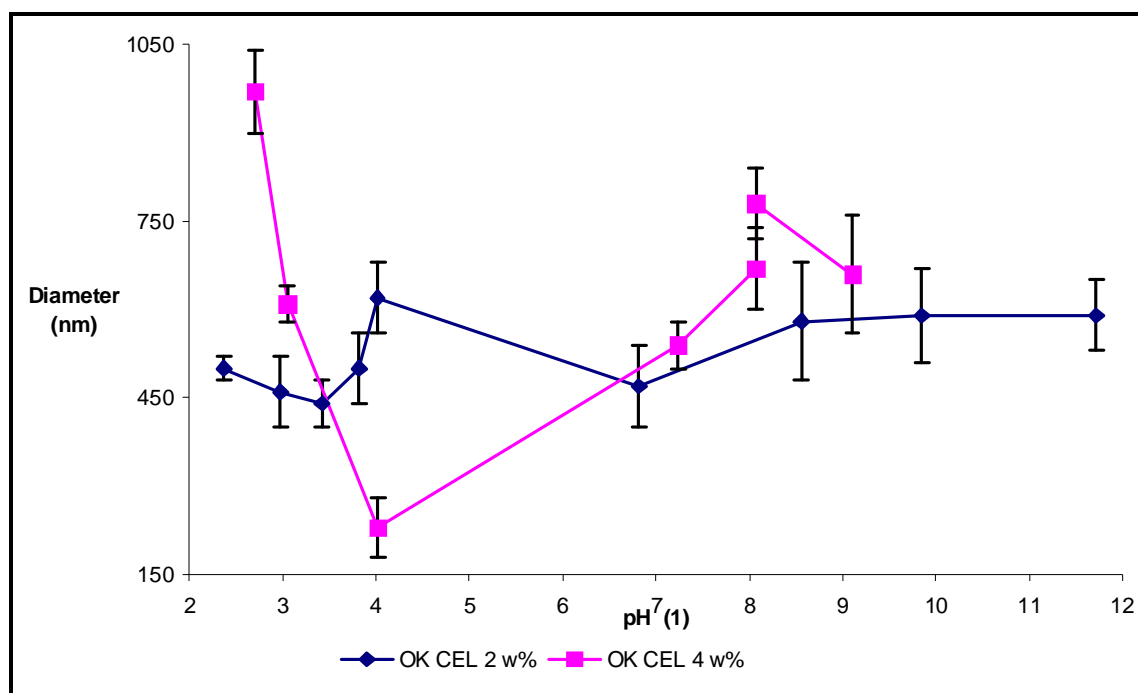


Figure 3.25: The changing OK CEL particle size in variable polymer solution pH.

The investigation also showed that diameter of OK CEL particles is much lower than for HEC and CMC. It is caused by lower ability to absorb water from surrounding solvent.

In case of HEC solution the diameter for 2 w% does not vary very significantly by the instrumentality of changing pH. For 4 w% solution of HEC, it could be concluded that the diameter decreases in pH range 2 – 7. Then the sudden increase is noticeable in pH range 7 – 10, which is followed by sweep decrease. So when solution pH is about 2 or 9, the conditions are good for molecules to absorb water from surrounding solution.

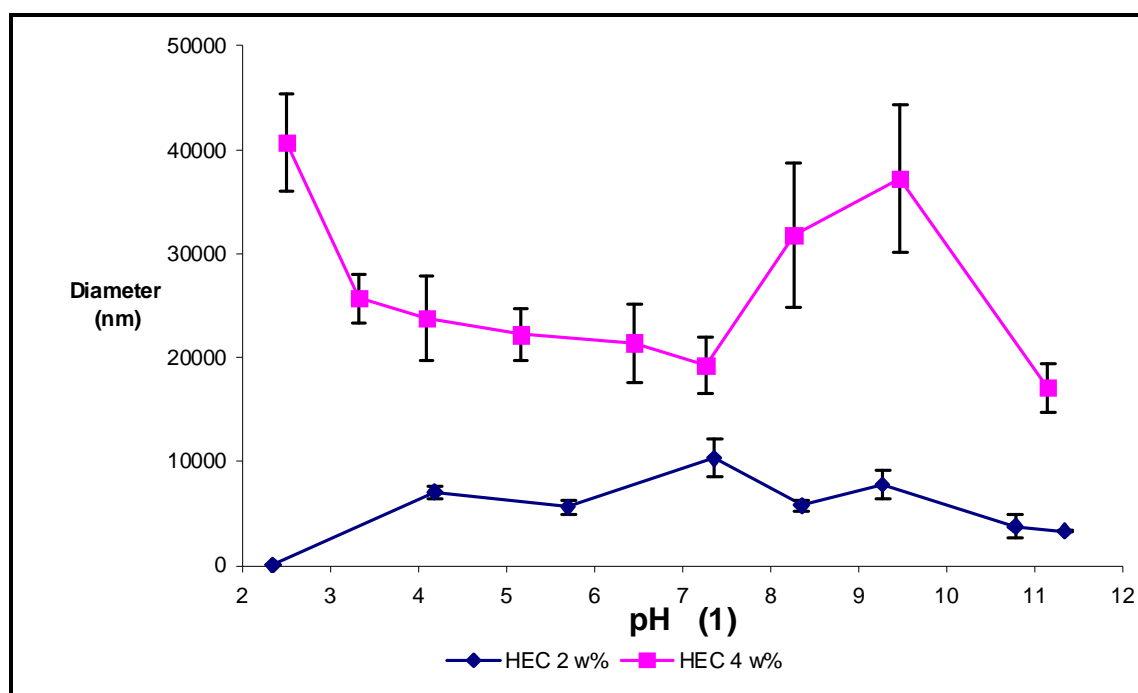


Figure 3.26: The changing HEC particle size with variable polymer solution pH.

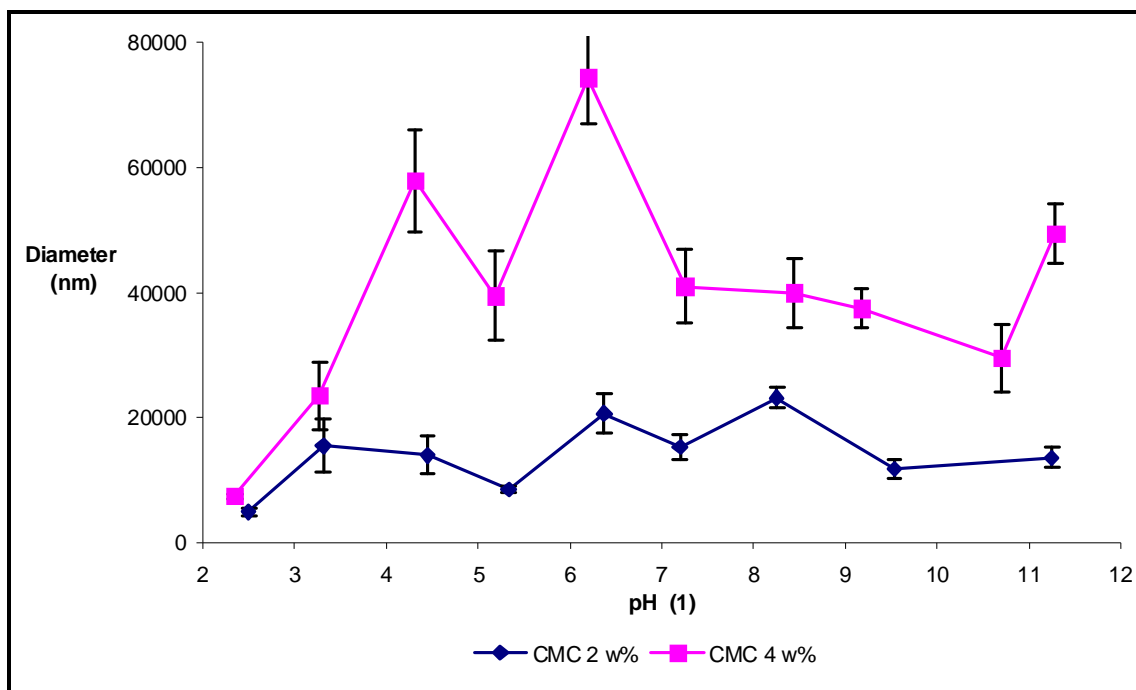


Figure 3.27: The changing CMC particles size with varying polymer solution pH.

The curves, which represent 2 and 4 w% of CMC solution, show that particle size depends on pH of solution. The apparent increase of diameter size could be observed in pH range 2 – 5. It is more visible for 4 w% samples. It could be concluded that water absorbability is pretty well, when the solution has pH about 4 and 6.

This part of study also investigated particle diameters and how could be influenced by changing ionic concentration. As previously mentioned the samples were prepared by diluting basic concentrated samples by NaCl solution in ratio 1:1. Newly obtained weight concentrations are 1 w% and 2 w%.

Measured values procured by this measurement are introduced on Figure 3.30. Here it is apparent influence of ionic concentration on particle size.

## Evaluation of cellulose derivates for pulsed drug delivery

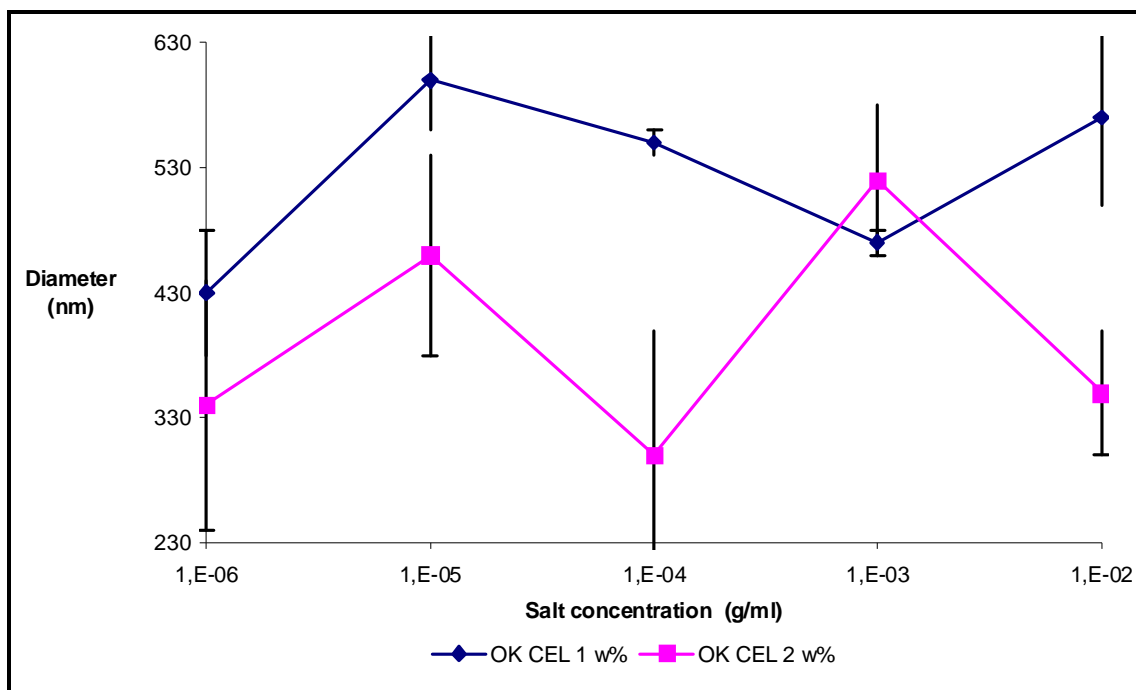


Figure 3.28: These curves represent data of particle diameter and their dependence on ionic concentration in OK CEL solution.

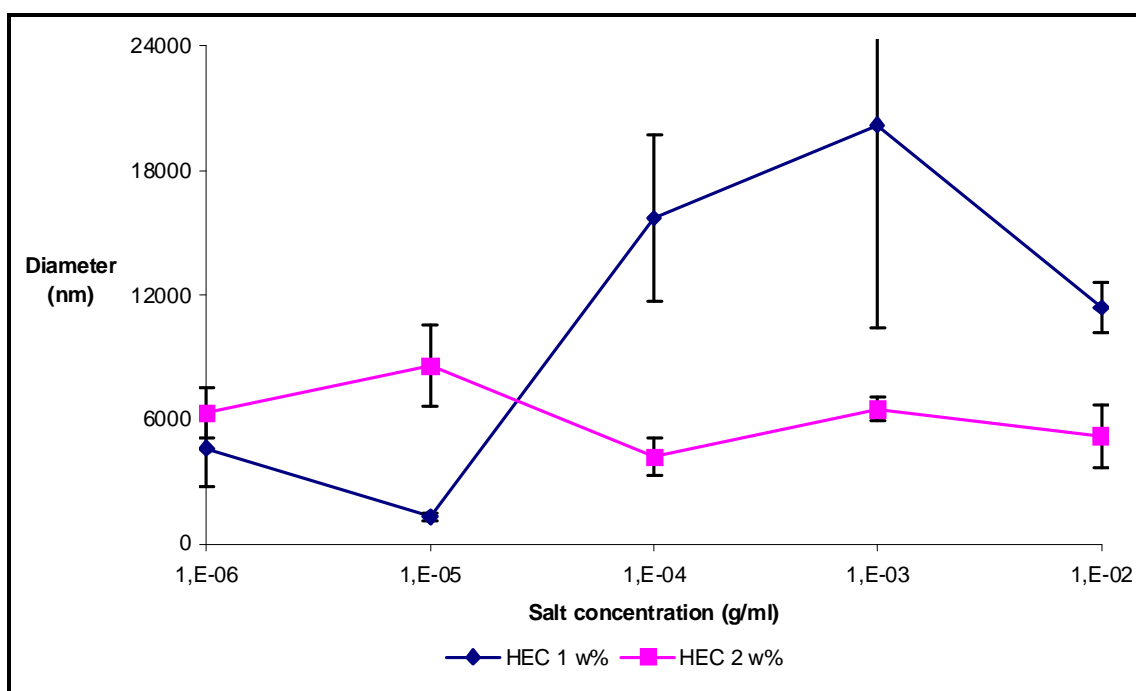


Figure 3.29: These curves represent data of particle diameter and their dependence on ionic concentration in HEC solution.

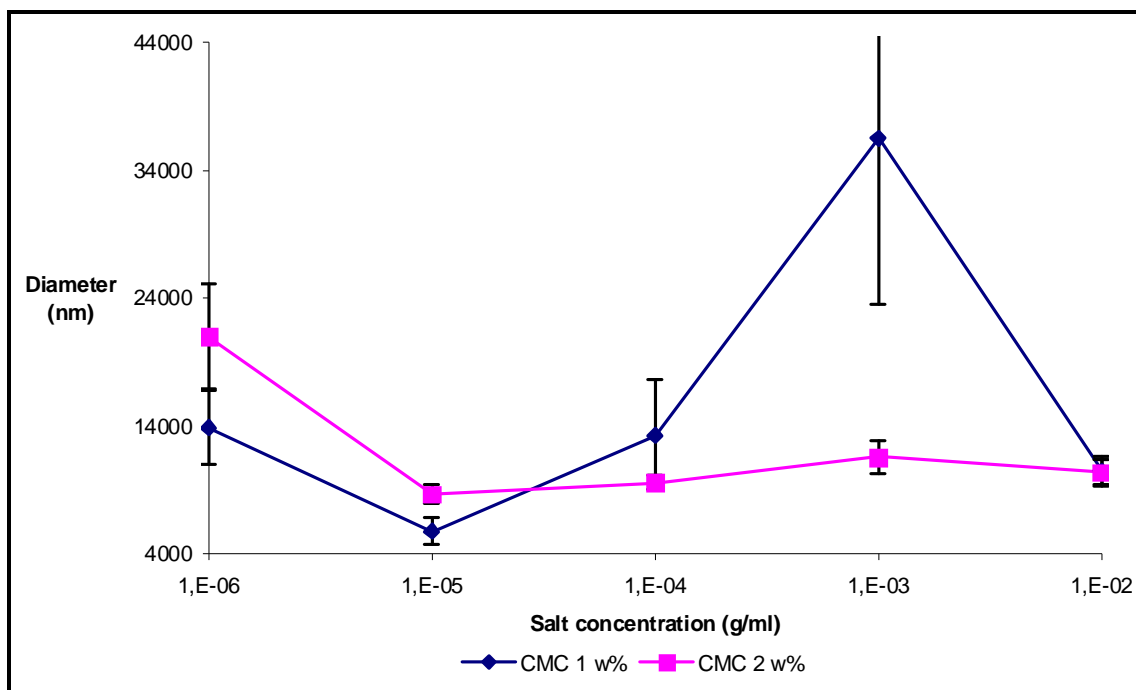


Figure 3.30: These curves represent data of particle diameter and their dependence on ionic concentration in CMC solution.

In case of OK CEL the influence is similar for both concentrations. From results of OK CEL solution measurements one could not concluded any reasonable dependence. In some concentrations of salts in surrounding solutions macromolecules can soak higher amount of surrounded solution in other concentrations macromolecules shrink.

On the other hand measurement of particle size of HEC and CMC solutions in variable ionic concentration. There is perceptible influence of ions, mainly for 1-weight % samples. The absorbability of molecules grows up with increasing ionic concentration. This particle size increasing is not possible for double concentrated solution. Molecules are very close each other and more marked swelling of molecules is not possible.



### 3.3.6 Measurement of zeta potential

The zeta potential measurement was provided on ZetaPlus instrument. The main point of this investigation was to evaluate the relation between pH of cellulose solution and zeta potential. Two weight concentrations (2 w%, 4 w%) of each cellulose derivate solution (OK CEL, HEC, CMC) were determined.

Data, which present solution pH influence on zeta potential, are presented as comprehensible charts in Figure 3.33. It is visible that zeta potential of particles is generally negative. These values present that OK CEL and CMC cellulose solutions are stable in whole measured pH range. HEC cellulose solution is not stable at pH area around 2,5 for 2 w% solution and 7,5 for 4 w% one.

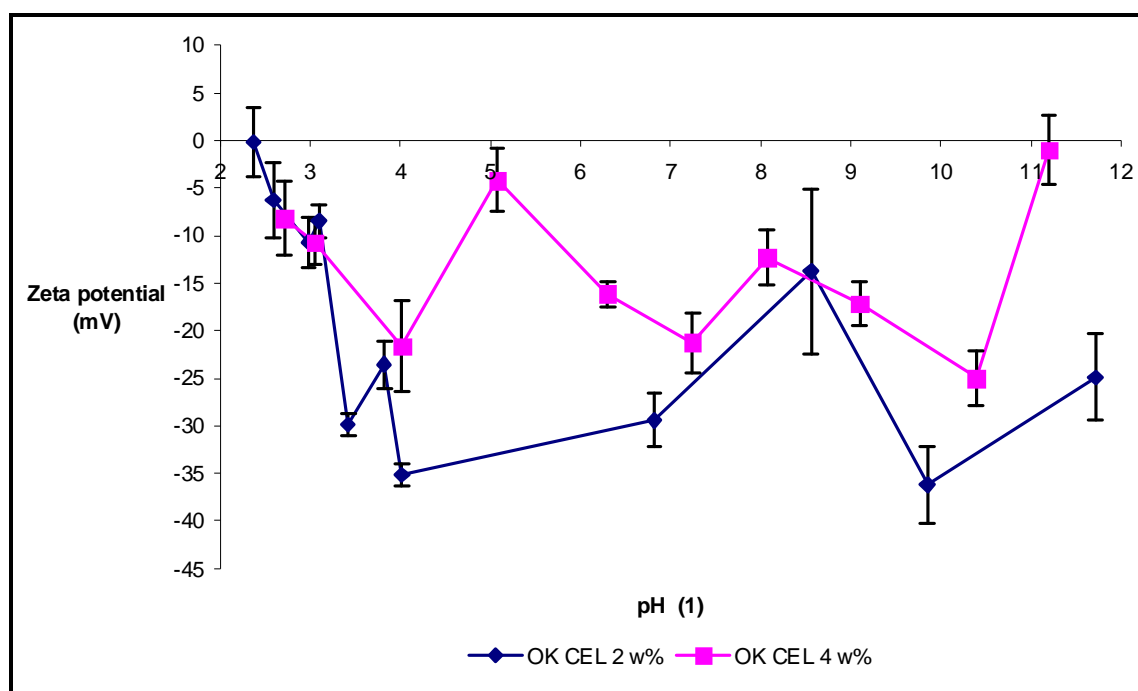


Figure 3.31: This graph shows the functionality of zeta potential and pH of OK CEL cellulose solution.

## Evaluation of cellulose derivates for wound healing dressing

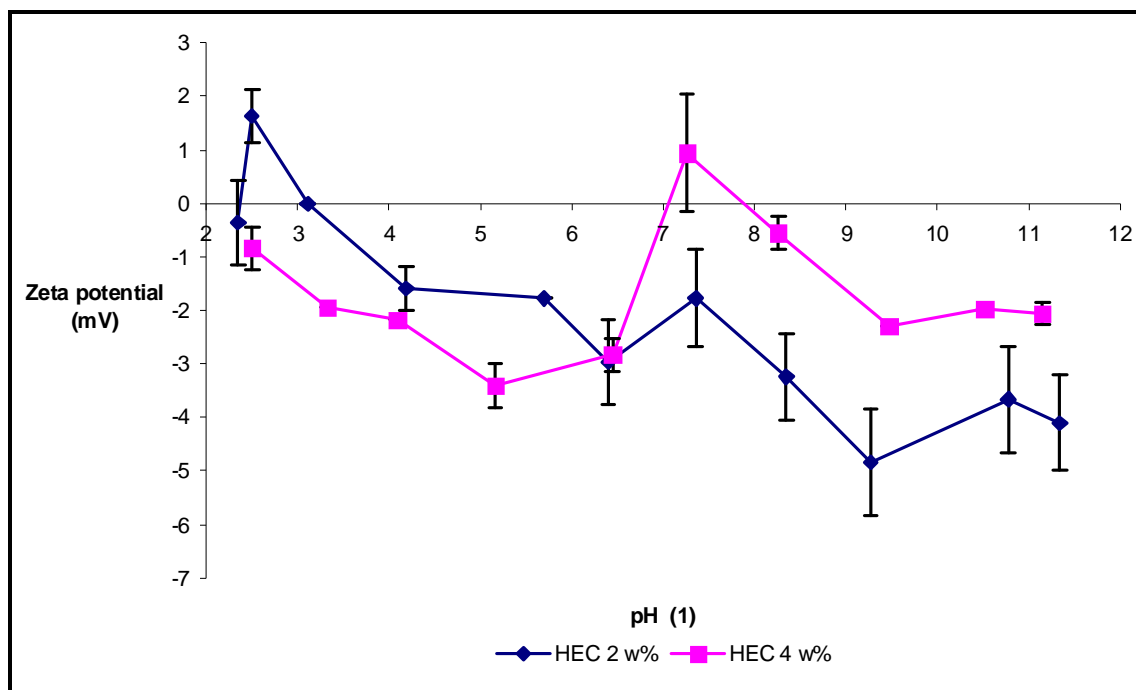


Figure 3.32: This graph shows the functionality of zeta potential and pH of HEC solution.

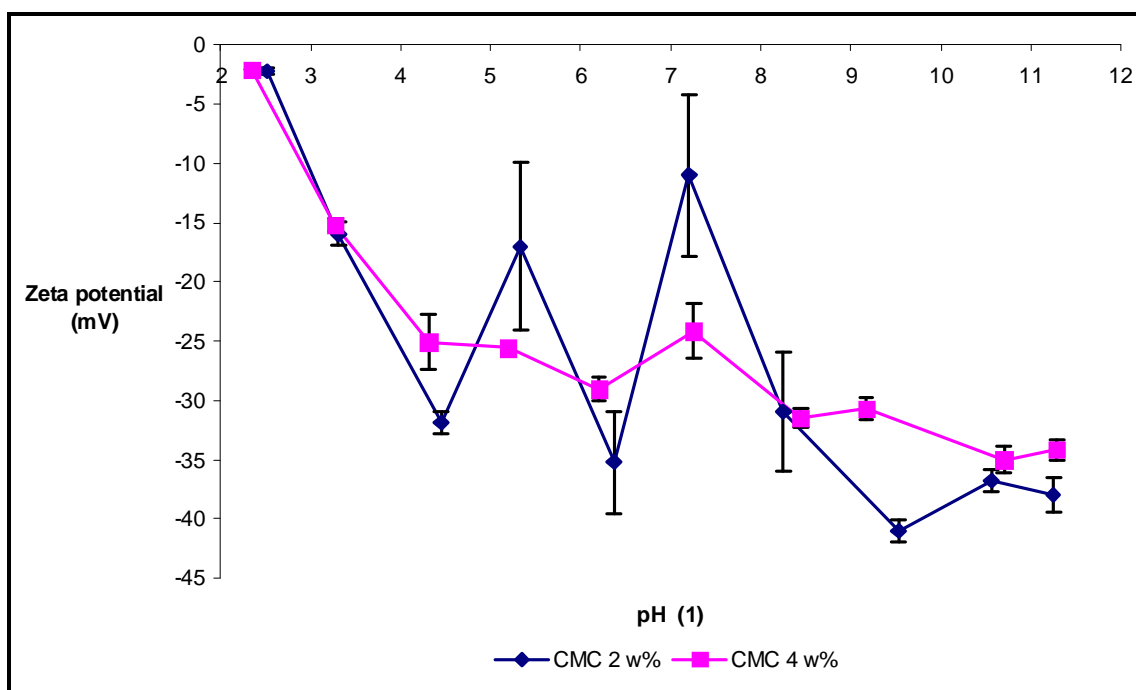


Figure 3.33: These three graphs show the functionality of zeta potential and pH of cellulose solution.

## Evaluation of cellulose derivates for pulsed drug delivery

As second the ion concentration on zeta potential was measured. Samples were again diluted by NaCl solution in ration 1:1 (1w%, 2w%). Measuring data are presented as curves in Figure 3.34.

These curves prove that zeta potential for these solution particles is negative. OK CEL and CMC solutions are stable in whole ionic concentration range, which was measured. HEC solution is less stable with ability to coagulate for ionic concentration about  $1 \cdot 10^{-5} \text{ g.ml}^{-1}$ . Otherwise it is stable in almost whole range.

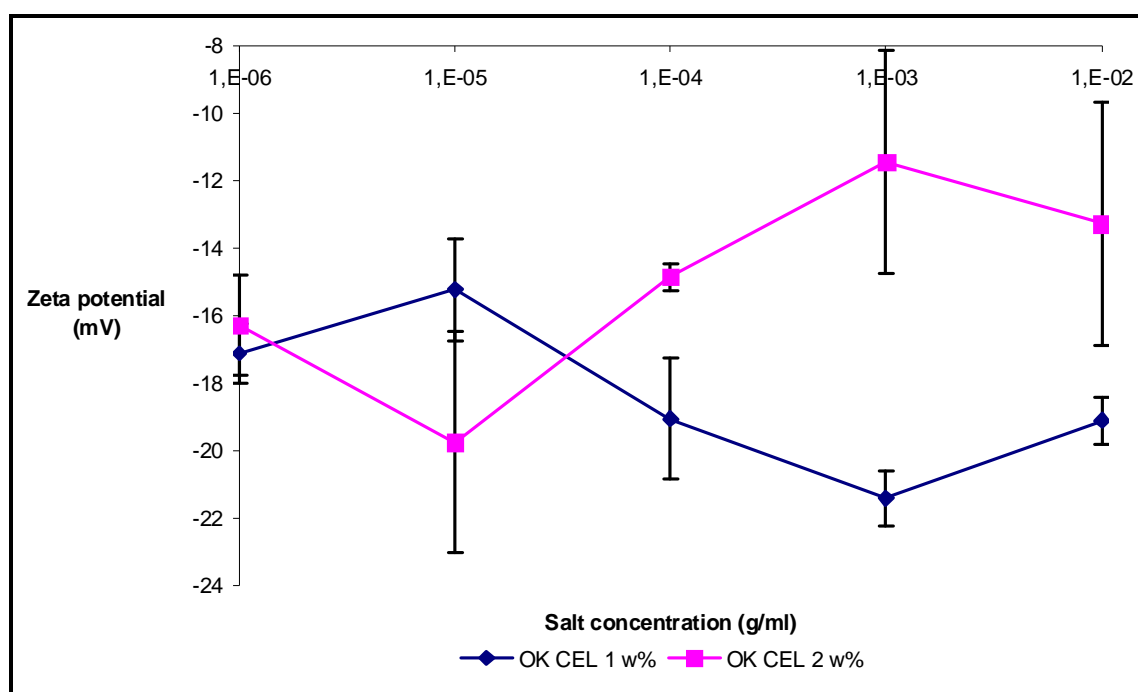


Figure 3.34: These three graphs show the functionality of zeta potential and ionic concentration in cellulose solution.

## Evaluation of cellulose derivates for wound healing dressing

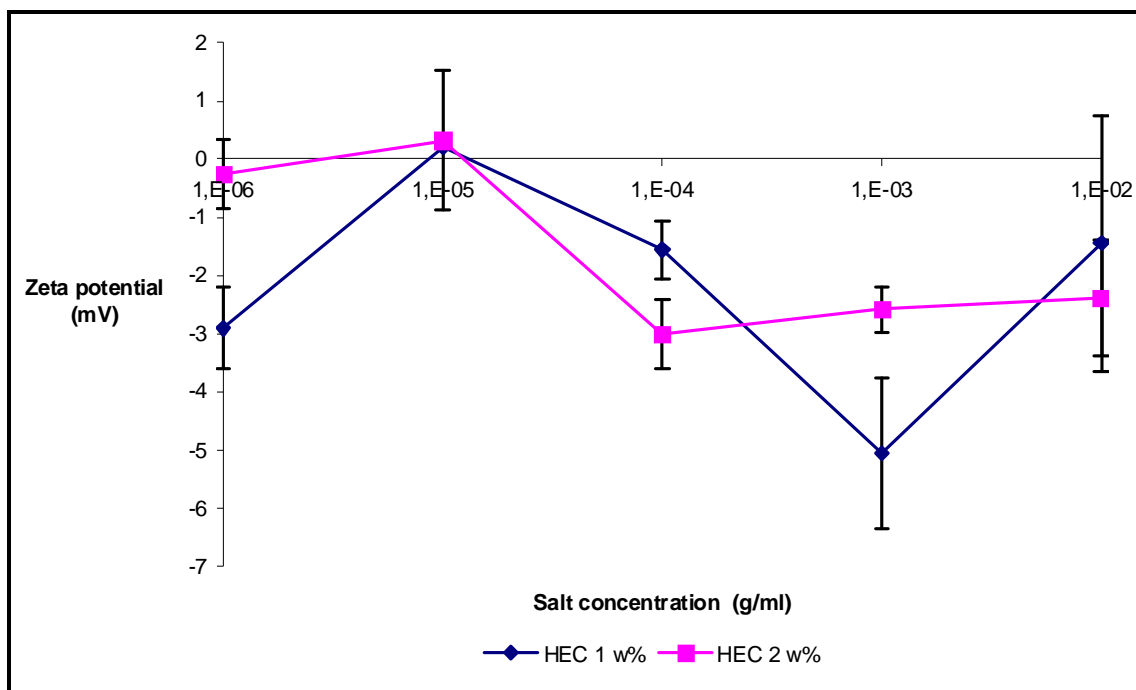


Figure 3.35: These three graphs show the functionality of zeta potential and ionic concentration in cellulose solution.

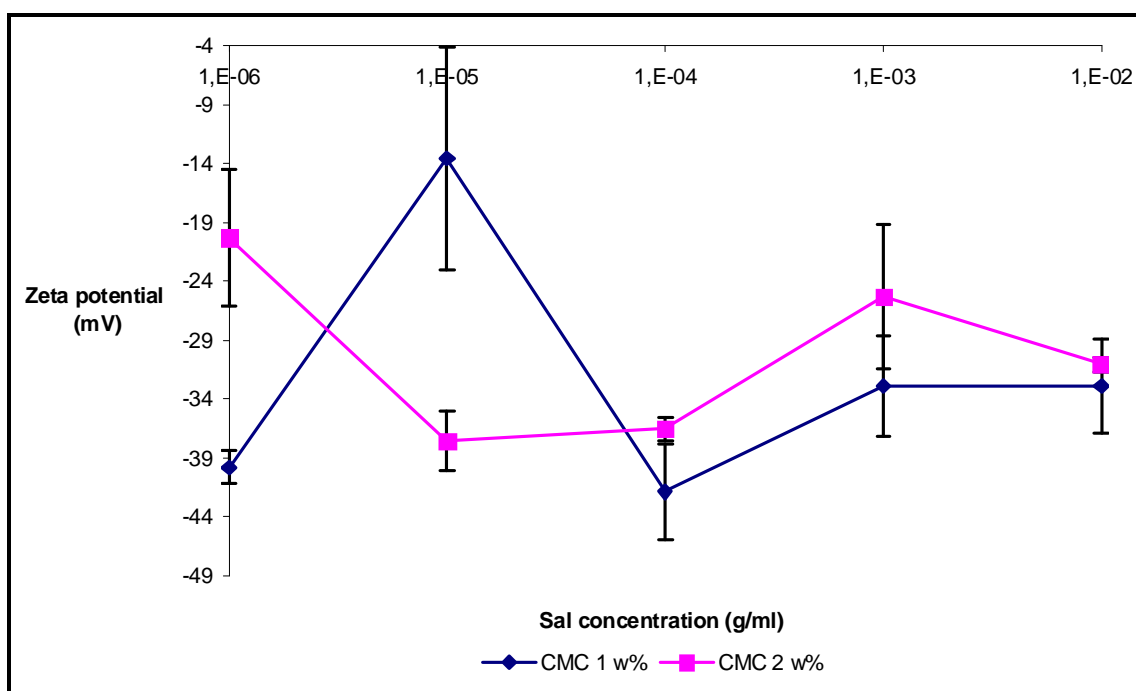


Figure 3.36: These three graphs show the functionality of zeta potential and ionic concentration in cellulose solution.

### **3.4 Conclusion**

The aim of this investigation was to determine basic physico-chemical properties of sorted cellulose derivatives (OK CEL, HEC and CMC). The evaluated properties were: density, surface tension, contact angle, UV-VIS light absorbance, particle size and zeta potential.

The study was also focused on temperature and concentration dependences of selected physical parameters (density, surface tension and contact angle of wetting) of cellulose derivatives in aqueous solutions. Similarly the effect of the latter conditions on UV VIS light absorbance was investigated to allow the calculation of the extinction coefficient. Last part of our work was focused on determination of the influence of counter ion concentration and pH of solution on particle size and zeta potential.

From our measurement we can conclude that density of solutions depends on solution temperature. The higher temperature means the lower density as comes from the basic theory. On the other hand higher solution concentration is the cause of higher density of solution.

Surface tension decreases with increasing temperature. But we do not have any definite conclusions for concentration of solution influence on surface tension. Obtained values of the surface tensions of cellulose aqueous solutions was around 50mN/m, the derivatives act as the surfactants.

The measurement of contact angle brings determinations that this is only slightly dependent on concentration and temperature.

The measurement on UV VIS spectrometer determined that absorbance increases with increases solution concentration. Ionic concentration and pH influence only the light absorbance by OK CEL solution. Other cellulose derivatives are stolid to these influences.

That the particle size varies by influence of varying pH of solutions or ionic concentration in cellulose solution was determined by measuring of particle diameter. This is more significant for HEC and CMC solutions; their molecules have higher absorbability.

Investigations of zeta potential brings conclusions that zeta potential is almost negative for cellulose determined in our work and that these cellulose solutions are stable in whole determined pH range and that adding of NaCl does not influence this behaviour.

We did the basic investigations of selected cellulose derivates. If we want to conclude that these derivates are suitable for applications in wound healing dressing.

### **3.5 List of abbreviations**

°C	Degree of Celsius
A	Absorbance (1)
b	Path length (m)
C	Carbon
c	Concentration of absorbing species (mol/m <sup>3</sup> )
cm	Centimetre
CMC	Carboxymethylcellulose
cos	Cosine
DNA	Deoxyribonose nuclei acid
DS	Degree of substitution
E <sub>s</sub>	Surface free energy (N/m)

## Evaluation of cellulose derivates for pulsed drug delivery

F	Force acting on the balance (N)
F <sub>b</sub>	Buoyancy force (N)
g	Gravitation acceleration (m <sup>2</sup> /s)
g	Gram
h	An hour
HCl	Hydrochloric acid
HEC	Hydroxyethylcellulose
K	Kelvin
L	Wetted length (m)
l	Liquid
m	Meter
ml	Millilitre
mm	Millimetre
NaCl	Sodium chloride
NaOH	Sodium hydroxide
nm	Nanometre
OK CEL	Oxycellulose
PMN	Polymorphonuclear leucocytes
r	Distance from diffusive element (m)
R <sub>v</sub>	Rayleigh's diameter (m <sup>2</sup> )
s	Surface tension (N/m)
s	Solid

## Evaluation of cellulose derivatives for wound healing dressing

s	Second
T	Absolute temperature ( $^{\circ}\text{C}$ ) or (K)
T	Transmittance (1)
UV	Ultraviolet
UV-VIS	Ultraviolet and visible
v	Vapour
V	Standard volume ( $\text{m}^3$ )
w	Weight (g)
w%	Weight percentage (%)
$\alpha$	Electric polarizability ( $\text{C}^2 \text{m}^2/\text{J}$ )
$\epsilon$	Electric permittivity (F/m)
$\nu$	Angle of light reflection ( $^{\circ}$ )
$\varphi$	Surface tension, between the corresponding interfaces (N/m)
$\varphi$	Luminous flux density of light after it passes through the sample (lm)
$\varphi$	Luminous flux density of incident light (lm)
$\varphi_0$	Luminous flux density of incident light (lm)
$\varphi_v$	Luminous flux density of diffused light (lm)
$\alpha$	Absorbitivity, constant of proportionality (m/mol)
$\lambda$	Wavelength (nm)
$\varphi$	Contact angle ( $^{\circ}$ )
$\rho$	Density of liquid ( $\text{g}/\text{m}^3$ )
$\tau$	Surface or interfacial tension (N/m)



### 3.6 List of References

- [3.1] ROYAL PHARMACEUTICAL SOCIETY of Great Britain. Structure and function of human skin. Pub. Great Britain: Pharmpress, 2000. <http://www.Pharmpress.com/shop/samples/T&T-ch 1.pdf>.
- [3.2] LANGMAIER, Ferdinand. Základy kosmetických výrob. 1st ed. Zlín: Univerzita Tomáše Bati ve Zlíně, 2001. 160 s. ISBN 80-7318-016-2.
- [3.3] RICHARDSON, Taylor. The Human Skin—Engineered by God. Pub. Montgomery, Alabama, U.S.A: *Apologetics Press*.
- [3.4] [http://www.eucerin.co.uk/skin/skincell\\_1.html](http://www.eucerin.co.uk/skin/skincell_1.html).
- [3.5] HÜBSCHMANN, Karel. Kůže: orgán lidského těla. *Pub. Praha: Nov*, 1972. 204 s.
- [3.6] SHAKESPEARE, Peter. Burn wound healing and skin substitutes. *Burns* 27 (2001) 517–522. [www.elsevier.com/locate/burns](http://www.elsevier.com/locate/burns).
- [3.7] Orthoteers syllabus [online]. Orthoteers: 2005 [cit. Wound healing]. <http://www.orthoteers.co.uk/Nrujp~ij33lm/Orthwound.htm>
- [3.8] SEDLAŘÍK, K. M. The process of wound healing. Hartmann [online]. <http://www.hartmann/online.de/english/produkte/wundbehandlung/wundforum/default.htm>.
- [3.9] BALASUBRAMANI, Manimalha; Kumar, T. Ravi; Babu Mary. Skin substitutes: a review. *Burns* 27. 2001, p. 534-544. [www.elsevier.com/locate/burns](http://www.elsevier.com/locate/burns).
- [3.10] RAMOS-E-SILVA, Marcia.; RIBEIRO DE CASTRO, Maria Cristina. New Dressings, Including Tissue-Engineered Living Skin. *Pub. New York: Elsevier Science Inc.*, 2002. *Clinics in Dermatology* 20:715–723.

- [3.11] DRURY, Jeanie L.; Mooney, David J. Hydrogels for tissue engineering: scaffold design variables and applications. *Biomaterials* 24. 2003, p. 4337-4351. [www.sciencedirect.com](http://www.sciencedirect.com).
- [3.12] BROWN-ETRIS, Marie.; and col. A New Biomaterial Derived From Small Intestine Submucosa and Developed Into a Wound Matrix Device. *Health Management Publications, Inc.: Wounds* 14(4): p.150-166, 2002.
- [3.13] EISENBUD, David.; and col. Biofilms and Their Potential Role in Wound Healing. *Health Management Publications, Inc.: Wounds* 16(7):234-240, 2004.
- [3.14] ALVAREZ, Oscar M. Effectiveness of a Biocellulose Wound Dressing for the Treatment of Chronic Venous Leg Ulcers: Results of a Single Center Randomized Study Involving 24 Patients. *Health Management Publications, Inc.: Wounds* 16(7):224-233, 2004. <http://www.medscape.com/viewarticle/484360>.
- [3.15] <http://www.medscape.com/viewarticle>
- [3.16] Yannas, Ioannis V. Regenerative Medicine I: Theories, Models and Methods. *Springer-Verlag GmbH*, 93 / 2005. ISBN: 3-540-22871-3.
- [3.17] Advances in Biochemical Engineering/Biotechnology. *Springer-Verlag GmbH*, 2005. ISSN: 0724-6145
- [3.18] FEI, Bin.; WACH, Radoslaw A.; MITOMO, Hiroshi.; YOSHII, Fumio.; KUME, Tamikazu. Hydrogel of Biodegradable Cellulose Derivatives. *Pub. John Wiley & Sons, Inc.: Journal of Applied Polymer Science*, Vol. 78, 278–283 (2000) 2000.
- [3.19] Cellulose.<http://www.lsbu.ac.uk/water/hycel.html>

- [3.20] O'SULLIVAN, Antoinette C. Cellulose: the structure slowly unravels. *Blackie Academic & Professional: Cellulose*. 1997, 4, p.173-207.
- [3.21] KÜFFER, Alfréd. Deriváty celulózy. Pub. Bratislava: TEI, VÚPC, 1961. 159 s.
- [3.22] TOMEČEK, Petr. Interfacial surface: characterization, physical and chemical modification, application: doctoral thesis. Zlín: UTB, FT, ÚFMI, 2004.
- [3.23] DORÉE, Charles. The methods of cellulose chemistry. London: Chapman & Hall LTD, 1947.
- [3.24] [www.aqualon.com](http://www.aqualon.com)
- [3.25] MAVON, A.; ZAHOUANI, H.; REDOULES, D.; AGACHE, P.; GALL, Y.; HUMBERT, Ph. Sebum and stratum corneum lipids increase human skin surface free energy as determined from contact angle measurements: A study on two anatomical sites. *Colloids and Surfaces B: Biointerfaces* 8. 1997, p. 147-155.
- [3.26] GUIDI, V. Surface Tension of Liquids.
- [3.27] KSV Instruments USA. surface and Interfacial Tension. [http://www.ksvinc.com/surface\\_tension1.htm](http://www.ksvinc.com/surface_tension1.htm).
- [3.28] Surface Tension. [http://www.brantacan.co.uk/surface\\_tension.htm](http://www.brantacan.co.uk/surface_tension.htm).
- [3.29] Kibron Inc. Surface Tension and Tensiometers. <http://www.kibron.com/index.html?http://www.kibron.com/Science/Science.html>.
- [3.30] <http://www.kruss.info/techniques/methods>.
- [3.31] KRÜSS GmbH. Manual DTV 30: Tensiometer K12. Hamburg, Germany.

- [3.32] ISHIKAWA, Yasuhiro.; KATOH, Yasuki.; OHSHIMA, Hiroyuki.  
Colloidal stability of aqueous polymeric dispersions: Effect pH and salt concentration. *Colloids and Surfaces B: Biointerfaces* 42. 2005, p. 53-58.
- [3.33] UV/Vis Spectroscopy Background.  
<http://www.chemistry.ccsu.edu/glagovich/teaching/472/uvvis/uvbasics.html>.
- [3.34] The Beer-Lambert Law.  
<http://www.shu.ac.uk/schools/sci/chem/tutorials/molspec/beers1.htm>.
- [3.35] UV-VIS: Theoretical principles.  
<http://www.shu.ac.uk/schools/sci/chem/tutorials/molspec/uvvisab1.htm>
- [3.36] Ultraviolet and Visible Absorption Spectroscopy (UV-Vis).<http://www.chem.vt.edu/chem-ed/spec/uv-vis/uv-vis.html>
- [3.37] Visible and Ultraviolet Spectroscopy.  
<http://www.cem.msu.edu/~reusch/VirtualText/Spectrpy/UV-Vis/spectrum.htm>.
- [3.38] Návodny pro laboratorní cvičení z Koloidní chemie. Určování distribuční funkce podle velikosti částic systému koloid/disperzní prostředí. Zlín: UTB, FT, ÚFMI.
- [3.39] Návodny pro laboratorní cvičení z Koloidní chemie. Určování zeta-potenciálu koloidních částic ve vodních roztocích. Zlín: UTB, FT, ÚFMI.
- [3.40] Brookhaven Instruments Corporation. Manual: ZetaPlus Zeta Potential Analyser. New York, USA.
- [3.41] What is Zeta Potential?<http://www.bic.com/WhatisZetaPotential.html>.

- [3.42] Hercules Incorporated. NATROSOL® 250L Hydroxyethylcellulose, For Pharmaceutical Uses. Wilmington, DE: Aqualon, 2004. NUMBER 4029-3.
- [3.43] Hercules Incorporated. Blanose: Refined CMC. Wilmington, DE: Aqualon, 2004.
- [3.44] Hercules Incorporated. Aqualon: Sodium Carboxymethylcellulose – Physical and Chemical properties. Wilmington, DE: Aqualon, 2004.
- [3.45] SURÝNEK, Martin. Stabilita koloidně dispergovaných soustav: Zeta potenciál a rozptyl světla. Diplomová práce. Zlín: UTB, FT, ÚFMI, 2004.
- [3.46] <http://www.ft.utb.cz/czech/ufmi/vybaveni.html>
- [3.47] ROYAL PHARMACEUTICAL SOCIETY of Great Britain. Structure and function of human skin. Pub. Great Britain: Pharmpress, 2000. Available at: <http://www.Pharmpress.com/shop/samples/T&T-ch1.pdf>.
- [3.48] LANGMAIER, Ferdinand. Základy kosmetických výrob. 1st ed. Zlín: Univerzita Tomáše Bati ve Zlíně, 2001. 160 s. ISBN 80-7318-016-2.
- [3.49] RICHARDSON, Taylor. The Human Skin—Engineered by God. Pub. Montgomery, Alabama, U.S.A: Apologetics Press.
- [3.50] EUCERIN COSMETICS , Available at: [http://www.eucerin.co.uk/skin/skincell\\_1.html](http://www.eucerin.co.uk/skin/skincell_1.html).
- [3.51] HÜBSCHMANN, Karel. Kůže: orgán lidského těla. Pub. Praha: Nov, 1972.
- [3.52] RAINEY, Joy. Wound Care. A Handbook for Community Nurses. London, England: Whurr Publisher Ltd, 2002.

- [3.53] COOPER, D. Managing malignant ulcers effectively. *Nursing Standard*, 8(2):p25-28. (1993).
- [3.54] ConvaTec A Bristol-Mayers Squibb Company. Available at:  
<http://www.convatec.com/convatec/jsp/CVTUSHHome.do>
- [3.55] FORENSIC MEDICINE FOR MEDICAL STUDENTS. Available at:  
<http://www.forensicmed.co.uk/index.htm>
- [3.56] SHAKESPEARE, P. Burn wound healing and skin substitutes. *Burns* 27 (2001) 517–522. Available at: [www.elsevier.com/locate/burns](http://www.elsevier.com/locate/burns).
- [3.57] ROSEN, M.R. *Delivery System Handbook for Personal Care and Cosmetic Products. Technology, Application, and Formulations*. 1st ed. Norwich, New York: William Andrew, Inc. 2005. 1091p. ISBN: 0-8155-1504-9.
- [3.58] Orthoteers syllabus [online]. Orthoteers: 2005 [cit. Wound healing].  
<http://www.orthoteers.co.uk/Nrujp~ij33lm/Orthwound.htm>
- [3.59] SEDLAŘÍK, K. M. The process of wound healing. Hartmann. Available at: <http://www.hartmann-online.de/english/produkte/wundbehandlung/wundforum/default.htm>.
- [3.60] BALASUBRAMANI, Manimalha; Kumar, T. Ravi; Babu Mary. Skin substitutes: a review. *Burns* 27. 2001, p. 534–544.
- [3.61] RAMOS-E-SILVA, Marcia.; RIBEIRO DE CASTRO, Maria Cristina. New Dressings, Including Tissue-Engineered Living Skin. *Pub. New York: Elsevier Science Inc.*, 2002. *Clinics in Dermatology* 20:715–723.
- [3.62] DRURY, Jeanie L.; MOONEY, David J. Hydrogels for tissue engineering: scaffold design variables and applications. *Biomaterials* 24 (2003) 4337–4351. [www.sciencedirect.com](http://www.sciencedirect.com).

- [3.63] BROWN-ETRIS, Marie.; and col. A New Biomaterial Derived From Small Intestine Submucosa and Developed Into a Wound Matrix Device. *Health Management Publications, Inc.: Wounds 14(4):150-166*, 2002.
- [3.64] BENBOW, M. Diagnosing and Assessing Wounds. *Journal of Community Nursing*. 2007, vol. 21, no. 8, p. 26-34.
- [3.65] EISENBUD, D. and col. Biofilms and Their Potential Role in Wound Healing. *Health Management Publications, Inc.: Wounds 16(7):234-240*, 2004.
- [3.66] ALVAREZ, Oscar M. Effectiveness of a Biocellulose Wound Dressing for the Treatment of Chronic Venous Leg Ulcers: Results of a Single Centre Randomized Study Involving 24 Patients. *Health Management Publications, Inc.: Wounds 16(7):224-233*, 2004.  
<http://www.medscape.com/viewarticle>
- [3.67] YANNAS, Ioannis V. Regenerative Medicine I: Theories, Models and Methods. *Springer-Verlag GmbH*, 93 / 2005. ISBN: 3-540-22871-3.
- [3.68] Advances in Biochemical Engineering/Biotechnology. *Springer-Verlag GmbH*, 2005. ISSN: 0724-6145
- [3.69] FEI, Bin.; WACH, Radoslaw A.; MITOMO, Hiroshi.; YOSHII, Fumio.; KUME, Tamikazu. Hydrogel of Biodegradable Cellulose Derivatives. *Pub. John Wiley & Sons, Inc.: Journal of Applied Polymer Science*, Vol. 78, 278–283 (2000) 2000.
- [3.70] Cellulose. Available at: <http://www.lsbu.ac.uk/water/hycel.html>
- [3.71] O'SULLIVAN, Antoinette C. Cellulose: the structure slowly unravels. *Blackie Academic & Professional: Cellulose*. (1997) 4, 173-207, 1997.

- [3.72] KÜFFER, Alfréd. Deriváty celulózy. Pub. Bratislava: TEI, VÚPC, 1961. 159 s.
- [3.73] TOMEČEK, Petr. Interfacial surface: characterization, physical and chemical modification, application: doctoral thesis. Zlín: UTB, FT, ÚFMI, 2004.
- [3.74] DORÉE, Ch. The methods of cellulose chemistry. London: *Chapman & Hall LTD*, 1947.
- [3.75] [www.aqualon.com](http://www.aqualon.com)
- [3.76] MAVON, A.; ZAHOUANI, H.; REDOULES, D.; AGACHE, P.; GALL, Y.; HUMBERT, Ph. Sebum and stratum corneum lipids increase human skin surface free energy as determined from contact angle measurements: A study on two anatomical sites. *Colloids and Surfaces B: Biointerfaces* 8. (1997) 147-155.
- [3.77] DEMBOSKI, G., BOGOEVA-GACEVA, G. Textile structures for technical textiles. Bulletin of the Chemists and Technologists of Macedonia. 2005, Vol. 24, p. 67-86. ISSN 0350-0136.
- [3.78] TEMPESTI, A. A Survey on Innovative Textiles and Their Application.
- [3.79] ANAND, S. C., SHAH, T. Recent Advances in Technical Textiles. Centre for Material Research and Innovation. The University of Bolton. United Kingdom. International Conference on Textile and Clothing 2006.
- [3.80] HORROCKS, A.R., ANAND, S.C. Handbook of technical textiles. Cambridge, England: *Woodhead publishing limited*, 2000. ISBN 1 85573 385 4.
- [3.81] MATHER, R.R. Developments in Textiles. Medical Device Technology. *ProQuest Medical Library*. p. 32. 2006.



- [3.82] KLEMM, D., HEUBLEIN, B., FINK, H.P., BOHN, A., Cellulose: Fascinating Biopolymer and Sustainable Raw Material. Weinheim: Angewandte Chemie. Int. Ed. 2005. Vol. 44, p. 3358-3393. Wiley-VCH Verlag GmbH & Co. KGaA, Weinheim.
- [3.83] KLEMM, D., SCHMAUDER, H.P., HEINZE, T. Cellulose. 5 *Biosynthesis*. p. 275 – 287. Jena, Germany 2004.
- [3.84] BAYER, E.A., CHANZY H., LAMED, R., SHOHAM, Y. Cellulose, cellulases and celulosomes. *Current Opinion in Structural Biology*. p. 548 -558. *Current Biology Ltd*. Israel. 1998. ISSN 0959-440X.
- [3.85] MIHRANYAN, A. Engineering of Native Cellulose Structure for Pharmaceutical Applications. Influence of Cellulose Crystallinity Index, Surface Area and Pore Volume on Sorption Phenomena. *Acta Universitatis Upsaliensis*, Uppsala, 2005, ISBN: 91-554-6130-1.
- [3.86] VINCENT, J.F. From Cellulose to Cell. *The Journal of Experimental Biology* 202, p. 3263-3268. Great Britain. The Company of Biologists Limited. 1999.
- [3.87] LADOUCE L., et al. Cellulose Microfibrils with Modified Surface, Preparation, Method and Use Thereof. *United States Patent*. US 6 703 497 B1. 9. March. 2004.
- [3.88] PANAITESCU. D.M., DONESCU, D. and coll. Polymer Composites with Cellulose Microfibrils. *Polymer Engineering and Science*. *Society of Plastics Engineers, Inc.* 2007.
- [3.89] CHALRABPRTY, A., SAIN, M., KORTSCHOT, M. Cellulose microfibrils: A Novel Method of Preparation Using High Shear Refining and Cryocrushing. *Holzforschung*. Vol. 59. p 102-107. Walter de Gruyter, Berlin. 2005.

- [3.90] MOHANTY, A.K., MISRA, M., DRZAL, L.T. Natural Fibres, Biopolymers, and Biocomposites. *Taylor & Francis Group*. New York, USA, 2005. ISBN: 978-0-8493-1741-5.
- [3.91] WOODINGS, C. Regenerated Cellulose Fibres. *Woodhead Publishing Limited*. Cambridge England, 2001, ISBN: 1-85573-459-1.
- [3.92] Rayon Fibre. Available at: [www.fibresource.com](http://www.fibresource.com)
- [3.93] MAHLIG, B., HAUFE, H., BÖTTCHER, H. Functionalisation of Textiles by Inorganic Sol-Gel Coatings. *Journal of Materials Chemistry*. 2005, vol.15, p. 4385-4398.
- [3.94] PEREPELKIN, K.E. Fibre Composite Materials, Polymer Fibre Composites, Basic Types, Principles of Fabrication, and Properties. *Fibre Chemistry*, Vol. 38. No1, Springer Science + Business Media, Inc. 2006.
- [3.95] EDWARDS, V.J., BUSCHLE-DILLER, G., GOHEEN, S.C. Modified Fibres with Medical and Specialty Applications. *Springer Dordrecht*. The Netherlands. 2006. ISBN-13: 978-1-4020-3794-8.
- [3.96] CARR, C.M. Chemistry of the Textile Industry. 1st ed. Glasgow: *Blackie Academic & Profesional*. 1995. 382 p. ISBN 0 7514 0054 8.
- [3.97] Encyclopaedia Britannica. Available at: [www.EncyclopaediaBritannica.com](http://www.EncyclopaediaBritannica.com)
- [3.98] SHANMUGASUNDARAM, O.L. Application of Nonwovens in Medical Field.
- [3.99] HONSHU SEISHI KABUSHIKI KAISHA. Adsorptive Nonwoven Fabric Comprising Fused Fibres, Non-fused Fibres and Absorptive Materials and Method of Making Same. SAMEJIMA, T. *United States Patent*, 4 160 059, 1979-07-03.

- [3.100] RUSSELL, S.J. Handbook of Nonwovens. The Textile Institute. *Woodhead Publishing Limited*. Cambridge, England, 2007, ISBN-10: 1-84569-199-7.
- [3.101] HUNTER, I. Handbook of Non-Woven Filter Media. 1st ed. Amsterdam: *Elsevier*. 2007. 477 p. ISBN: 1 8561 4417.
- [3.102] E.I. DU PONT DE NEMOURS AND COMPANY. Apparatus for Making Non-woven Fibrous Sheet. BRETHAUER, D. M., PRIDEAUX, J.P. *United States Patent*, 3 860 369, 1975-06-14.
- [3.103] E.I. DU PONT DE NEMOURS AND COMPANY. Process for the Preparation of Nonwoven Fibrous Sheets. MCGINTY, D.J. *United States Patent*. 5 603 885. 1997-02-18.
- [3.104] ZHANG, X. Investigation of Biodegradable Nonwoven Composites Based on Cotton, Bagasse and Other Annual Plants. A Thesis. Louisiana State University , Louisiana, 2004. 73 p.
- [3.105] JOHNSON & JOHNSON. Methods of Making Nonwoven Textile Fabrics. PLUMMER, CH. H. *United States Patent*. 3 753 826. 1973-08-21.
- [3.106] History of wound care. Wikipedia. Available on World Wide Web: [www.wikipedia.com](http://www.wikipedia.com)
- [3.107] SIPOS, P., GYORY, H., HAGYMASI, K., ONDREJKA, P. BLAZOVICS, A. Special Wound Healing Methods Used in Ancient Egypt and the Mythological Background. *World Journal of Surgery*. 2004, vol. 28, p. 211-216.
- [3.108] GOTTRUP, F., LEAPER, D. Wound Healing: Historical Aspects. *EWMA Journal*. 2004. vol. 4, no. 2, p. 26.

- [3.109] MITCHELL, B.S. An Introduction to Materials Engineering and Science for Chemical and Materials Engineers. *A John Wiley & Sons, Inc.*, Publication. Hoboken, New Jersey. 2004.
- [3.110] OTŘÍSALOVÁ, K. Evaluation of Cellulose Derivates for Wound Healing Dressing. Master Thesis. Tomas Bata University in Zlín. Zlín. 2005.
- [3.111] SAVILLE, B.P. Physical testing of textiles. *Woodhead Publishing Limited*. Cambridge, England. 1999. ISBN: 1-85573-367-6.
- [3.112] FÄLT, S. Model Studies of Cellulose Fibres and Films and Their Relation to Paper Strength. Licentiate Thesis. *KTH Stockholm*, 2003. 46 p.
- [3.113] Article Made From Perforated Cellulose Sheets. HEYMAN, W.A. *United States Patent Office*, 2 137 243, 1936-04-20.
- [3.114] Articles for Reducing Atmospheric Odors. MCKAY JR., N. D. *United States Patent Application Publication*, US 2008/0009560 A1, 2008-01-10.
- [3.115] UNITIKA Ltd., NIPPON UNICAT COMPANY LIMITED. Biodegradable Nonwoven Fabrics. TANAKA, H., MIYAHARA, Y., KASETANI, S., ESAKI, K. NISHIMARA, S., INOUE, T. *United States Patent*, 5 506 041, 1996-04-09.
- [3.116] ASAHI KASEI KOGYO KABUSHIKI KAISHA. Composite Nonwoven Fabric. FUKUI, M., KIYOTAKI, T. *United States Patent*, 5 298 315, 1994-03-29.
- [3.117] HEINZE, T., VIEIRA, M., HEINZE, U. New Polymers Base on Cellulose. Jena, Germany.

- [3.118] OMNOVA SOLUTIONS INC. Nonwoven Fabric of Non-Cellulose Fibres and a Method of Manufacture. DIEHL, D.F. United States Patent. 6 034 005. 2000-03-07.
- [3.119] RUTGERSWERKE AKTIENGESELLSCHAFT. Non-woven Textiles. JELLINEK, K., GARDZIELLA, A., SCHWIEGER, K., ADOLPHS, P., SUREN, J. *United States Patent*. 4 745 024. 1988-05-17.
- [3.120] TAMFELT OY AB. Planar Textile Structure. SALMINEN, A., RAUTENEN S. *United States Patent*. 5 006 399. 1991-04-09.
- [3.121] SQUIBB; E.R. & SONS, INC. Polymeric Support Wound Dressing. FREEMAN, F. *United States Patent*. 5 681 579. 1997-10-28.
- [3.122] RHONE-POULENC FIBRES. Process for the Treatment of Non-woven Sheets and the Product Obtained. BARAVIAN, J. *United States Patent*. 4 560 385. 1985-12-24.
- [3.123] JOHNSON & JOHNSON. Skin Treatment Article. EKNOIAN, M. W., GUBERNICK, D., MCLAUGHLIN, R.A. *United States Patent Application Publication*. US 2007/0299410 A1, 2007-12-27.
- [3.124] CIBA SPECIALTY CHEMICALS CORPORATION. Stabilized Body Care Products, Household Products, Textiles and Fabrics. LUPIA, J. A., SUHADOLNIK, J., WOOD M.G. United States Patent Application Publication. US 2008/0009550 A1. 2008-01-10.
- [3.125] Textile-like Patterned Nonwoven Fabrics and Their Production. EVANS, F.J. *United States Patent*. 3 485 706. 1969-12-23.
- [3.126] ESTABLISSEMENTS LES FILS D' AUGUSTE. Multilayer Textile Composites Based on Fibrous Sheets Having Different Characteristics. CHOMARAT, G. *United States Patent*. 5 175 042. 1992-12-29.

- [3.127] RHODIA FILTEC AG. Technical Fabrics for Airbags. LALONDE, R., HURSCHLER, F. *United States Patent*. 6 153 545. 2000-11-28.
- [3.128] Wound and Ulcers. Basic Definitions and Introduction. Available at: WWW.
- [3.129] Dressing Materials. Basic Overview. Available at: WWW.
- [3.130] FOUDA, M.M.G. Use of Natural Polysaccharides in Medical Textile Applications. Doctoral Thesis. University of Duisburg-Essen. 2005. 135 p.
- [3.131] DUTKIEWICZ, J. Some Advances in Nonwoven Structures For Absorbency, Comfort and Aesthetics. *AUTEX Research Journal*. vol.2, no. 3, 2002.
- [3.132] KIMBERLY-CLARK WORLDWIDE INC. Absorbent Structure and Method. DUTKIEWICZ, J. *United States Patent*. 6 329 565 B1, 2001-12-11.
- [3.133] DOW CORNING KABUSHIKI KAISHA. Artificial Skin. IKADA, Y., GEN, S., OHI, S., URABE, Y. KAWASHIMA, H. *United States Patent*. 4 882 162. 1989-11-21.
- [3.134] ALZA CORPORATION. Medical Bandage. ZAFFARONI, A. *United States Patent*. 3 996 934, 1976-12-14.
- [3.135] TOWNSEND AND TOWNSEND AND CREW. Multifunctional Textiles. SUN, G. *United States Patent Application Publication*. US 2003/0056297.
- [3.136] THE WEBB LAW FIRM. Wound dressing. CRISP, W.E. *United States Patent Application Publication*. US 2006/0015052 A1, 2006-01-19.
- [3.137] YUDANOVA, T.N., RESHETOV, I.V. Drug Synthesis Methods and Manufacturing Technology. *Modern Wound Dressings*:

Manufacturing and Properties. *Pharmaceutical Chemistry Journal*.  
vol. 40, no. 2, 2006.

- [3.138] BRISTOL-MEYERS SQUIBB COMPANY. Wound dressing.  
BOWLER, P., PARSON, D., WALKER, M. United States Patent  
Application Publication. US2004/0001880 A1, 2004-01-01.
- [3.139] MANEERUNG, T., TOKURA, S., RUJIRAVANIT, R. Impregnation  
of Silver Nanoparticles into Bacterial Cellulose for Antimicrobial  
Wound Dressing. *Carbohydrate Polymers*. 2007.
- [3.140] MANO, J.F. and collective. Natural Origin Biodegradable Systems in  
Tissue Engineering and Regenerative Medicine: Present Status and  
Some Moving Trends. *J. R. Soc. Interface*. 2007.
- [3.141] XYLOS CORPORATION. Microbial Cellulose Wound Dressing for  
Treating Chronic Wounds. SERAFICA, G.C., MORMINO, R.,  
OSTER, G.A., LENTZ, K.E., KOEHLER, K. P. European Patent  
Specification. EP 1 356 831 B1. 2002-06-24.
- [3.142] AM INTERNATIONAL TESSLA AG. Super Absorbent Wound  
Dressing. TIMMERMANS, C.J. United States Patent. 5 961 478.  
1999-10-05.
- [3.143] COLOPLAST A/S. Dressing. NAESTOFT, R., HANNE, J. United  
States Patent. 5 643 187. 1997-07-01.
- [3.144] SMITH & NEOHEW PLC. Dressings. ROBINSON, J.W. United  
States Patent. 6 191 335, 2001-02-20.
- [3.145] DORITY & MANNING, P.A. Wound or Surgical Dressing.  
VILLANUEVA, J., SAYRE, C.N. United States Patent Application  
Publication. US 2007/0141130 A1, 2007-06-21.

- [3.146] MOLNLYCKE HEALTH CARE AB. Wound Dressing.  
ARESKOUG, S., LINDQUIST, B.W. United States Patent. US 4 797 24 B1, 2002-11-12.
- [3.147] ACORDIS FIBRE LIMITED. Wound Dressing. BAHIA, H.S.,  
BURROW, T.R. United States Patent. US 6 075 177, 2000-06-13. Wound Dressing. BAY, M. United States Patent. US 5 064 652, 1991-11-12.
- [3.148] BRISTOL-MYERS SQUIBB COMPANY. Wound Dressing.  
BUGLINO, D.E., BARRY, C., HUDAK, J.C., KADASH, M.A. United States Patent. 6 011 194. 2000-01-04.
- [3.149] BRISTOL-MYERS SQUIBB COMPANY. Wound Dressing.  
BARRY, C. United States Patent. US 5 603 946, 1997-02-18.
- [3.150] THE KENDALL COMPANY. Wound Dressing. QUARFOOT, A.J.  
United States Patent. US 4 759 354, 1988-07-26.
- [3.151] BRISTOL-MYERS SQUIBB COMPANY. Wound Dressing. SHAW, H., LINNANE, P.G. United States Patent Application Publication. US 2004/0181182 A1, 2004-09-16. Wound Dressing. EAKIN, T.G. United States Patent Application Publication. US 2002/0091347 A1, 2002-07-11.
- [3.152] KURARAY CO., LTD. Wound Dressing. TANIHARA, M.  
FUKUNISHI, Y., KINOSHITA, H. United States Patent. 5 679 371, 1997-10-21.
- [3.153] SPENCO MEDICAL CORPORATION. Wound Dressing. SPENCE, W.R. United States Patent. 4 226 232, 1980-10-07.
- [3.154] 3M INNOVATIVE PROPERTIES COMPANY. Wound Dressings and Methods. BURTON, S.A., HYDE, P.D., POPKO, D. T. United



Evaluation of cellulose derivatives for pulsed drug delivery

States Patent Application Publication. US 2005/0123590 A1, 2005-06-09.

[3.155] Wound Dressing and Wound Dressing Kit. KURATA, S. United States Patent Application Publication. US 2006/0094997 A1, 2006-05-04.

[3.156] SQUIBB; E.R. & SONS, INC. Wound Dressing System. FRANK, M.A., FREEMAN, F.M., CHERRY, G. United States Patent. US 4 909 243, 1990-03-20.

[3.157] OGITA BIOMATERIAL LABORATORIES CO. LTD. Wound-Covering Material and Wound-Covering Composition. KUBOTA, S. United States Patent. US 5 834 007, 1998-11-10.

[3.158] CHIRON OPHTHALMICS, INC. Wound-Healing Dressing and Methods. REICH, C. United States Patent. US 4 973 466, 1990-11-27.

## MAIN CONCLUSION

The aim of this Doctoral Thesis is focused on investigation and selection of basic materials and techniques necessary for preparation of the currently used planar materials mainly used as wound healing material for healing of injuries after mechanical injuries as well as on surface burn injuries. These materials are also being possible to use in case of problems related with bedsores and other types of ulcerations of tissue deprived e.g. by nutrition or prolonged pressure.

Based on such critical vigorous review the new prospective planar based candidate articles are selected and their physic-chemical properties and their influence ability were tested.

As the most progressive materials systems of engineered planar wound healing article components building blocks will be mainly on natural biopolymer bases (polysaccharides).

With respect to the latter mentioned practical oriented aims, the need of detail study of systems suitable for controllable drug delivery in situ of direct wound/article interface on dex-HEMA bases was studied. As followed from above mentioned aims, important issue was also detaining high sterility and antibacterial functionality of the article based on silver and titanium oxide anti-inflammatory agents attached on cellulose fibres.

This study shows that chosen HEC and CMC polysaccharides are able to swallow in specific pH and salt concentrations better than other chosen polysaccharide OK CEL. Ability to swallow is very important for polymers to be able to disintegrate from crosslinked gel what is necessary condition for polymers suitable for pulsed drug delivery, as it is shown in the case of dex-HEMA and PEG-HEMA.

This study also presents two different successful ways of polymerization of natural polymers. Their degradation process is then studied by increasing swelling pressure, increasing concentration of free polymer particles. Degradation process is necessary for realising of entrapped drug molecules from crosslinked polymer matrix.

Basic construction units will be exposed to different agents from surrounding during application. That is way it is so necessary also to protect them against influences. One possibility of protection is also shown in this study, where inorganic/ organic nanocomposites are built up. We present process of covering fibre surface with inorganic oxides. These can protect fibres, but they can be also used as base for growing Ag metal particles on their surface. Ag, as well known, has high sterile and antibacterial functionality. Which can brings other possibilities for application of, on these basis, prepared planar articles.

This study investigates possible candidates from natural polymer row, which can be chosen as basic construction materials for planar articles. Molecules of drugs could be entrapped in crosslinked matrix and by slow swallow process could be further released in to the wound. Because of using of different factors, which can also influence the physico-chemical properties of fibres, this can be protected or even improved by building nanocomposites. This can bring other opportunities for natural polymers in medical textiles and their medical application.

## CONFERENCE CONTRIBUTION

OTŘÍSALOVÁ, K., DE SMEDT, S., DEMEESTER, J., VAN THIENEN, T.,  
LAPČÍK, L. Biodegradable hydrogels for pulsed drug delivery. *Poster on international conference CHISA 2004*, (22-26.8.2004), Praha.

OTŘÍSALOVÁ, K., DE SMEDT, S., DEMEESTER, J., VAN THIENEN, T.,  
LAPČÍK, L., BLAHA, A. Syntéza hydroxyethylmetakrylát-dextran pro pulzní rozptyl léčiva. *Presentation on national conference Aprochem 2004*, (Milovy, 20-22.9.2004).

OTŘÍSALOVÁ, K., Characterization Of dex-hema For Pulsed Drug Delivery. *Student expert works. SVOČ 2004*. (1. místo).

OTŘÍSALOVÁ, K., LAPČÍK, L. Charakterizace fyzikálně-chemických vlastností celulozových derivátů pro povrchovou léčbu ran. *Presentation on national conference CHISA 2005*, (Srní, 17 – 20.10.2005)

OTŘÍSALOVÁ, K., LAPČÍK, L. Colloidal stability of aqueous calcium pyrophosphate dispersions: effect of annealing temperature and solution ionic strength. *Poster on national conference NANO 06*, (Brno, 13 – 15.11.2006).

OTŘÍSALOVÁ, K., LAPČÍK, L. Colloidal stability of aqueous calcium pyrophosphate dispersions: effect of annealing temperature and solution ionic strength – advanced study. *Poster on international conference COST and SURUZ Workshop. KRAKOW 2007, (Krakow, 19-21.3.2007).*

LAPČÍK, L, jr., NOVOTNÁ, K., LAPČÍKOVÁ, B., Minařík, A., Evaluation of cellulose Derivates Gels for Wound Healing Dressing. *Poster on international conference ICCE/17, HAWAII, 2009.*

## CURRICULUM VITAE

### Personal Data:

Name: Ing. Karin Novotná (Otřísalová)  
Date of birth: 6.2.1982  
Address: Dlážděná 69, 691 05 Zaječí  
Contact: karinovotna@seznam.cz, +420 776 736 900

Employment: Tyco Electronics Czech s.r.o., Automotive, Kuřim  
2010 – so far Department of Inlay Molding  
Supervisor of Inlay Molding  
2009 – 2010 Department of Mechatronics and Inlay Molding  
Manager of Mechatronics and Inlay Molding  
Supervisor of Mechatronics and Inlay Molding  
2008 – 2009 Process Engineer of Mechatronics department

### Education:

2005 - so-far Tomas Bata University in Zlín, Faculty of Technology  
Department of Physics and Materials Engineering  
Doctoral Degree Specialization: Materials Chemistry  
2000 – 2005 Tomas Bata University in Zlín, Faculty of Technology

Department of Physics and Materials Engineering

Study Program: Materials Engineering

Thesis topic: Evaluation of cellulose derivates for wound healing dressing.

1993 – 2000                      High school T.G. Masaryka, Hustopeče, General studies

Stays Abroad:

07-08/2003                      National Technological University Athens, Greece

Study: Evaluation of natural and artificial pozzolana used for preparation of restoration mortars.

09-12/2003                      University Ghent, Belgium

Study: Evaluation of Dex-HEMA for pulsed drug delivery.

08-09/2005                      Martin Luther University, Halle, Germany

Study: Viscoelastic and anisotropic behaviour of bones.

05-08/2006                      University Aveiro, Portugal

Study: Coating of cellulose fibres with silica to protect it against UV rays.

Courses:

January 2006    Measuring of Vibration Spectra and Interpretation of Vibration Spectra (Ioannes Marcus Marci Spectroscopic Society).